12-2004

Fumed Metallic Oxides and Conventional Pigments for Glossy Inkjet Paper

Hyunkook Lee
Western Michigan University

FUMED METALLIC OXIDES AND CONVENTIONAL PIGMENTS FOR GLOSSY INKJET PAPER

by

Hyunkook Lee

A Dissertation
Submitted to the
Faculty of The Graduate College
in partial fulfillment of the
requirements for the
Degree of Doctor of Philosophy
Department of Paper Engineering, Chemical Engineering, and Imaging

Western Michigan University
Kalamazoo, Michigan
December 2004

THE GRADUATE COLLEGE
WESTERN MICHIGAN UNIVERSITY
KALAMAZOO, MICHIGAN

Date November 10, 2004

WE HEREBY APPROVE THE DISSERTATION SUBMITTED BY

Hyunkook Lee

ENTITLED FUMED METALLIC OXIDES AND CONVENTIONAL PIGMENTS FOR GLOSSY INKJET PAPER

AS PARTIAL FULFILLMENT OF THE REQUIREMENTS FOR THE

DEGREE OF Doctor of Philosophy

Paper Engineering, Chemical Engineering, and Imaging
(Department)

Dr. Margaret K. Joyce
Dissertation Review Committee Chair

Paper and Imaging Science and Engineering
(Program)

Dr. Paul D. Fleming
Dissertation Review Committee Member

Dr. Molly W. Williams
Dissertation Review Committee Member

APPROVED

Wm. Wiener
Dean of The Graduate College

Date DECEMBER 2004

TABLE OF CONTENTS

Table of Contents—continued

Table of Contents—continued

CHAPTER

Table of Contents—continued

CHAPTER

APPENDICES

LIST OF TABLES

LIST OF FIGURES

List of Figures—Continued

List of Figures—Continued

List of Figures—Continued

List of Figures—Continued

CHAPTER I

INTRODUCTION

Inkjet printing has proven to be the first digital technology that has achieved an acceptable level of color quality at an affordable price for the majority of home/office end users (1). As a result, there is a demand for inkjet media with intermediate and high gloss finishes, so that the inkjet printed image may resemble a photographic image (2). It is foreseen that as image quality improves and throughput speeds increase, inkjet printing will continue to expand into additional printing markets and may begin to challenge electrophotography in many high-end applications. A key to meeting the needs of this evolving market is the development of coated inkjet media capable of providing the desired glossy image characteristics of photographic papers.

The basic imaging technique in inkjet recording involves the use of one or more inkjet assemblies connected to a source of ink. Each inkjet nozzle includes a small orifice that is electro magnetically energized by magneto restrictive, piezoelectric, thermal, or similar means to emit uniform droplets of ink as a continuous stream or as individual droplets on demand (3).

The droplets are directed onto the surface of a moving web and controlled to form printed characters. The quality of the record obtained in an inkjet recording process highly depends on jet operation, the properties of the ink, and the recording

paper. Among these the recording sheet must absorb the ink rapidly and at the same time immobilize the ink dye on the sheet surface. The former property reduces the tendency for set-off (i.e. transfer of the ink from the paper to sheet handling rollers and the like) whereas the latter property insures that images having high optical density are obtained. Unfortunately, these two properties are in conflict with one another. Papers having high absorbency draw the ink deeply into the paper and the optical density of the image formed at the paper surface is reduced. They also suffer from feathering, poor edge security, and show-through. Papers with low absorbency, such as highly sized papers, provide good optical density by retaining the ink at the paper surface, but have a high tendency to set-off because the ink vehicle does not absorb rapidly (5).

Gloss is the degree to which the surface simulates a perfect mirror in its capacity to reflect incident light (4). Specular reflection refers to the portion of incident light that is reflected from the surface of an object with an angle of reflection equal to the angle of incidence. According to the Fresnel theory, the specular reflection of light off an optically smooth surface is a function of the index of refraction of the object, wavelength of the incident light, and angle of the incident light. For rough surfaces, Chinmayanadam showed gloss to be a function of the same parameters, as well as the surface roughness:

$$\%\text{Gloss} = I/I_o = f(n,i)\ \exp[-(4\pi\sigma\cos(i/\lambda)]^2$$

I and I_o are the specularly reflected and incident light intensities. f(n,i) is the Fresnel coefficient of specular reflection as a function of refractive index, n, and angle of incident light, i. σ is the standard deviation of the surface roughness, and λ is the wavelength of incident light.

According to TAPPI standards, gloss is defined as the 75° spectral reflectance of light at λ=0.55μ. Based on this definition, coating gloss is optimized by increasing the refractivity of the coating layer and minimizing the roughness of the coated surface layer.

Previous studies by Do Ik Lee (4) have shown that the gloss of paper coatings is mainly affected by the following factors:

1) The effect of the particle size and shape

Coating gloss decreases with increasing particle size.

2) The effect of particle size distribution

Since small particles increase the packing efficiency of particles by filling the void spaces, coating gloss can be improved by increasing the fraction of small size particles.

3) The effect of colloidal stability

The flocculation or destabilization of suspended particles leads to a porous sediment or coating. It has been noted that the gloss values of certain coatings

reach a maximum at the point of optimum deflocculation. Ammonium sulfate and calcium chloride are examples of some deflocculating agents.

4) The effect of binder level

It can be seen that coating gloss decreases with increasing binder level. These results are consistent with the idea that film shrinkage roughens the coating surface, and increasing the binder level increases surface roughness.

5) The effect of drying conditions

Although there is no significant influence of drying conditions on the gloss of low temperature film forming polymer coatings, the gloss of high temperature film forming polymer coatings is strongly dependent upon the drying conditions. It can be seen that the gloss of high temperature film forming polymer coatings decreases with an increase in drying temperature.

6) Effect of binder composition:

Binder composition also has an influence on the gloss of the coating in certain cases. For example, the ratio of styrene to butadiene in styrene-butadiene latex binders has an influence on gloss. It has been noted that increasing the level of styrene increases the hardness of the binder and reduces the amount of shrinkage that occurs during drying. Unfortunately, increasing the hardness of the binder also reduces its strength properties.

Recent research by Lee (5) and Ramakrishan (6) showed that fumed metallic oxide pigments are capable of producing semi-gloss and high-gloss inkjet papers with acceptable print quality after calendering. Both researchers found the gloss of fumed alumina pigments to be higher than fumed silica. An important finding of Ramakrishan's studies was that the gloss of the inkjet papers increased with an increase in silica particle size. Smaller particle silicas were shown to produce coatings that contained severe coating cracks. Ramakrishan concluded that the presence of these coating cracks increased the microroughness of the papers, consequently reducing the gloss of the silica coatings. Coating cracks were not observed in the scanning electron microscopy images of alumina-coated papers at the same magnification. These results correlate with previous findings by Do Ik Lee (4), which showed that shrinkage during drying is the cause of surface roughening and loss of coating gloss. Do Ik Lee attributed the roughening of the coated surface to the shrinkage of the binder and removal of coating waters upon drying. In his work, Do Ik Lee showed that the %shrinkage is related to the amount of free water in the coating remaining to be removed during drying by the following equation:

The Extent of Film Shrinkage = $(V_{immobilized} - V_{dried}) / V_{immobilized} \times 100(\%)$

$V_{immobilized}$ = Pore volume present in the coating at the point of coating immobilization (60-74% depending on the binder system, starch or latex, respectively).

V_{dried} = Cumulative pore volume present in the dried coating layer as measured by mercury porsimetry.

The findings by Do Ik Lee supports the free volume theory of Vrentas and Duda (7) which has emerged as a convenient and accurate method for predicting drying diffusivities rates from limited experimental data (8). Mass transfer coefficients and heat transfer coefficients are related by the Chilton-Colburn analogy (9).

In paper coating operations, beyond the take-away zone of the coater (10 and 11) comes the solidification zone, or zones. Solidification may begin by consolidation, for example by filtration as liquid is pressed or absorbed into the substrate; or by physical gelation, for example coalescence of latex binders. Most often the solidification proceeds by drying, chemical reaction (curing), colloidal change, phase change, or combination of these.

The basic function of solidification can be accomplished in a variety of ways as depicted in Figure 1. The elemental processes are water removal from the outer surfaces of the coating; water movement to the surfaces from within the coating; energy delivery to supply the latent heat of evaporation of water, to initiate or drive enhance the removal of water by raising is diffusivity or partial pressure; colloidal transformations, phase separations, fusion (coalescence) and binding; and polymerization and other chemical reactions of curing if crosslinkers are present. Not all these elemental processes need to be present: at one extreme, solidification is a simple matter of water diffusion to and removal from the surface of the coating; at another extreme, the coating is polymerized in place or reaction cured, so that no

vaporation or drying whatsoever is involved. The elemental processes of solidification may all result in stresses that are produced by shrinkage, capillary pressure, and syneresis (composition-stress coupling). The stresses may be exacerbated when these phenomena occur non-uniformly or are incompatible with adherence to the substrate. Proper control and understanding of stress development and relaxation mechanisms makes it possible to produce coatings without stress-related defects.

Solidification is generally accompanied by stress development, because departure of water from the coating, consolidation of particulates, colloidal flocculation and coagulation almost always tend to produce shrinkage. But stresses that are thereby induced also tend to diminish by various mechanisms. Consequently, the state of stress in a coating at any stage of solidification is the outcome of the competition between stress development and stress relief and relaxation. If stress grows large enough it can produce a variety of defects, among them curling, crazing, cracking, peeling (delamination), and microstructural alterations Carincross (12).

Unlike coatings formulated with standard pigments for conventional printing, ink jet coatings use high surface area, nano sized, pigments. This causes extreme stresses to develop during drying that are further exacerbated by the low application solids of the coating. As menisci recede into pores during drying, capillary pressures and surface tension forces at the menisci cause stresses to develop. These stresses tend to be non-uniform because pores vary in size and the drying rate may vary locally. If the stresses are large enough and non-uniform they can cause

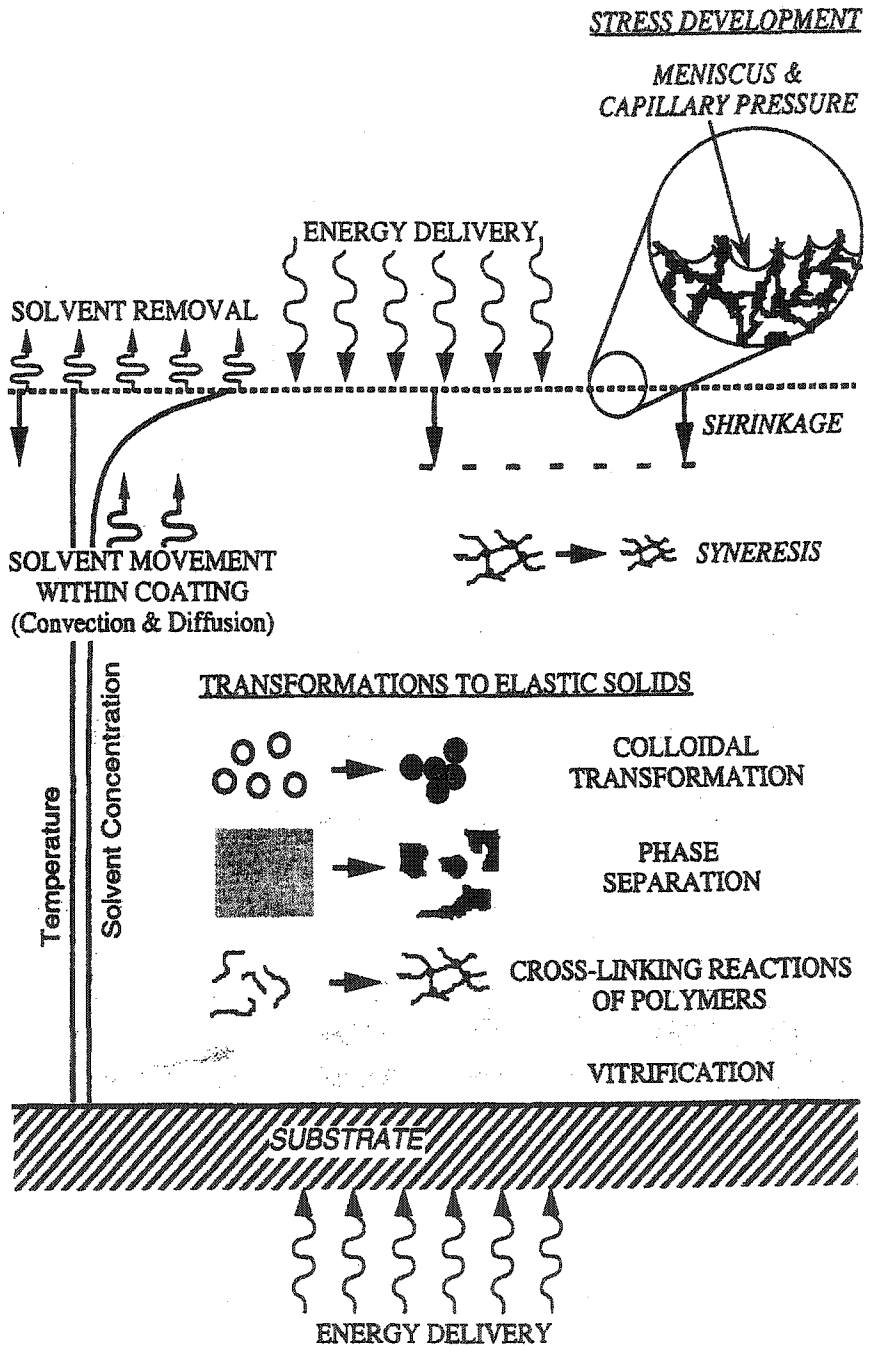

Figure 1. Elemental processes of solidification and stress development in coatings (adapted from Caincross1994)

microcracking to occur. However, they can also be extremely important to the consolidation and compaction of the coating layer, which may or may not be desired in order to obtain the proper ink liquid update for good print quality. The stronger they are, the more they may promote the sintering, fusion, or coalescence of the pigment and binder into a continuous coating (13). Film-formation is required for pigment adhesion to the paper substrate.

Based on this understanding, studies are required to better understand the factors influencing the shrinkage and cracking of glossy ink jet coatings containing nano particle metallic oxides. Studies are needed to minimize the shrinkage, hence roughening of the coating surface, to optimize gloss while maintaining print quality.

In this work, nano metallic oxide containing composite pigments were formulated with well characterized pigments. The packing structures of the wet and dry coating layers were examined to determine if the application solids could be increased to immobilize the coating layer more quickly. To minimize the %shrinkage, coating solids greater than 55% solids were targeted. Since the immobilization solids point is defined as the point at which the free drainage of coating water to the basesheet ceases, raising the application solids will reduce the amount of free water lost to the basesheet upon its application and metering. As a result, the amount of basesheet roughening due to fiber swelling and shrinkage during drying should be diminished, reducing the amount or size of the microcracks, enabling higher gloss to be obtained.

CHAPTER II

LITERATURE REVIEW

Paper plays an important role in determining image quality in inkjet printing. For high print quality, halftone dots should have minimal dot gain and sharp, circular edges, the receiving surface must have a fine, high-porosity structure and be hydrophilic. Paper structure and surface chemistry requirements for good inkjet print quality are so unconventional that new paper grades for inkjet printing should be specially designed (1).

M.G. McFadden and D.W. Donigian stated that non-impact inkjet printing needs are very different from the requirement of conventional coating pigment. One reason is that desktop inkjet printer inks are dye solutions or carbon black dispersions in aqueous media. Thus, there is no resin and a distinct ink layer is not formed. The primary requirement is that the pigments in the coating layer traps and holds the colorant on its surface. The primary pigment component of most matte coated inkjet paper is silica; precipitated, fumed, or gelled. The accepted rationale for the use of silica is that it is porous and hydrophilic, so it is able to trap the large volumes of water based ink applied. Precipitated calcium carbonate inkjet coating pigments, on the other hand, specifically bind the dyes used to produce color (7).

In inkjet printing systems, images are produced on the recording surface by an electrically controlled flow of high velocity, tiny fluid ink droplets or tiny solid ink

stream. The ink drops are controlled by digital signals to produce images on the ink-jet paper surface. Paper for inkjet printing is coated with fine silica and water-soluble binder. These coated papers exhibit excellent color reproducibility due to an improved color deposition, since the absorbed ink dyes are retained in the coating layer (8).

Generally, the interactions of ink and coatings in inkjet printing are complex because many parameters are present. The most basic objective to achieve with water- based inks is to render printouts that are as waterfast and lightfast as possible. These are the key functions for color graphics with outdoor applications. Niemöller et al. first used silica because they absorb ink very fast into the inner void volume of the coating layer by a viscous flow mechanism and are re-fixed by the binders to render the coating waterfast (9).

Silica

M.C. Withiam stated that commercial inkjet applications rely on synthetic silica pigments to deliver the proper combination of physical and chemical properties. The optimum combination of properties will deliver a print with good dot quality and excellent color production (10). He reported the processes of commercial silica production; fumed, gelled and precipitated silica as follows:

Fumed silica

$$SiCl_4 + 2H_2 + O_2 + 3.76N_2 \xrightarrow[1000\ ^\circ C]{} SiO_2 + 4HCL + 3.76N_2$$

Fumed silica pigments have little or no internal microporosity. It is produced by the flame hydrolysis of silicon tetrachloride. The result is an aerosol of small primary particles typically 7-40 nm in diameter, which again are non-porous. These particles stick together by hydrogen bonds forming aggregates and the aggregates form into micro-sized agglomerates. These clusters are solid and non-porous. The fumed silica is a very fine particle size product with high levels of microporosity. Particle sizes in the range of 10- 30μm are typical. Figure 2. shows the structure of fumed silica.

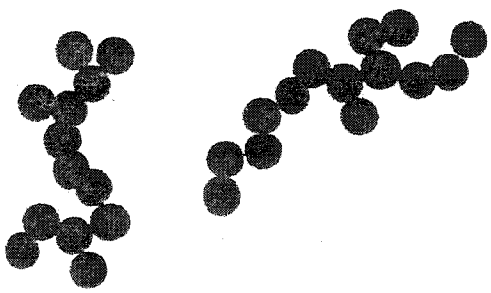

Figure 2. Illustration of fumed silica agglomerate particle chains (11)

Gelled silica

The silica gel process forms a cage-like structure that is up to 75% water. The way in which the product is dried determines the type of gel. Particle shape is considered to be irregular. The silica gel process is like that of a large piece of Jello gelatin being broken into smaller pieces. The particles will not take on any specific

shape. The macro pore volumes are low, at 60 to 75 cc/100g. However, surface area is very large, typically between 200-700 m^2 / g.

Silica gel pigments tend to be very porous materials. The pore structure is controlled by the washing and drying conditions employed. The cage-like particles are full of water. As this water is removed the particles tend to collapse due to surface tension forces. Figure 3 shows the structure of silica gels.

Generally, silica gel products have a high degree of fine mesoporosity or microporosity as is evidenced by their high specific surface areas. The pores that are present are tightly distributed. The surface of these water-borne particles is occupied with hydroxyl groups and layers of hydrated water.

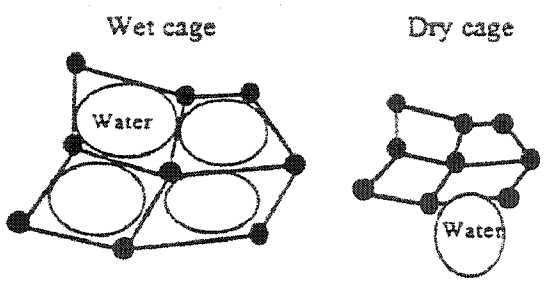

Figure 3. Illustration of gel particle shrinkage upon drying (11)

Precipitated silica

Particle size of precipitated silica is typically between 1-12 μm. There is also a broad range of macro pore volumes that are attainable. Oil absorption is between 70-300 cc/ 100g. Surface areas tend to be less than gelled silica with 60-250 m^2 /g B.E.T.

Precipitated silica is prepared by mixing sodium silicate and mineral acids. The reaction system is typically sheared during the silicate polymerization process. As a result of the pH and temperature of the reaction system, which favor silicate dissolution and re-precipitation, the primary, non-porous particles grow in size from 5 to 100 nm. As a result of the shear forces applied during the reaction, the developing network between these particles is continually broken down, and the primary particles are again only weakly bonded together as in the case of fumed silica. Conceptually, fumed and precipitate silica agglomerates resemble a cluster of grapes rather than the sponge structure of silica gels.

Figure 4 shows the structure of precipitated silica. Figure 5 shows the silanol groups reacting with the molecules of water.

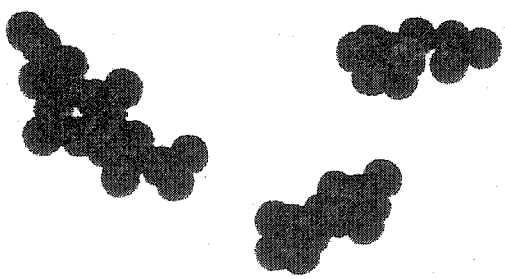

Figure 4. Fumed silica particle chain agglomerates (11)

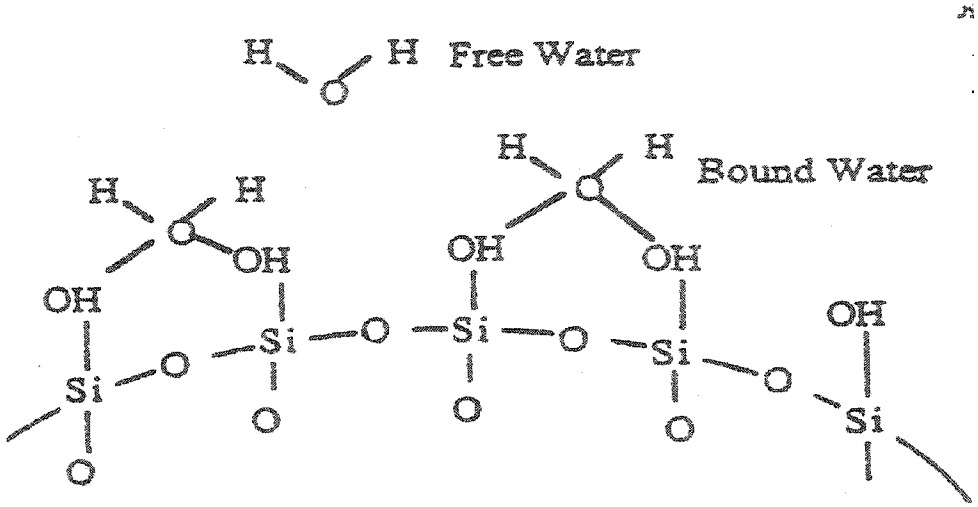

Figure 5. Association of synthetic silica surface with water

According to D.M. Chapman, silica gels derive their name from the hydrogel phase that the material passes through during synthesis (11). The gels are prepared by acidification of concentrated sodium silicate with mineral acids. Molecular-sized silicate oligomers with a nominal diameter of 2.5 nm are present in the starting solution, and these "micelles" can be regarded as the fundamental, non-porous building blocks for the hydrogel network. Because of the high porosity that remains after the hydrogel is dried, these silicas can be conceptualized as a having sponge-like structure. Typical commercial silica gels have porosities that range from 0.4 cm^3 /g to 2.0 cm^3 /g. In addition to the three amorphous synthetic silicas discussed, there is a fourth type of crystalline silica, colloidal silica, which will now be discussed.

Colloidal silica

Colloidal silica is a stable dispersion of non-porous particles in water. These particles, which are termed primary particles because they are composed of dense-phase silica, can range in size from roughly 10 nm to over 100 nm. Porosity in coatings comprised of colloidal silica arises from the packing of the particles. Thus, surface area is a direct measure of the external surface of the spherical particles.

Polyvinyl alcohol (PVOH)

Polyvinyl alcohol (PVOH) is a water soluble, synthetic film-forming polymer that exhibits excellent adhesion to cellulose. Films of PVOH are extremely tough and flexible as well as clear and colorless (12). The hydrophilic nature of PVOH makes it highly resistant to non-polar solvents, oils, and greases. The chemical structure of PVOH is often shown as hydroxyl bearing vinyl units (Figure 6). Its true structure is more complex and involves other structural variables (Figure 7). The most important variables are the number of residual vinyl acetate units. They may vary from 0.1 to 20 mole percent and significantly affect the end-use properties such as water solubility and specific adhesion. The molecular weight of the PVOH grade influences factors such as viscosity (runnability) and strength.

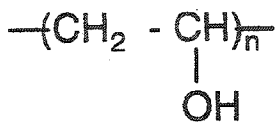

Figure 6. Simplified chemical structure of PVOH (12)

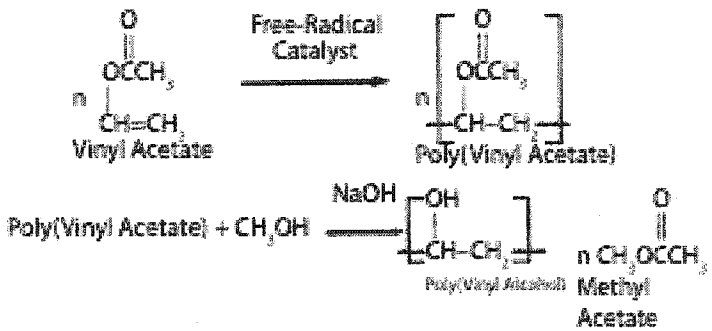

Figure 7. Actual chemical structure of PVOH (12)

More than any other factors, degree of hydrolysis determines the chemical and performance properties of PVOH, and differentiates the end-use applications for which it is used in various grades. Commercial grades range from a low of about 72 mole percent hydrolysis (28 percent acetate groups) to a high of 99.6+ percent (or less than 0.4 percent acetate). The most commonly used grades start at 88 percent, called "partially hydrolyzed", and proceeds to the 95-96 percent grades, called "intermediate hydrolyzed", the 98-99 percent grades, called "fully hydrolyzed", and the 99.3+ percent grades, called " super hydrolyzed". Hydrolysis in effect results from the change in the hydroxyl/acetate balance. The hydroxyl group imparts hydrophilicity

and hydrogen bonding effects (Figure 8); the acetate group imparts hydrophobicity and bulky steric effects (Figure 9).

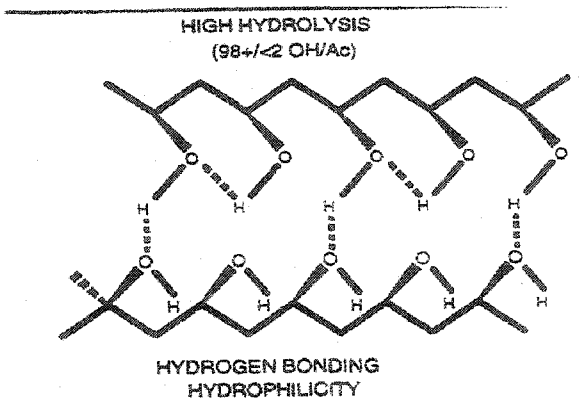

Figure 8. Molecular effects of high hydrolysis PVOH (12)

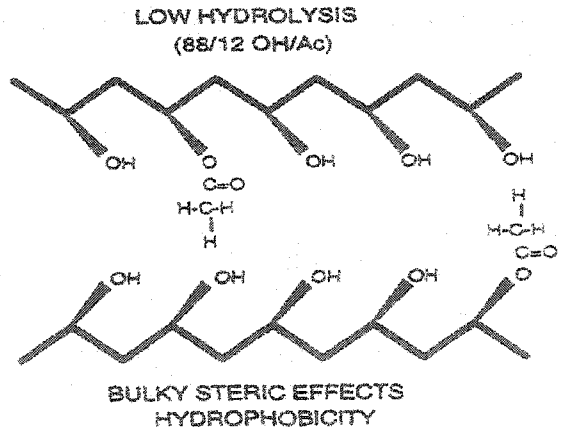

Figure 9. Molecular effects of low hydrolysis PVOH (12)

Maximum water solubility occurs within the 86-94 percent hydrolysis range. Within this range, the polymer is sufficiently hydrophilic for water solubility, and contains a sufficient number of bulky acetate groups (12%) to prevent molecular

association and crystallization through hydrogen bonding. As the acetate content decreases, as with higher hydrolysis grades, molecular association makes them more difficult to solvate. Consequently, fully and super hydrolyzed grades, having even greater hydrophilicity, are much more water resistant both in terms of being more difficult to dissolve and rewet. Films of partially hydrolyzed (88%) grades, for example, dissolve within 30 seconds of immersion in room temperature water; whereas films of super (99.3 %+) hydrolyzed grades do not dissolve at all. Other properties, listed in Table. 1, are significantly affected by hydrolysis levels. Because the higher hydrolysis grades form hydrogen bonds better, they exhibit greater film cohesive strength, and greater adhesion to cellulosic substrates. Add to this the fact that they foam much less than the lower hydrolysis grades and it is easy to understand why the fully and super hydrolyzed grades are more commonly used in paper coatings than the lower hydrolysis grades.

PVOH producers specify molecular weight as a function of solution viscosity at 4 % solids and describe their various viscosity grades as "high", "medium", "intermediate", and "low". From Table 2, these viscosities may range from 2 to 70 centipoises, as measured by Brookfield viscometry. These viscosities correspond to degrees of polymerization, or number of repeating vinyl alcohol units, ranging from about 300 to 2500, and to number average molecular weights, ranging from roughly 25,000 to in excess of 90,000. Molecular weight primarily affects polymer strength and solution viscosity, both increasing with molecular weight.

Table 1. The effect of hydrolysis on properties

High hydrolysis (98+%)	Low Hydrolysis (88%)
* High hydrogen bonding	* Reduced hydrogen bonding
* High film strength	* Surfactant-like properties
* High adhesion to cellulose	* Adhesion to hydrophobes
* Films cold water insoluble	* Films cold water soluble
* Non-foaming	* Latex compatible
* Non-lumping	* Greater tendency to foam and lump

PVOH is commonly used in inkjet coating formulations due to the high surface area of the silica pigments used. The high surfaces area of these materials results in a pigment binder demand that is much higher than typical clays or other conventional pigments used in typical coating or pigmented size press formulations. PVOH finds utility due to its tremendous binding power and hydrophilic properties. The strength of PVOH allows for greater pigment loading levels in comparison to other binders leading to enhanced inkjet printability without dusting. The hydrophilic surface enables the quick absorption of ink into the silica coating layer.

Table 2. Typical molecular weights of polyvinyl alcohol

Viscosity description	Viscosity, mPa•s	Degree of polymerization	Number average molecular weight
High	45-70	2400-2500	95,000
Medium	25-35	1700-1800	65,000
Intermediate	12-16	900-1000	43,000
Low	2-7	300-700	28,000

John R. Boylan reported that PVOH provides excellent binding strength and improved inkjet print quality verse typical latex binders used in other pigmented coating applications. Formulations of PVOH and silica do, however, create a very viscous coating at relatively low solids. The viscosity that is developed is dependent upon the desired coating solids, the pigment-to-binder ratio and grade of PVOH used (10).

Coating formulations utilizing typical latex binders produce inkjet printed images that are mottled, low in ink density, and have poor ink bleed control. These undesirable results may be due in part to the surfactants used to stabilize the latex particles. These surfactants may interfere with the wetting properties of the inkjet inks. PVOH is hydrophilic and can quickly absorb water-based ink, helping to prevent wicking and bleeding. In particular, partially hydrolyzed grades of PVOH provide the best inkjet printability in terms of ink optical density and dry time when

used with silica pigments. This is due to the more open coating structure provided by the partially hydrolyzed grades. Due to hydrogen bonding between the PVOH hydroxyl groups and the silanol groups on the silica pigment, the final viscosity of PVOH/silica coating increases sharply with small increases in solids. This phenomenon maximizes solids at 25-30%, depending on the grade of PVOH, the pigment-to-binder ratio, and the type of silica pigment used in the formulation.

Partially hydrolyzed low/medium molecular weight grades allow for the highest level of coating solids. Therefore partially hydrolyzed (87-89%), ultra low/medium molecular weight grades are recommended for coating applications.

PVOH possesses a non-ionic charge and is compatible with most coating additives, including all types of cationic additives and surface sizing agents.

Coating formulations

Baryta coating

Higher quality applications, especially for continuous-tone reproduction, have used coated paper from the very early days of photography (14). Paper coated with barium sulfate as reflective pigments were first mentioned in 1866. These coatings consisted of barium sulfate as the reflective pigment in a gelatin binder and various additives such as hardeners, surfactants, and plasticizers. Calendering or embossing these coatings produced glossy or textured surfaces. These, combined with a wide range of tints and basis weights, provided a whole spectrum of photographic base

papers for a host of conceivable end uses. For about one hundred years, baryta coated papers were the principal support material for photographic reflection prints, gradually improving in quality from a physical and chemical standpoint, to meet the increasing requirements of more sensitive photographic emulsions.

Colored inkjet imaging

For superior color fidelity, image intensity, color resolution, and proper drying characteristics, the baryta formulation used for a photographic emulsion coating must be modified for inkjet printing. These modifications control the depth, breadth, and uniformity of ink penetration. The superior paper for inkjet imaging allows the ink dots deposited on the coated surface to be rapidly absorbed into the coating layer while controlling the spread of the ink dot applied on the surface to provide optimum image quality. The superior paper using the modified baryta coating formulation shows improved optical density, excellent ink receptivity, and is able to regulate the spreading of ink dots.

Michael J. Cousin et.al. stated that some lateral spreading of the ink dot may be desirable in order to obtain good solid coverage, but the lateral spread for a particular paper must be matched to the resolution of the printer and the amount of ink ejected per drop in order to obtain the desired print quality. The base paper's density, good formation, high surface planarity, and water holdout ability enhance the subsequent coating application and its contribution to physical and optical requirements of a superior inkjet printing paper. The control of coating weight on the

paper web in both the web-direction and cross-direction is critical. Coat weight controlled within ± 1.0 g/m^2 of the desired coat weight target must be achieved. This precision is critical for the control of lateral spread of the inkjet dots, dot resolution, and optical density. They suggested a few physical and optical tests to quantify print quality; optical density measurements, show through, edge acuity (feathering), and spread.

Optical density measurement

The intensity of the inked area can be measured using any densitometer. However, care must be taken to avoid including any uninked areas while measuring the test specimen. The high reflectance of the uninked surface will greatly distort any measurement of optical density.

Show through

Show through is a measure of the depth of penetration for ink colorants through a printed sheet of paper. It is affected by the opacity of the paper. Show through can be defined by any one of a number of optical measurements of the back-side of the inked area of the sheet.

Edge acuity (feathering)

Feathering can be defined as the non-uniform spread of ink on paper. Furnishing, filler, sizing, and coating affect feathering. Consequently, it is a measuring of the uniformity of the composition of the substrate. The tendency to

feather can be measured from dots obtained using a designated printer or independently from the printer using the system's ink. An image analyzer is used to measure the perimeter and area of the dots. The dot area is measured and used to determine the circumference of a circle of equal area.

Spread

The degree to which a single ink droplet spreads over the substrate has an important influence on the ultimate print quality. Drop volume, drop velocity, ink surface tension, ink viscosity, temperature and ink-paper contact angle significantly affect dot sizes. The size of the dot, in turn, affects resolution, line width, intensity of tones, bleeding, and offsetting.

Waterfastness

Images created using water-based inks may not be stable in conditions of high humidity and moisture. In particular the water-soluble dyes have a tendency to smudge and run if rewetted. A test has been developed to quantify waterfastness. The optical density of the image is determined prior to placing the sample into a pan of deionized water. The specimen is removed after it has been allowed to soak for 1 minute. After drying, the optical density of the immersed test sheet is determined using a densitometer. Waterfastness is the loss in optical density resulting from the immersion.

According to the research of Lori Shaw-Klein, waterfastness by soaking was evaluated by immersing the printed samples in room temperature deionized water for

5 minutes. Retained optical density was recorded. Values of retained optical density of 100% were indicative of dye immobilization; values below 100% indicated that the dye was dissolved out of the receiver, and values over 100% indicated that while the dye is confined in the layer, bleed occurs (15).

K. Khoultchaev and T. Graczyk mentioned that the charge density on the chain of the macromolecule or on the surface of the colloidal particles has an influence on the formation of soluble and insoluble associates in the coating formulation (16). Any classic inkjet formulation described in the patent literature consists of a silica type pigment, resin binder and dye mordant. The dye mordant is usually a specific additive to the formulation facilitating the fixation of the dyes in the coating layer. The ink receiving layer may contain one or more water-soluble and water-dispersible polymers. A suitable example of such a water-soluble binder for an inkjet coating formulation is polyvinyl alcohol. The water absorptivity is dependent upon its structure, the hydrophilicity of the functional groups and molecular weight. Furthermore, water itself hydrates various binders and influences the interaction of polymer binders with both water and various liquids.

Polymer interactions

K. Khoultchaev and T. Graczyk divided the interactions between components of the coating mixture into ionic and nonionic interactions. Ionic interactions involve oppositely charged polymers and pigment particles. Negative charges are due to the

presence of acid groups in the resin structure. Positive charges in most cases relate to the presence of groups of quaternized nitrogen. Reaction between oppositely charged ingredients would result in the formation of complexes and complex associates. The equilibrium of this reaction can be affected by several factors like pH and ionic strength of the surrounding media. In some cases the complex formation could be followed by precipitation of insoluble polymer-polymer associates. Depending on certain individual properties of blended ingredients (charge density, molecular weight) and mixing conditions (concentration, pH, and ionic strength) complex formation might not cause the solid-liquid phase separation of the system. In the pigment- polymer interactions, when the number of colloidal particles is small, polymer-colloid complexes coexist with free polymer chains. A further increase in the content of colloidal particles in the system results in the formation of the complex having the composition of the mixture. The constructive diagram of state for a polymer-colloidal particle system is showed in Figure 10. At some polymer/colloid ratio, the system breaks into two different phases and the precipitate coexists with the stable complex. The curve of the Figure 10 represents the relative turbidity of the system. It is reported that the formation of a precipitate increases the optical density of the mixture. The nonionic interaction between the two polymers occurs mostly due to hydrogen bonding, which is strongly dependent on pH.

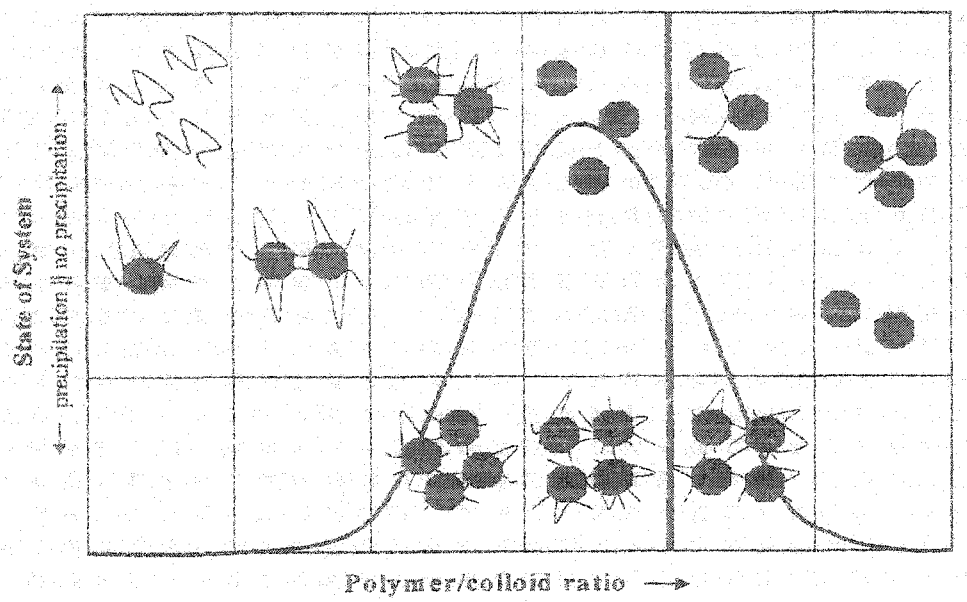

Figure 10. State of polymer-colloid system at different component ratios (16)

Inkjet media

Ink jet papers can be classified into four major categories as shown in Table 1. Depending on the grade, the coating formulation, and application process (air knife, pre-metering size press, rod, or blade), cost can vary substantially.

Glossy inkjet papers are by far the best papers to use when photo realistic images are desired, better even than electrophotographic (laser) papers. They best replicate silver halide photographs. They are currently made by one of three processes. One uses a double or triple coat process. Another coats a dense layer composed of a hydrophilic resin onto a plastic film or laminated paper (see Figure 11). This is called a resin-coated paper.

Table 3. The classification of the media

• Plain or surface-sized paper	Lowest cost, good monochrome text, poor color (limited coverage, poor gamut, high bleed, strike-through, cockle/curl)
• Coated matte paper	High cost, good color gamut, fast dry time, excellent resolution, 100% coverage
• Coated glossy paper	Higher cost, non-porous, slow dry time, poor waterfastness, slow dry, photo realistic image
• Cast coated paper	Highest cost, highest gloss, photo realistic image, multiple coating layers, good waterfastness

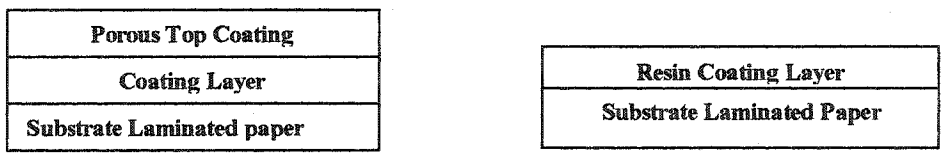

(a) (b)

Figure 11. (a) Cross section multicoated paper, and (b) film-substrate glossy based paper

The third process uses a cast coater to apply a special coating that produces a porous coating layer on a pre-coated paper substrate. The process for making cast coated papers is shown in Figure 12. The coagulation-method (cast) is specifically suitable for production of glossy inkjet papers due to the replication of the chrome cylinder. It is a highly specialized coater, limited in speed.

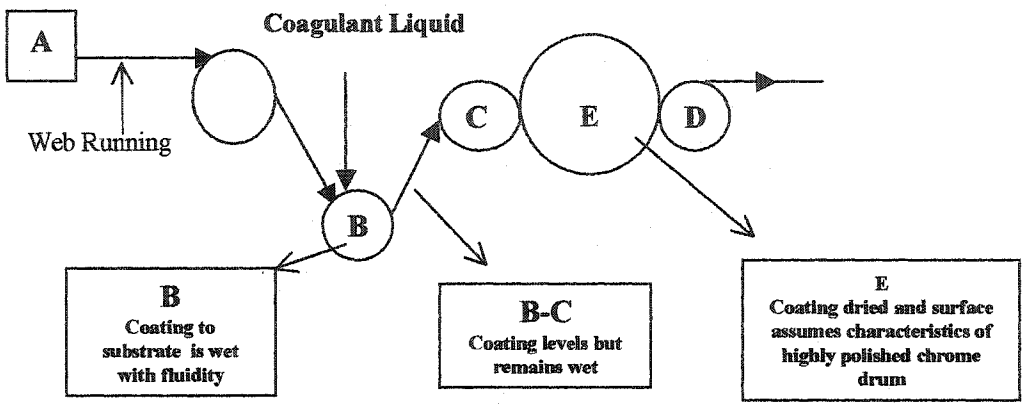

A: Coating Operation Part, B: Coagulant Roll, C: Forming Roll, D: Strip Off Roll,
E: Heated Metal Drum with Specular Surface called "Cast Drum"

Figure 12. Schematic of the cast-coating process

The quality of the inkjet recorded image by the multicolor inkjet process is comparable to that of the image produced by the conventional multicolor printing process and the printing cost is lower than that needed in the conventional printing plate process when the number of copies is not large (18). For these reasons, attempts are being made to apply the inkjet recording techniques to the field of multicolor printing and the printing of color photographs.

In the inkjet recording process, the surface type of a recording sheet is one of the major factors affecting image quality. If used in the inkjet recording, plain and baryta paper all have poor ink absorptivity, arising from the ink remaining unabsorbed for a certain period of time. One problem, smudging, occurs when unabsorbed ink touches some part of the recording equipment or an operator of the equipment or when the successively delivered recorded sheets come into brushing contact with each other. Another problem arises in the case of recording densely

arranged images or when performing multicolor recording. In these instances, where crowded ink droplets remain unabsorbed, larger droplets of mixed color bleed together. The requirement for inkjet recording sheet include formation of an image of high density and bright color (sharp tone); rapid absorption of the ink to prevent the ink droplet from spreading out and from smudging upon contact with some object immediately after recording; and prevention of the ink dot from lateral or horizontal diffusion in the surface layer of the sheet to obtain an image of desirable resolution without feathering.

For the purpose of producing an inkjet recording sheet having a high rate of ink absorption so as to make the ink apparently dry immediately after the application, applying a uppermost layer of pigment particles of a suitable size to utilize the capillary effect of the interparticle voids or to provide a porous layer of similar pore size or pore radius to absorb the ink is needed. It was also found that in order to maintain a high image resolution and a high ink absorptivity, it is necessary to provide an ink receptive layer having an extremely large cumulative void volume by using a pigment having primary particles of very small size.

For double layer coatings, the intermediate layer (second layer) should have a rate of ink absorption larger than that of the uppermost layer. This will allow the ink to permeate deep into the interior of the sheet without lateral or horizontal diffusion, thus rendering the sheet competent as an inkjet recording sheet. However, for double layer coatings, there is limitation to the improvement in the resolution of the recorded image that can be obtained. The uppermost layer behaves as a rate-determining step

for ink absorption. As a consequence, ink is set-up in the secondary layer. Therefore, it is difficult for the sheet to acquire a high rate of ink absorption comparable to that achieved with a single layer coating.

Most high-quality matte inkjet sheets are coated with a system containing binder (typically polyvinyl alcohol, PVOH) (11). Micronized amorphous (typically gelled silica) and other additives (e.g., cationic polymers). Print performance depends in a complex way on many factors, such as the printer, substrate, coating properties and coating application method. With regard to the coating, almost all variables affect print quality. For example, for PVOH binder, the degree of hydrolysis and molecular weight affect print performance. Within a particular coating formulation, however, the silica properties, such as porosity, surface chemistry, and particle size and size distribution play the primary roles on determining inkjet printing properties.

Inkjet printing on a variety of substrates has become a very popular method for output of digital color images, primarily because of the low cost of the printers and the high quality of output that can be achieved. With regard to narrow-format substrates for home and office use, there are three types of coatings that are encountered commercially. Surface-sized papers can be used for monochrome or low quality color output; coated matte media containing synthetic amorphous silicas offer excellent overall performance; and glossy, coated media are capable of producing very high-quality color images.

A typical coating formulation for silica-based matte sheets includes binder (e.g. PVOH), silica, and additives (e.g. cationic polymer). Micronized amorphous silicas are the main functional ingredients and silica properties such as porosity (pore volume, surface area and pore size distribution). Overall print quality depends on many factors that include the printer (hardware, software and ink), the substrate (type, weight, porosity, internal and surface sizing), coating formulation variables (binder type, silica type, additive type, etc.) and coating application and finishing method (calendering, etc.). In the study of dot roundness, the group of fumed silica formulation showed that an increased pore diameter in the coating layer improved roundness. The group of gelled silica pigments showed lower roundness values.

The air content of the coating has an important effect on coating optical properties, since it creates scattering centers and hence controls coating opacity and transparency. The refractive index of silica is 1.46-1.48, while the refractive index of PVOH is 1.49-1.53, and the refractive index of air is 1.00. If the coating contained no air, that is, the silica is present in an amount below the critical pigment volume concentration, the coating would be nearly transparent since the difference in the silica and binder refractive indexes is small. By contrast, for typical matte coatings, if the silica is present in an amount well above the critical pigment volume concentration, so that the coating contains air/silica and air/binder interfaces that effectively scatter light, the opacity of the coating becomes a function of the silica/binder ratio.

The total capacity of the coating for liquid uptake is a sum of the void fraction between the silica particles and the void fraction within the silica particles that results from their porosity. In real sheets, there likely is leakage of the fluid into the substrate, and hence the substrate properties also influence print appearance. Nonetheless, it is of interest to determine the relative contributions to the overall capacity for liquid uptake from the silica pores and the inter-particle voids.

Droplet absorption

Liquid flow through pores is important for inkjet media performance, since it affects, among other things, the dry time of the sheet. For example, the Hewlett Packard 550C printer places droplets of ink that are roughly 150 pL in volume, and these droplets give rise to a resulting dot that is nominally 100 μm in diameter on a coating that is nominally 25 μm thick. The free volume of this cylindrical area, given a void fraction of 0.6, is 118 pL. It is thus clear that the coating pores must transport ink liquid away from the surface and distribute it throughout the coating and base sheet in order to immobilize the dye or pigment quickly. Failure to immobilize the colorant quickly can lead to smearing of the image and loss of image quality.

Capillary flow through a cylinder is usually described by balancing capillary forces, which drive the flow with the viscous drag of the liquid, and is given by the Lucas-Washburn equation (Eq. 1). In this equation, the liquid surface tension, viscosity, contact angle, and pore radius are parameters, so that liquid flow depends

on both the nature of the ink fluid as well as the pore size and chemical nature of the porous surface. The flow is faster for flow between the silica particles and the binder particles (2μm), and uptake into the silica particles (20 nm) is relatively slower. However, the driving force (capillary pressure) is much greater than in the smaller pores. It is thus evident that the interparticle pore network in silica is responsible for bulk fluid flow, while the porous network in the silica is responsible for the driving force and provides the ultimate sink for the liquid. Other raw material properties such as the silica particle-size distribution, binder nature, silica/binder ratio, additives and the ink fluid all affect the flow of liquid in the coating.

$$H^2 = \sqrt{Rg(\cos\theta)t/2h} \qquad \text{(Eq. 1)}$$

Where

H = the height of rise of the liquid in the capillaries

R = the radius of the capillary

g = the surface tension of the liquid

θ = contact angle between the liquid and the substrate

t = time

h = the viscosity of the liquid

According to Oliver, the capillary absorption of inkjet ink is crucial in the inkjet process as the image is formed directly on the paper surface with low viscosity inks (19). He described the capillary absorption using the Lucas-Washburn equation.

The equation is a quite simple equation that is often used in its integrated form (where gravitation is neglected).

P. Wägberg and L. Wägberg mentioned that even though Eq. 1 is often used when trying to describe capillary absorption, it has some fundamental limitations (20). First of all the contact angle is assumed to be a single value, whereas in reality on rough and porous surfaces it is quite variable and dependant on time. Secondly, it is based on an infinite reservoir of fluid, which is very seldom the case. The model does not take into account that there is often an irreversible swelling of fibrous structures upon liquid absorption, especially with polar liquids. Equation 1 obviously states that capillary absorption is dependent not only on the porous structure of the substrate but also on the characteristics of the liquid used (surface tension, contact angle and viscosity).

Droplet spreading

The tendency of a liquid to spread on a smooth surface with an equilibrium amount of absorbed liquid vapor is defined by the contact angle, θ, and this is determined by the solid-liquid, solid-vapor and liquid-vapor surface energies (tensions) according Young's equation (Eq. 2). The solid-liquid surface tension is further divided into three components, for hydrophobic, which are useful for specifying the nature of the chemical interaction between the solid and liquid. Thus, a predominant determinant of the contact angle or degree of droplet spreading in the

chemical interaction between the droplet and surface, and this in turn is influenced by the silica/binder ratio, the chemical nature of the binder, the chemical nature of the ink fluids, and the effect of added surfactants. Porosity affects contact angle. However, the porous surface serves to reduce the volume of the droplet on the surface, which will also affect the overall radial coverage if the liquid absorption rate is comparable to the spreading rate.

$$\gamma_{SG} = \gamma_{SL} + \gamma_{LG}\cos\theta \qquad \text{(Eq.2)}$$

Where

γ_{SG} = Surface tension between solid and gas (vapor) phase

γ_{SL} = Surface tension between solid and liquid phase

γ_{LG} = Surface tension between liquid and gas (vapor) phase

θ = Contact angle

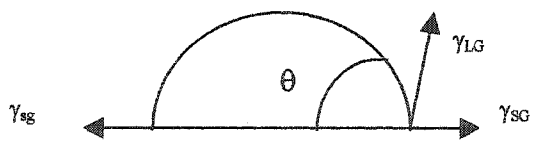

Figure 13. Surface forces involved in wetting

Inkjet printing process

It is desirable that ink spreading be kept at the minimum needed for setting of the ink. The paper should have high enough void volume to allow sufficient ink

uptake and a high enough permeability to allow rapid uptake for quicker setting. Papers coated with conventional clays or calcium carbonate have insufficient void fraction to prevent drop splatter or excessive spreading before ink uptake. Control of the coat weight and void volume is critical for proper drop resolution and density. Their effect on drop spreading, drying time, and image intensity are important. The larger void volume of a coating minimizes spreading. As the number of drops per inch increases, the need for spreading decreases, and high void volume papers are needed for good resolution.

A high color density for the print is one of the most critical requirements of quality ink-jet reproduction. This property is obviously not only related to the ink formulation but also to the concentration of dye left at the surface of the paper after the ink has dried. A coating that promotes the segregation of the dye molecules in its upper layer will contribute to a print with bright, vivid colors.

When an inkjet recording paper contains a dyeing component and the amount of jetted ink is small, as in the case of monochromatic inkjet recording, the water resistance properties of the paper may be satisfactory if the dye or dyes themselves have good water resistance properties. However, for multicolor inkjet printing, the amount of jetted inks is relatively large, and papers having sufficient water resistance properties cannot be obtained even when a dye with good water resistance is used. When inkjet printed papers are used for outdoor advertisements, they are required to have particularly good water resistance. But unfortunately, multicolor inkjet printed

products formed by the combination of conventional inkjet papers and inks have been utterly unsuitable for such use (21).

In the case of multicolor inkjet recording, it frequently happens that inks are ejected from two or more nozzles of an inkjet printer causing two or more ink dots to overlap at various points on the recording paper. When this occurs, if the prior ink drop is not quickly absorbed into the inside of the recording paper, the ink drop is mixed with the subsequent ink drop ejected and if rubbed in handling, the ink drops remaining on the surface without being absorbed can stain the recording paper. Therefore, papers having particularly excellent ink absorbing properties are required for successful multicolor inkjet recording. However, a paper having good ink absorbing properties generally is not only needed but controlled spreading properties for good dot resolution is also desirable for good color reproducibility.

Thus, for obtaining color images having good color density, resolving power, and color reproducibility by multicolor inkjet recording, such properties, which are contrary to each other. Spreading of the coloring components in the ink drops in the longitudinal direction of a recording paper needs to be minimized, permeation of the coloring components into the paper should needs to be minimized, yet the recording paper must have good ink absorption properties.

Morea-Swift, G. and Helen Jones reported that the various printing techniques of inkjet printers use of inks that are low in solids and predominantly based on polar (water/alcohol) dispersions (22). Consequently, the coated media must be able to:

Assist the drying of the ink before the ink drop penetrates deeply into the paper. Fix the dye chemically and maintain it physically at the surface of the paper. They also reported that increasing the porosity of the coating in the micro pore region allows for the rapid adsorption of the ink's solvent (water) by the substrate for quick drying. Generally, high porosity synthetic silicas are used for this purpose. In the research of Morea-Swift, G. and Helen Jones, an improvement in print quality was observed with increased pore volume regardless of the type of silica used (gelled or precipitated). This observation was most likely related to the rate at which the ink dries as a result of the total pore volume available in the coating.

Color density increased with increasing particle size in the study. They concluded that the observation must be a result of differences in distributions of pore size. If the distribution of pore size is wide, optical density decreases. And they stated that the probability of the ink to "sink" i.e. penetrate downwards into the paper before the drying of ink, increased with increasing pore size. It was also mentioned that the greater the number of pores around the 0.1-1 μm size, the larger the probability for the ink to "sink" below the surface before it dries with a consequent loss in color density.

If a large number of mesopores and micropores are present, the color density increases because the large surface area available and the size exclusion effect on the dye molecules that are segregated at the paper surface facilitate the drying of the ink at the surface of the paper. This explains the high color densities observed with low pore volume, small pore size silicas.

Typical home inkjet printing is unique among important paper printing processes in the amount and mobility of the applied inks. Offset, gravure, flexo, and newsprint inks are applied in layer about 1μm-5μm in thickness for each color. In contrast, inkjet ink layers may be 15 μm or more in thickness for each color. Offset, gravure, and flexo inks have binders to hold the colorants in position. Most aqueous inkjet ink do not contain a binder. Binder containing inks increase markedly in viscosity when small amounts of solvents are removed; inkjet inks remain mobile even when most of their solvent volume is removed (23).

Most inkjet color inks are dilute solutions of one or more acid dyes. The solvents account for up to 98% of the ink weight and are blends of water and various organic materials, typically high boiling alcohols. For good printed appearance, the dyes should be fixed on the paper's outer surface with only enough lateral spreading from the position of drop impact to merge adjacent drops in solids colors. In fact, proper dye fixation is the key to several components of inkjet print quality including high optical density or intensity of the color, high resolution or sharpness of the ink boundaries, low image print through to the back side of the paper, and high resistance of the image to smearing when wetted.

Uncoated paper is treated with sizing agents to balance lateral ink spreading and Z-direction penetration. Higher quality can be obtained with pigmented coatings. These provide the well known benefits of finer pore structure and surface smoothness but require the dyes to adhere to non-cellulosic coating ingredients: pigments, coating binders, and functional additives.

For inkjet coatings, silica pigments are most commonly applied. A few grades of silica including precipitated, fumed, and gelled have found application. Recently, pigments based on clay and precipitated calcium carbonate (PCC) have been offered. One of the major differences between the specialty PCCs, clays, and silicas being offered these grades, is the mechanism by which they trap and adhere the ink at the surface.

Silica coatings work by providing pore volume to trap the entire ink volume and provide surface area on which the dye can deposit and adhere as the solvent evaporates. Higher silica pore volumes, even with lower surface area, causes faster inkjet ink setting (11). Specialty PCCs and clays hold only the dye and allow the fluid phase to pass through. Silica provides space to hold large volume of ink solvent. Specialty PCCs and clays provide fine pores with high surface to volume ratios so that the dye molecules have a high probability of making contact with the pigment surface in a short time. In this practice, a relatively low coat weight is needed since only the dye remains in the coating layer. Another difference between pigment types is that silica has a higher relative affinity for the solvent components of the dyes whereas PCC has a higher relative affinity for the dye components in the ink.

There are a number of factors to consider when a colorant interacts with a substrate (24). The colorants consist of hydrated anionic dyes and this hydration sphere must dissociate from the colorant to interact effectively with the substrate. For the dye to be attracted to the substrate the dye-substrate combination must have a lower energy than the combination of the hydrated dye and the hydrated substrate.

Other important factors include: (i) the print head which influences the ink concentration (drop volume) and the frequency of drop formation and (ii) the ink.

The interaction between colorant and media are reviewed in order of decreasing strength of interaction below.

Covalent bonding

This is the strongest interaction that can occur and results from a chemical reaction between the colorant and the substrate. The electrophilic reactive group on the dye reacts with a nucleophilic group (a primary hydroxyl group on the cotton) producing an irreversible chemical reaction. This produces a print with excellent fastness properties.

Electrostatic or ionic interactions (coulombic attraction)

Anionic dyes contain water solubilizing groups such as, SO_3, COO^-, PO_3^{2-} and these are attracted by cationic groups on the media e.g. Ti^{4+}, Al^{3+}, Ca^{2+} producing a strong interaction, effectively immobilizing the dye molecules, giving excellent image quality.

π:π interactions

These are important in dye-dye interactions and can lead to dye aggregation or crystallization. These are relatively strong interactions and may occur for media

containing aromatic groups capable of interaction with the colorants. Chromophores such as the phthalocyanines aggregate undergo such interactions.

Hydrogen bonding

This is a fairly weak interaction, but for cellulosic substrates this is often the most important interaction between colorant and media. For a large dye molecule, there may be a large number of sites for hydrogen bonding to increase the binding strength of media and colorants. In addition, the hydroxyl groups of the cellulose will interact with the π–cloud of an aromatic group on a colorant.

Hydrophobic interactions

This attraction occurs for solvent soluble dye systems that contain hydrophobic groups such as alkyl chains. These interact with similar hydrophobic groups on the substrate and this is quite favorable particularly when the colorant is applied from an aqueous phase. The interaction consists of a combination of hydrogen bonding and Van der Waals interactions.

Dipole-dipole interactions

These are relatively weak and result from the induced polarity in the interacting groups.

Van der Waals forces

These tend to be quite weak at long range but become stronger when the interacting groups are brought close together. A weak repulsion occurs between cellulosic substrates and anionic dyes when they are far apart. However, as the water soluble dyes are absorbed then the interaction between colorant and media becomes quite strong. This is observed for most of the dyes and is also important in preparing aqueous dispersions of insoluble colorants.

Interaction with plain paper

All of these modes of interaction are present in textile inkjet application. However, for plain papers hydrogen bonding and Van der Waals bonding are the key interactions, whereas for coated papers and film, ionic or coulombic forces are also important. Plain and modified papers consist of mainly cellulose and this is what the colorant interacts with when printed onto the paper surface. For these papers, the furnish as well as the internal and surface sizing play an important role in determining the print properties. For these papers, the capillary absorption of the aqueous inks influences how rapidly the ink diffuses into the substrate.

It is possible to design coated media to maximize the binding energy derived from the non-covalent interactions.

Interaction of the colorant with coated media

There has been considerable growth in the development of coated media particularly for color inkjet printing. This is a consequence of the increased demands placed on color printing particularly in the photorealistic and wide-format application areas and the choice of the media is key to achieving optimum performance. The coating formulations are a complex mixture of binders (polymers), pigments, fixing agents (cationic reagents), optical brighteners etc. The selection of the components of both the coating and ink formulation has a significant influence on the image quality, fastness properties, and the rate of ink absorption. The coating layer must also retain its original surface characteristics such as gloss and avoid distortion or cracking of the coating.

Coated media can contain inorganic oxides such as alumina, silica, talc, clay, titanium dioxide, calcium carbonate etc and also polymers such as polyvinyl-pyrrolidone (PVP), polyvinyl alcohol (PVA), gelatin, carboxymethylcellulose and polyvinyl acetate. The nature of the coating largely determines the image properties of the print. The interaction of the ink with plain paper, coated paper and photo paper is contrasted in Figure 14. For plain paper the ink is absorbed by the cellulose and spreads out in all directions both on and beneath the paper surface.

For anionic dyes the color-media interactions are relatively weak and are mainly due to hydrogen bonding and Van der Waals interactions. Coated papers however, interact much more effectively with dyes fixing the colorant in the vicinity

of where it was printed. The increased interaction is largely due to the presence of electrostatic interactions between the anionic dyes and the inorganic oxide. This interaction greatly increases the binding energies for the dyes and leads to high strength, high chroma prints with no color-to-color bleed, excellent dot definition and perfect waterfastness in most cases.

Inkjet inks

The distinguishing characteristic of inkjet inks compared with other conventional printing inks is that inkjet inks are fluid. This is especially true for the continuous stream inkjet method where rapid drop formation requires viscosity near 1 mPas. In thermal jetting, viscosity is commonly less than 5 mPas, 10 mPas is the upper limit. Table 4. gives a summary of the main components of inkjet inks.

The use of pigments instead of soluble dyes as the source of color in inkjet inks is increasing due to their better lightfastness properties. Low levels of viscosity and freedom from nozzle clogging, however, can be more easily reached with soluble dyes. Dye concentration is considerably below 10%. Low viscosity and desired drying properties are the main criteria in selecting solvents for the inks.

Water is preferred, especially in home and office environments. Rapid charging of the drop requires a high electrical conductivity. This is the reason for the charge generation additives.

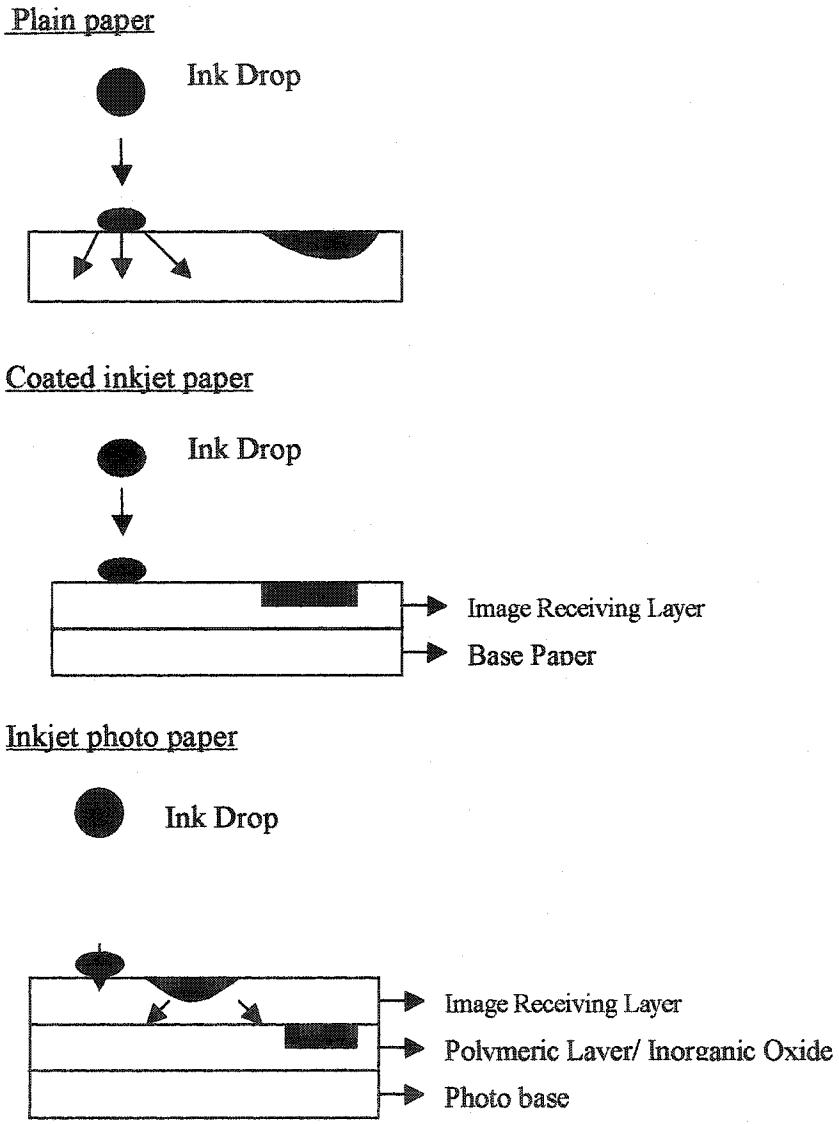

Figure 14. Ink absorption by plain and coated media

Table 4. Composition of inkjet inks

Component	Purpose
Dye or pigment	Coloring Material
Binder	Binding the pigment on the paper (not always used)
Liquid phase	Carrier phase for the dye or pigment and binder
Continuous jet: water + alcohol and DOD jet: water + glycol	Allows the desired low viscosity of the ink and prevents ink from drying in the nozzle
Charge generation additives (continuous jet)	Enhances the electrical charging capability of the ink
Preservatives	Prevents bacterial decomposition

Influence of the ink

The ink properties have a considerable influence on performance. A penetrating ink can be absorbed by a plain paper within milliseconds with most of the aqueous ink vehicle being absorbed by the cellulose. If the internal sizing is low, or the paper is unable to cope with the volume of ink, then strike-through can occur.

Non-penetrating inks are absorbed more slowly, taking 10-30 seconds to be absorbed into the paper. This produces high optical density prints with no strike-

through. Future printers will require rapidly penetrating inks to give fast dry times and faster print speeds. This will almost certainly require the media to be able to cope more effectively with the absorption of the ink vehicle.

Drying time

Drying time is one of the major characteristics of inkjet media. There is no concern for cast coated and matte coated papers because the water absorption power of the base itself significantly reduces the dry time. For photo glossy inkjet paper, drying time is dependent on coating chemistry (16).

If the ink- receiving layer has a polymer with high water absorption capacity like polyvinyl alcohol, the print images will dry fast. The ability to absorb water depends on the hydrophilicity of the functional groups of these polymers. Water molecules from the ink would be readily accommodated if those functional groups were available to them. The water absorbing capacity of the same polymer would be dramatically reduced if the functional groups were engaged in bonding with other functional groups. Subsequently, coating consisting of resins capable of forming too many bonds with each other would have long dry time characteristics in comparison with the coating where polymers do not react.

S. Yuan et. al. divided inkjet drying mechanisms into absorbing drying and evaporative drying (26). Absorptive drying was broken down into two components: capillary drying and molecular diffusion. In media with porous structures, like simple

sized papers, the absorptive drying process primarily involves capillary movement of the ink droplets from the media surface. In most coated inkjet media, the absorptive drying mechanism involves molecular diffusion of ink vehicle into the bulk media through ink-medium interactions.

Mercury porsimetry method

This method, introduced by Ritter and Drake in 1945, uses intrusion capillary pressure curves to calculate the pore size distribution and the void volume, and the model of Lucas-Washburn to calculate pore diameters. The complete pore size distribution spectrum is obtained by applying pressure to fill the pores with non-wetting mercury (27). The pores (capillaries) are filled when the applied pressure is equal or greater than the capillary pressure. Thus, at low applied pressures the largest capillaries are first penetrated and filled by the mercury. The smaller pores require higher pressures. The pore diameter penetrated at a given pressure, P, is obtained with the following equation,

$$D = -(1/P)\, 4\gamma_{Hg}\cos\theta \qquad \text{Eq.3}$$

where P is the applied pressure, γ_{Hg} the surface tension of mercury, and θ is the contact angle of mercury on the pores. The accepted value of γ_{Hg} for mercury is between 480 and 485mPa·s, although it is known that it varies with purity. The contact angle θ varies with the materials investigated. For paper, values between 130 and 140 degrees are usually used.

The volume of mercury penetrating the pores is measured directly as a function of the applied pressure, *P,* which can be converted to a plot of cumulative intrusion volume versus the pore diameter D calculated with the equation. With this information the mean pore diameter of the samples can be calculated. The peak shape is a measure of the pore size distribution and its area represents the total pore volume. The void fraction, ε^{Hg}, is then calculated using Eq 3.

The usual practice of applying a simple model of straight capillaries to represent the porous system is one of the criticisms of this method. It is well known that porous materials have complex porous structures in the form of three-dimensional networks of irregular geometries, sizes and topographies. Another major criticism of mercury porsimetry for determining pore size distribution is that it does not give the true internal pore dimensions. This has been inferred from comparisons of mercury porsimetry data with data obtained from microscopic examination of sample cross sections. Mercury porsimetry gave narrower distributions with maxima at lower pore diameters than optical measurements. The reason is that the large pores with narrow entry pores (necks) will not be filled with mercury until the applied pressure is high enough to overcome the capillary pressure of the entry pore. As a result these large pores will be assigned a much smaller diameter than the actual one. This is known as the "ink-bottle" effect. Therefore, the pore diameters obtained with this method should be considered as "apparent" and not "absolute" pore diameters.

CHAPTER III

STATEMENT OF THE PROBLEM AND OBJECTIVES

Although coatings formulated with fumed metallic oxide pigments have proven to be capable of producing glossy inkjet media, their high cost and the inability to run them at high solids (>30% solids) limits their commercial application.

Previous research showed the presence of coating cracks to increase the microroughness of papers, consequently reducing the gloss of silica coatings. Coating cracks were not observed in scanning electron microscopy images of alumina coated papers at the same level of magnification. Studies are, therefore, needed to minimize the roughening of the silica coatings to optimize their gloss properties. Additional studies are also needed to determine if composite pigments can be formulated which would enable the solids of silica based coating formulations can be increased to reduce the difference between application solids and coating immobilizations solids to minimize the roughening of the basesheet and shrinkage of the coating layer. Coating solids at or near 55% solids should be targeted since the immobilization solids of most coatings containing soluble binders occur around the 55-60% solids level. Since the immobilization solids point is defined as the point at which the free drainage of coating water to the basesheet ceases, raising the application solids will reduce the amount of free water lost to the basesheet upon its application and metering.

This research also seeks to determine if less expensive conventional pigments can be blended with the aluminas and silicas to form a composite pigment with equal or better glossing properties.

The objectives of this research were:

(A) To study the influence of fumed metallic oxide and conventional pigments on the optical properties of coated paper,

(B) To compare the print quality among fumed metallic oxide and conventional pigments coated papers and commercial coated inkjet papers,

(C) To study the influence of protein on the optical properties and printing qualities of fumed silicas and conventional pigmented coatings

(D) To quantify gloss related to the ratio of pigments, and

(E) To study the influence composite pigment structures on microcracking and pore structure using SEM (scanning electron microscopy), dynamic contact angle measurements, and mercury porsimetry.

CHAPTER IV

EXPERIMENTAL DESIGN

The experimental program is divided into four phases: (1) drawdown (2) analysis of the selected fumed silica coating papers prepared using a cylindrical laboratory coater (CLC) (3) analysis of select fumed alumina coated papers prepared using a cylindrical laboratory coater (CLC). Figure 15. shows a flow chart of the experimental design.

Phase I

- Drawdowns were made to test coating properties with fumed metallic pigments and conventional pigments ratios (100: 0, 90:10, 80:20, 70:30, 60:40, 50:50, and 0:100)
- Use conventional pigments of well-defined shape and size.
- Determining optimum ratio of fumed metallic pigments and conventional pigments

Phase II

Analysis of fumed silica and conventional pigments with different ratio using CLC

1. Measure optical properties and printing properties
2. Analyze coating porous structure using contact angle machine, Hg porsimetry.

Phase III

Analysis of fumed alumina and conventional pigments with different ratio using CLC

1. Measure optical properties and printing properties
2. Analyze coating porous structure using contact angle machine, Hg porsimetry.

Figure 15. Flow chart of experimental design

Materials

Selected pigments were obtained from several pigment companies. Fumed silica (FS), aluminum oxide (AO), precipitated calcium carbonates (PCC), ultrafine ground calcium carbonate (UFGCC), alumina trihydrate(ATH), and baumite pigments were applied. The physical properties of the pigments are shown in Table 5 and ratios of each in the applied coatings are shown Table 6.

Table 5. The physical properties of pigments as supplied

Sample	Solids Content	Color	Specific Gravity	pH	Refractive Index	Avg. Particle size (nm)
AO	40%	White	1.40	3.8-4.2	1.76	160
FS	30%	White	1.20	10.0-10.3	1.46	225
PCC	70%	White	2.72	9.0-10.0	1.58-1.63	544
UFGCC	75%	White	1.92	9.0-10.0	1.58	600
Baumite	30%	White	1.1-1.3	4.0-6.0 (5% sol)	1.65-1.66	200
ATH	65%	White	2.42	6.70	1.57	400

The binder used in the coating formulation was a partially hydrolyzed, low viscosity, polyvinyl alcohol (Airvol 203S, Air Products Inc.). This polyvinyl alcohol was chosen to optimize the percent coating solids by minimizing the interaction between pigments and PVOH. Polyvinyl alcohols with a higher degree of hydrolysis

are known to interact more strongly with silica pigments, thus limiting the percent coating solids that can be feasibly prepared. Solutions of polyvinyl alcohol were prepared at 30% solids by adding the required amount of dry PVOH powder to cold alkaline water (pH 9.0-10.0) under agitation and heating the mixture to 185 °F.

Table 6. Ratio of Coatings

Sample	Pigments	Parts	Viscosity* (cP)	pH
Sample A	Fumed silica/UFGCC	70:30	572	9.2
Sample A-1	Fumed silica/UFGCC	50:50	704	8.94
Sample B	Fumed silica/ PCC	70:30	254	9.7
Sample B-1	Fumed silica/PCC	50:50	608	9.05
Sample E	Fumed Silica	100	72	9.8
Sample C	Aluminum Oxide/ATH	70:30	984	5.9
Sample C-1	Aluminum Oxide/ATH	50:50	1370	4.90
Sample D	Aluminum Oxide/Baumite	70:30	1766	6.9
Sample D-1	Aluminum Oxide/Baumite	50:50	1130	4.2
Sample E	Fumed Silica	100	72	9.8

The solution was held at this temperature for 35-40 minutes to assure complete dissolution and hydration of the PVOH. A defoamer was then added (Foam master VF, Henkel, Inc.). The solids content of the solution were measured using a

CEM Labwave 9000 microwave moisture analyzer. The solution was cooled to 40°F before adding the slurried pigment at a slow rate of agitation. The coatings were mixed for 30 minutes, and the pH and viscosity measured. Aluminum oxide coatings were prepared to determine the influence of pH on their coating properties. Coatings were prepared at a pigment-to-binder ratio of (7:1).

The viscosities of the coatings were measured using a Brookfield RVT digital viscometer (#4 spindle @ 100 rpm).

Protein (Procote 4000) was applied as a co-binder by adding the dry protein powder directly to the pigment slurry. This protein was selected for its inability to solvate with heat. The mixture was agitated for 25-30 minutes. Then, PVOH was added to the mixture. Study of the coated papers prepared from these coatings had extremely low gloss, and were difficult to coat so these coatings were not carried forward into the next phase of the study.

Drawdowns

The coatings were applied to the uncoated base paper using several different Meyer rods. The Meyer rods were selected to enable 6-12 g/m^2 coating to be applied. The coatings were made 3 batches per 1 coat weight. The samples were allowed to air dry, until they were dry to the touch. The samples were then cut into 5 inch diameter circles using a press punch. The coat weights of the samples were then determined, taking the difference between the weights of the uncoated and coated samples after

being dried in the CEM Labwave 9000 microwave moisture analyzer. The samples were then conditioned in a humidity-controlled room before performing optical and physical property measurements.

The brightness of the papers was measured using a Technidyne Brightness meter, TAPPI procedure T 452 om-92. Gloss was measured using a Hunter 75° gloss meter according to standard TAPPI procedure T 480 OM-92. The surface smoothness and porosity of the sheets were measured using a Parker Print Surf (PPS) tester (TAPPI T555 pm-94). The rate of liquid absorption of the papers was measured using a First 10 Angstrom Dynamic Contact Angle measuring device.

After reviewing the results of the drawdown studies, pigments were selected for additional CLC studies. CLC studies were performed to obtain larger dimensional samples for print studies and to optimize the surface smoothness of the samples by using a blade applicator and infrared drying under tension.

Cylindrical Laboratory Coater (CLC) Studies

The base papers were blade coated using a Cylindrical Laboratory Coater (CLC) at a speed of 2000 fpm. Coatings were prepared using fumed silicas (A), an aluminum oxide, and conventional pigments. The samples were pre-dried at 25% power for 10 seconds and post-dried at 100 % power for 60 seconds. Four different coat weights were applied: 6 g/m^2, 8 g/m^2, 10g/m^2, and 12 g/m^2.

The samples were printed on an Epson Stylus 900, Hewlett Packard 932C and Canon S450 inkjet printers using a proprietary test print pattern created with ADOBE software. The Epson 900 is a piezo electric printer with a resolution of 1440 x720dpi. The HP 932C is thermal inkjet printer with a resolution of 2400 x 1200 dpi. And the Canon S450 printer is thermal inkjet printer with a resolution of 1440 x 720 dpi. The print gloss and print density of the samples were then measured. Print gloss and delta gloss were measured using a Gardener 60° Micro-Gloss meter. Print density was measured using a BYK Gardner densitometer. Roundness was measured at 30% tone scale by means of a Hitachi HV-10 camera (Hitachi Density, LTD., Japan). Computer software, Image-pro plus, version 3.0, was used for image detail analysis.

The CLC samples were calendered on one side through 3 nips at 123 kN/m and 60°C. The optical, surface, and printing properties were repeated and the results compared to the uncalendered samples.

CHAPTER V

CONCLUSION

The results obtained from the research indicate that the optical properties, brightness and gloss, were affected by pigment type and coat weight. In the case of brightness, as the addition of precipitate calcium carbonate (PCC) and ultra ground calcium carbonate increased, the brightness increased due to their inherent blue shade and high purity. In the case of the fumed alumina group coatings, the addition of alumina trihydrate increased brightness.

Improvements in gloss were due to increase in smoothness and refractive index. In all coatings, the optical properties were influenced by the ratio of fumed metallic oxides and conventional pigments. The correlation between improvements in optical properties and smoothness indicates that the property improvements were due to an increase in surface coverage with coat weight.

Print quality as measured by ink density, and ink gloss were dependent on pigment ratio and type such as the optical properties. The print properties were also influenced by pigment particle size and packing volume. Print qualities as measured by ink density and ink gloss were strongly dependent on pigment particle size and packing volume. Inks used in the printers influenced print quality. From the research, there was not a reduction of printing quality due to the addition of conventional pigments

The porosity of the fumed silica and PCC was more porous, thus the print quality of the coatings was better. Coat weight did not significantly affect ink density. Calendering decreased the pore size of the pigments and improved its smoothness. Ink gloss and ink density consequently increased. From the results, specially, the increase in gloss with fumed silica and PCC demonstrates that the co-pigment system is sufficient to produce a high glossing ink jet coating.

In the respect to economics, the coating cost can be saved by the addition of PCC because it considerably less expensive than fumed silica, it improved the runability of the coater enabling which enables more throughput and the ability to apply these coatings at higher solids reduces the energy costs associated with drying.

From the SEM (scanning electron microscope) pictures, the microcracks of the coatings were reduced by the addition of PCC and UFGCC. It is believed that the high solids and large particles of PCC and UFGCC relieve some of the drying stresses.

From the results of these experiments, it is evident that the composite coatings had optical properties and printing qualities comparable to the 100% fumed metallic oxide coatings. The finding that print quality did not diminish coupled with the economic benefits discovered make them the more desirable product for this application.

REFERENCES

1. Lyne, M.B. and Aspler, J.S., "Paper for inkjet printing," TAPPI, 68(5):106-110 (1985).

2. Mills, R.N., "Inkjet printing - past, present and future." IS&T's tenth international congress on advances in non-impact printing technologies, IS&T, p. 410-414, 1994.

3. Le, H.P., "progress and Trends in ink-jet Printing Technology", Journal of Imaging Science and Technology, 42,1,1998,p.49-62.

4. Cousin, M. J. and Hill, L.O., U.S. Patent 4, 554, 181, Nov. 19, 1985.

5. Lee, D.I., "A fundamental study on coating gloss", 1974 Coating conference proceedings, TAPPI press, p. 183-200, (1974).

6. Lee, Hyunkook., "The influence of fumed metallic oxides on coating structure and their relationships to print quality", Western Michigan University, 1998 MS thesis, submitted.

7. Ramakrishnan, Raja., "Coating and Basesheet Influences on the Development of Gloss for Inkjet Papers Containing Fumed Metallic Oxides." Western Michigan University, 1999 MS thesis, submitted.

8. Vrentas, J.S., and Duda, J.L., " Diffusion in Polymer-Solvent Systems III Construction of Deborah Number Diagrams, Journal of Polymer Science 15,19977,p.441-453.

9. Zielinski, J. M., and Duda, J.L, "Prediction of diffusion Coefficients for Polymer-solvent Systems, AIChE Journal, 38,1992,p. 405-415.

10. Chilton, T. H., and Colburn, A. P., " Mass Transfer (Absorption) Coefficients, Industrial Engineering Chemistry, 26, 1934, p1183.

11. Benjamin, D.F., et al., "Coating Flows: Form and Function, Industrial Coating Research, 1,1991, p. 1-37.

12. Benjamin, D.F., et al., "Coaters Analyzed by Form and Function, Industrial Coatings Research 2, 1992.

13. Cairncross, R.A.,et al., "Competing Drying and Reaction Mechanisms in the Formation of Sol-to-Gel Films, Fibers, and Spheres, Drying Technology Journal, 10, 1992, p. 893-923.

14. Eckersley, S. T., and Rudin, A., " Mechanism of Films Formation from Polymer Latexes, Journal of Coatings Technology, 62,1990, p. 89-100.

15. McFadden, M.G. and Donigan, D.W., " Effects of Coating Structure and Optics on Inkjet Printability", 1999 TAPPI Coating conference, TAPPI press, p. 169-177, (1999).

16. Nakamura, K., "Recent trends in inkjet printing inks and papers", Color Hard Copy and Graphic Arts II, SPIE Vol. 1912,p.91-101 (1993).

17. Niemöller, A. and Becker, A., " Interactions of inks with inkjet coatings", IS&T's NIP 13: 1997 international Conference on Digital Printing technologies, IS&T, p. 430-436, 1997.

18. Withiam, M.C., " Silica pigment porosity effects on color inkjet printability", IS&T's NIP 12: 1996 international Conference on Digital Printing technologies, IS&T, p. 430-436, 1996.

19. Chapman, D.M., " Coating structure effects on inkjet print quality", 1997 Coating conference proceedings, TAPPI press, p. 73-93, (1997).

20. Miller, G.D., Jones, R.B. and Boylan, J.R., " Polyvinyl alcohol-a specialty polymer for paper and paperboard", Air Product & Chemical, Inc, p1-14, (1997).

21. Boylan, J.R., "Using polyvinyl alcohol in inkjet printing paper", TAPPI, v.80, no. 5:p. 68-70 (1985)

22. Cousin, M. J., King, A. F. and Hill, L.O., "Interaction of inkjet inks with photographic type substrates", Journal of Imaging Technology, Vol. 12, no. 1: p. 40-46, Feb. (1986).

23. Shaw-Klein, L., " Effects of mordant type and placement on inkjet receiver performance", IS&T's NIP 14: 1998 international Conference on Digital Printing technologies, IS&T, p. 129-132,1998.

24. Khoultchaev, K. and Graczyk, T., "Polymer-polymer and polymer-pigment interactions-implications on inkjet universal media", 1999 TAAPI Coating conference, TAPPI press, p. 155-168, (1999).

25. Lee, H., Joyce, M. K. Joyce, Fleming, P.D., and Cameron, J.H., "Production of a single coated glossy inkjet paper using conventional coating and calendering methods", 2002 TAPPI Coating Conference, May 2-6, Orlando, Florida.

26. Shigenhiko, M. et. Al., U.S. Patent 4, 460, 637, July 17, 1984.

27. Oliver, J.F. Agbenzuge, L., and Woodcock, K., "Development of a realistic drying model for water based inkjet inks printed on paper", IS&T's 7th International congress on advances in non-impact printing technology., Oct. 1991.

28. Wägberg, P. and Wägberg, L., " Inkjet printing on uncoated fine papers." 1996 International Printing & Graphic Arts Conference, p. 187-197.

29. Sugiyama, M. et. Al., U.S. Patent 4, 371, 582, Feb. 1, 1983.

30. Mores-Swift, G. and Jones, H., "The use of synthetic silicas in coated media for inkjet printing", 2000 TAPPI Coating Conference and Trade Fair, p.317-327.

31. Donigian, D.W., "Inkjet dye fixation and coated pigments", 1998 TAPPI Coating/Papermaking Conference, 1998, p.393-412.

32. Lavery, A. and Provost, John. " Color-media international in inkjet printing", IS&T's NIP 13: 1997 international Conference on Digital Printing technologies, IS&T, 1997, p. 437-441.

33. Oittinen, P. and Saarelma, H., "Electronic Printing", Printing, Chapter 6, TAPPI press, Atlanta, GA, p.186-188.

34. Yuan, S., Sargeant, S., and Rundus, J., " The development of receiving coatings for inkjet imaging applications", IS&T's NIP 13: 1997 international Conference on Digital Printing technologies, IS&T, 1997, p. 413-442.

35. Larrondo, L. and Monasterios, C., " The porous structure of paper coatings-a comparison of mercury porsimetry and stain-imbibition methods of measurement", 1995 TAPPI Coating Conference., 1995, p.79-93.

CHAPTER VI

ARTICLES

INFLUENCE OF PIGMNT PARTICLES ON GLOSS AND PRINTABILITY FOR INKJET PAPER COATINGS

Hyun-Kook Lee, Margaret K. Joyce, and Paul D. Fleming

Department of Paper Engineering, Chemical Engineering and Imaging

Center for Coating Development

Western Michigan University

Kalamazoo, MI 49008

Abstract

Previously, we have shown that coatings formulated with fumed silica pigments are capable of producing glossy inkjet media, despite the presence of these coating cracks, caused by shrinkage of the coating layer. However, their high cost and the inability to run them at high solids (>30% solids) limits their commercial application. Raising the coating solids with the addition of conventional pigments reduces the amount of shrinkage that occurs during drying, and thereby reduces the coating cracks, improving the final gloss of the coating layer.

In this research, the solids of fumed silica coating systems were increased by adding co-pigments of different particle sizes. Fumed silica was used as the main pigment and precipitated calcium carbonate (PCC) and ultra fine ground calcium carbonate (UFGCC) were used as co-pigments. The ratio of fumed silica to co-pigments were 100:0, 90:10, 80:20, 70:30, 60:40, 50:50, 0:100. These blends of pigments were previously shown to produce high gloss and good printability. The coatings were applied using Meyer rods to obtain a coat weight of 10g/ m^2 on one side. The optical brightness, printability, ink density, and ink gloss were compared. Based on the findings, it is concluded that the co-pigment systems had optical properties and printing qualities as good as the mono pigment coatings.

Introduction

Most high-end publication printing and photo finishing employ a glossy paper because the readers associate gloss with high surface smoothness and print quality. Gloss is associated with high surface smoothness[1] and commonly regarded as a smoothness index. However, it does not always correlate with physical smoothness, since it is possible to have a glossy surface that is quite rough. For example, some photo glossy inkjet paper has high gloss although it has rough surface. However, the average observer instinctively tends to downgrade the rougher paper, even though the gloss is the same.

Previous studies by Do Ik Lee[2] have shown that the gloss of a paper coating is mainly affected by the following factors:

- The effect of the particle size and shape.
- The effect of particle size distribution.
- The effect of colloidal stability.
- The effect of binder level.
- The effect of drying conditions.
- Effect of binder composition.

Product development of inkjet printing papers has accelerated greatly to meet the rapidly growing market for inkjet[3-6] printing. Advancements in inkjet printing technology have also placed new demands on the glossy substrate that produces photo quality images[3,5,6]. To meet these requirements, papermakers are turning to pigmented coating systems. In the glossy inkjet coating field, fumed silica is used. The particle size of these glossy pigments is typically in the range of 100-300 nm. This particle size range offers possibilities for glossy inkjet applications.

Research by Lee[7,8] and Ramakrishan[9] showed that fumed metallic oxide pigments are capable of producing semi-gloss and high-gloss inkjet papers with acceptable print quality, after calendering. Both researchers found the gloss of fumed alumina pigments to be higher than fumed silica. An important finding of Ramakrishan's studies was that the gloss of the inkjet papers increased with an increase in silica particle size. Smaller particle silicas were shown to produce coatings that contained severe coating cracks. Ramakrishan concluded that the presence of these coating

cracks increased the microroughness of the papers, consequently reducing the gloss of the silica coatings. Coating cracks were not observed in the scanning electron microscopy images of the alumina-coated papers. These results correlate with previous findings by Do Ik Lee[2], which showed that shrinkage during drying is the cause of surface roughening and loss of coating gloss. Do Ik Lee attributed the roughening of the coated surface to the shrinkage of the binder and removal of coating waters upon drying.

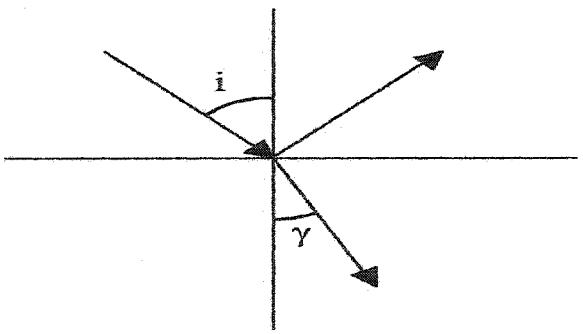

Figure 16. The angle of refraction γ is governed by Snell's law

Basic theory

On plain surfaces like glass, when a beam of light strikes the surface part of the light is reflected from the surface and the remainder is transmitted and scattered[1]. The reflection and refraction that can occur are illustrated in Figure 1. The relationship between the incident and refracted angle is given by Snell's law[1] (Equation 1):

$$\sin i / \sin \gamma = n, \qquad (1)$$

where n is a constant known as the refractive index. Since γ can be changed depending on the material of the plane, the refractive index can be also changed.

Due to the angles i and γ, the intensity of light reflected from surface affecting the surface gloss is fixed by Fresnel's law[1].

$I_{rfl}/I = [\sin^2(i-\gamma)/\sin^2(i+\gamma) + \tan^2(i-\gamma)/\tan^2(i+\gamma)]/2$,(2)

where I is the intensity of the incident beam, I_{rfl} is the intensity of the reflected beam. For normal incidence, the equation may be written in the form:

$$I_{rfl}/I = [(n-1)^2/(n+1)^2]. \qquad (3)$$

If n is approximately 1.5, about 4 % of the incident light is reflected and if n is about 2.4, about 17 % of the incident light is reflected.

For wavy surfaces, Chinmayanadam[10] tried to account theoretically for the reflection from rough surfaces by hypothesizing that the reflecting elements of an optically rough surface are distributed according to the probability law, and he derived the expression:

$$I = e^{-(8\pi^2\cos^2R)/\alpha\lambda^2} \qquad (4)$$

where R is the angle of viewing and α is a constant having dimensions of length^{-2}. For moderate angles of incidence (up to 54°), it shows good agreement with practice. For higher angles, Chinmayanadam falls back on an empirical formula, which has been found to give good agreement with observed values:

$$I = e^{-(\alpha\tan^2R+b\cos^2R/\lambda^2)} + (1-e^{-\alpha\tan^2R})e^{-(c\cos R+d\cos^2R)/\lambda} \quad .(5)$$

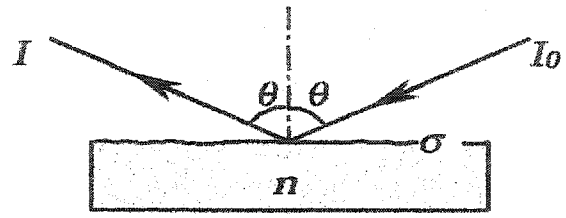

Figure 17. Light path of specular reflectance

Gloss is the degree to which the surface stimulates a perfect mirror in its capacity to reflect incident light. From a study of the different existing gloss instruments and properties that they measure, six types of gloss have been defined[1,11,12]; specular gloss, sheen, contrast gloss, absence-of – bloom, distinctness –of- reflected image gloss, and absence-of-surface texture gloss. In the paper industry, specular gloss (reflection) is sought[11]. Specular reflection refers to the portion of incident light that is reflected from the surface of an object with an angle of reflection equal to the angle of incidence (Figure 2).

From Figure 2, the light path on the surface at certain incident and reflect angle (θ) is seen[13]. Specular gloss is related to the ratio of the incident light intensity (I_0) to reflected light intensity (I), and more exactly defined as the ratio of the luminous flux reflected by the test surface into a specified angle and luminous flux from the standard reflecting surface. Therefore, specular gloss can be formulated as:

$$G_s(\theta) = \rho_v(\theta)/\rho_0(\theta) \times 100, \qquad (6)$$

where $\rho_v(\theta)$ is the Fresnel Equation of the test surface, $\rho_0(\theta)$ is the Fresnel Equation for the standard, and θ is the incident light angle. From the Fresnel theory, the equation of the reflectance of opaque or black glass with a perfectly smoothnesssurfaceisshownby[13,14]:

$$\rho(\theta,\lambda)=\frac{1}{2}\left[\left(\frac{\cos\theta-\sqrt{n(\lambda)^2-\sin^2\theta}}{\cos\theta+\sqrt{n(\lambda)^2-\sin^2\theta}}\right)^2+\left(\frac{n(\lambda)^2\cos\theta-\sqrt{n(\lambda)^2-\sin^2\theta}}{n(\lambda)^2\cos\theta+\sqrt{n(\lambda)^2-\sin^2\theta}}\right)^2\right], \quad (7)$$

where $n(\lambda)$ is the refractive index at wavelength λ.

The equation for rough surfaces like paper is as follows:

$$\%Gloss = I/I_0 = f(n, \theta)\exp[-(4\pi\sigma\cos\theta/\lambda)^2] \quad (8)$$

where I_0 and I are the specularly reflected and incident light intensities,

$f(n, \theta)$ is the Fresnel coefficient of specula reflection as a function of refractive index n and angle of incident light I, σ as the surface roughness (standard deviation of the surface profile), and λ is the wavelength of incident light.

From Equation 8, the paper gloss is determined by the incident angle of light, incident light wavelength, refractive index, and surface roughness of the paper.

According to TAPPI standards[15], gloss is defined as the 75° spectral reflectance of light at λ=0.55 m. Based on this definition, coating gloss is optimized by increasing the refractivity of the coating layer and minimizing the roughness of the coated surface layer.

$$\text{TAPPI } 75°\text{gloss}=384.6f(n,75°)\exp\{-(4\pi\sigma\cos75°/0.55)^2\} \quad (9)$$

From the Equation 9, TAPPI 75° gloss is dependent on the refractive index and surface roughness. Theoretically, sheet gloss should be responsive to the effective index of refraction of a surface. It is the index of refraction that depends on both void volume and the material present in the coating. Increasing the void volume should decrease the index of refraction and thus the gloss.

The ideal surface should catch and reflect the light, when the light source is behind the observer and at a high angle of incidence, but should absorb the light when viewed at a low angle with the light source in front. The proportion of light at the glare angle need not be much greater than light reflection at the glare angle to cause appreciable glare. Gloss can be reduced by coating the paper with highly opaque pigments, provided that the pigment-coated surface is not too highly finished.

Materials

Silica

The ink used for inkjet printing is usually a water-soluble-dye based system. Comparisons between ink jet printing with water-soluble dye and water dispersible pigments are given elsewhere[16,17]. Most inkjet inks consist of 90% water[18]. Therefore, the paper must absorb water quickly to avoid wicking and maintain sharp edge acuity. The highly-absorbent, porous nature of silica pigments make them an excellent pigment for inkjet printing papers. These pigments quickly absorb the vehicle and set the toner, which maintain edge acuity, proper color balance and saturation. The excellent water absorptivity of high-structure silicas minimizes banding caused by the

improper absorptivity of the paper for the ink. High water absorptivity also decreases the drying time for print.

Polyvinyl alcohol

In comparison to latex and natural binders, polyvinyl alcohol (PVOH) is the strongest binder[19,20]. Polyvinyl alcohol is an excellent film former and is resistant to wetting by oils, greases, and organic liquids[19,20]. Since it is a water-soluble synthetic binder, the properties of polyvinyl alcohol can be controlled precisely over a wide range of values. Although water soluble, it can be made water-resistant. It forms clear, colorless, non-blocking, abrasion resistant, yet flexible, films at room temperature. PVOH shows outstanding adhesion to cellulose, and provides high pigment binding strength. It is compatible with other hydrocolloids, natural and synthetic binders, pigments and other commonly used additives in the paper industry. PVOH provides unique enhancement of fluorescent whitening agents[21,22], which are commonly used in inkjet papers. It is used in clear and pigmented paper and paperboard coatings. Paper grades using PVOH include release liners, carbonless, flexible packaging, and high brightness papers.

The quality of the record obtained in an inkjet recording process depends highly on the properties of the ink and the recording paper. The recording sheet must absorb the ink rapidly and at the same time precipitate the ink dye on the sheet surface. From two properties, the ink property reduces the tendency for set-off (i.e. transfer of the ink from the paper to sheet handling rollers and the like) whereas the recording sheet

property insures that images having high optical density are obtained. Unfortunately, there is a problem with these two properties compromising each other. Papers having high absorbency allow the ink to penetrate deeply into the paper, decreasing the printing density of the image at the surface. They also show feathering, poor edge acuity, and show-through. Papers with low absorbency, such as highly sized papers, provide good optical density by retaining the ink at the paper surface, but have set-off problems because the ink vehicle is not absorbed rapidly[23-26].

For high-grade coated paper, to which major attention regarding print gloss is directed, print gloss develops frequently irrespective of sheet gloss. Since the 1960's, it has been stated that print gloss is more normally associated with holdout of ink vehicle on the stock surface, rather than directly with the smoothness of the stock or ink film, because it is the vehicle holdout that contributes to the smoothness of the final print and to print gloss. Leveling of an ink film and menisci development, among ink pigment particles, play an important role in achieving print gloss. In the printing industry, leveling of an ink film is the primary mechanism[24].

In order to study the relationship between gloss and pigments, surface modifications to increase the refractive index of the silica pigments should also be studied, because refractive index can affect the gloss of the coated paper. Additional studies are also needed to determine if composite pigments can be formulated that would enable the coating solids of the formulations to be increased. To minimize shrinkage, coating solids greater than 55% solids should be targeted to reduce the difference between application solids and the coating's immobilization solids point.

Since the immobilization solids point is defined as the point at which the free drainage of coating water to the basesheet ceases, raising the application solids will reduce the amount of free water lost to the basesheet upon its application and metering.

Experimental design

This project is divided into two phases: (1) relative sediment volume (RSV) of coatings studies, (2) drawdown coating studies, characterization of the optical properties, printing properties after calendering. One fumed silica and PCC and UFGCC were used. The physical properties of pigments are shown in Table 7.

Table 7. The physical properties of pigments as supplied.

Sample	Solids Content	Specific Gravity	pH	Refractive Index	Particle size (nm)
FS	30%	1.20	10.0-10.3	1.46	225
PCC	70%	2.72	9.0-10.0	1.58-1.63	544
UFGCC	75%	1.92	9.0-10.0	1.58	600

The ratio of fumed silica + PCC and fumed silica + UFGCC were 100:0, 90:10, 80:20, 70:30, 60:40, 50:50, and 0:100.

The binder used in the coating formulation was a partially hydrolyzed and low viscosity, polyvinyl alcohol (Airvol 203, Air Products Inc.). This polyvinyl alcohol

was chosen to increase the coatings solids by minimizing the interaction between pigments and PVOH. Polyvinyl alcohols with a high degree of hydrolysis are known to interact more strongly with silica pigments, thus limiting the coating solids that can be feasibly prepared. Stable solutions of polyvinyl alcohol were prepared at 30% solids by adding the required amount of dry PVOH powder to cold water under agitation and heating the mixture to 185° F. The solution was held at this temperature for 35-40 minutes to assure complete dissolution and hydration of the PVOH. A defoamer was then added (Foam master VF, Henkel, Inc.). The solids content of the solution was measured using a CEM Labwave 9000 microwave moisture analyzer. The solution was cooled to 40° F before adding the slurried pigments at a slow rate of agitation. The coatings were mixed for 20-30 minutes and the pH and viscosity measured. Coatings were prepared at one pigment-to-binder ratio (7:1). In the previous research, the ratios of pigment to binder were 4:1 and 5:1 but in this research, the binder ratio was reduced because PCC and UFGCC with low binder demand were added.

The viscosities of the coatings were measured using a Brookfield RVT digital viscometer (#5 spindle @ 100 rpm). Twenty-five ml of each coating was centrifuged at 25,000 RPM for one and one half hours to determine its Relative Sediment Volume (RSV) at 30% solids.

Drawdowns

The coatings were applied to the uncoated base paper using several different Meyer rods. The Meyer rods were selected to enable 10g/m^2 of coating to be applied. The samples were allowed to air dry, until they were dry to the touch. The samples were then cut into 5-inch diameter circles using a press punch. The coat weights of the samples were then determined, taking the difference between the weights of the uncoated and coated samples after being dried in a CEM Labwave 9000 microwave moisture analyzer. The samples were then conditioned in a humidity-controlled room, before performing optical and physical property measurements.

The brightness of the papers was measured using a Technidyne Brightness meter, TAPPI procedure T 452 om-92. Gloss was measured using a Hunter 75° gloss meter according to standard TAPPI procedure T 480 OM-92. The surface roughness and permeability of the sheets were measured using a Parker Print Surf (PPS) tester (TAPPI T555 pm-94).

The samples were printed on a Canon S450 inkjet printer using a proprietary test print pattern created with Adobe software. The print gloss and print density of the samples were then measured. Print gloss was measured using a Gardener 60° Micro-Gloss meter. Print density was measured using a BYK Gardner densitometer.

The samples were calendered on one side through 3 nips at 123 kN/m at and 60°C.

Results and discussion

Figure 18 shows that RSV (relative sediment volume) of each coating. From the graph, the RSV of fumed silica and UFGCC coatings decreased as the addition of a UFGCC increased.

The following equation was applied to quantify the RSV:

① =weight of water/density of water

+ weight of pigment/ density of pigment

weight of water/① = % volume of water

100 - % volume of water = % volume of pigment

Volume of pigment = Total volume of coating x

% volume of pigment/100

Then, RSV = separated water from centrifuge

machine/ volume of pigment

Figure 18 shows how RSV was changed by the addition of PCC and UFGCC.

In the case of FS and PCC coatings, RSV volume did not change much until 30% PCC was added. It is believed that the aragonite (needle shape) particles of PCC did not reduce the internal void volume of the fumed silica of grape-cluster shape. Therefore, the coating layer absorptivity of 70% fumed silica and 30% PCC coating maintains the same level of 100% fumed silica coating. After 40% addition of PCC, RSV decreased because the particles of PCC filled the internal void volume of fumed silica. In the case of FS and UFGCC, RSV decreased from the 10% addition of

UFGCC. From the data, the rhombohedral shape of UFGCC more readily reduced the internal void volume of the fumed silica.

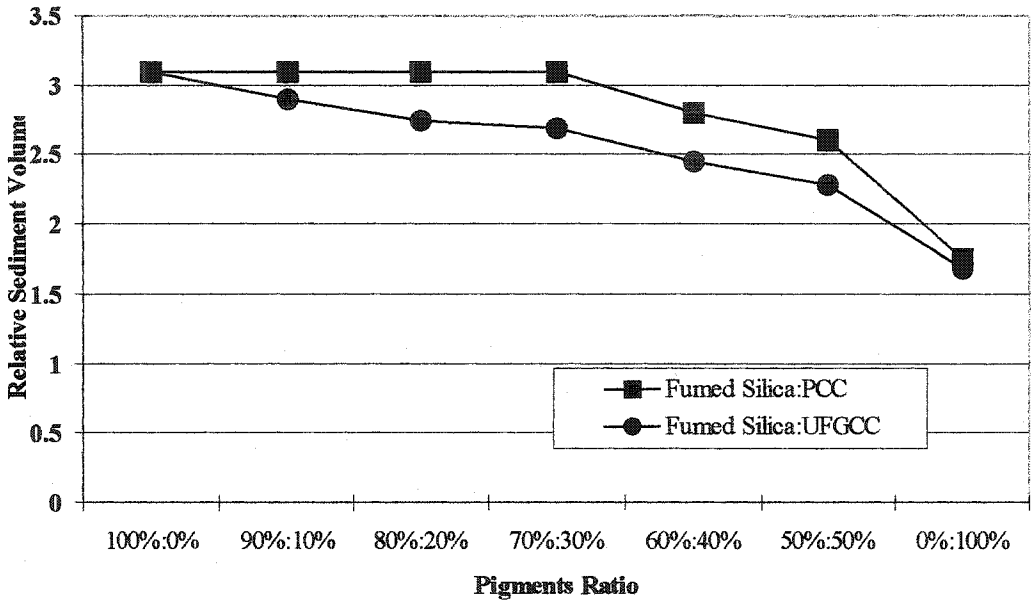

Figure 18. Relative sediment volume comparison of each coatings (Coat weight:10 gsm, Calendered samples, Pigment:Binder =7:1).

Figure 19 shows the relationship of brightness to the addition of UFGCC and PCC. As the addition of PCC and UFGCC increased, the brightness value increased. The brightness value of fumed silica and PCC coating was higher than that of fumed silica and UFGCC. Brightness was influenced by the amount of light scattered and absorbed. Since scattering is influenced by the surface area of the pigments and the number of air-to-pigment interfaces, the fumed silica and PCC coating may have more air voids in the coating structure enabling more light to be scattered.

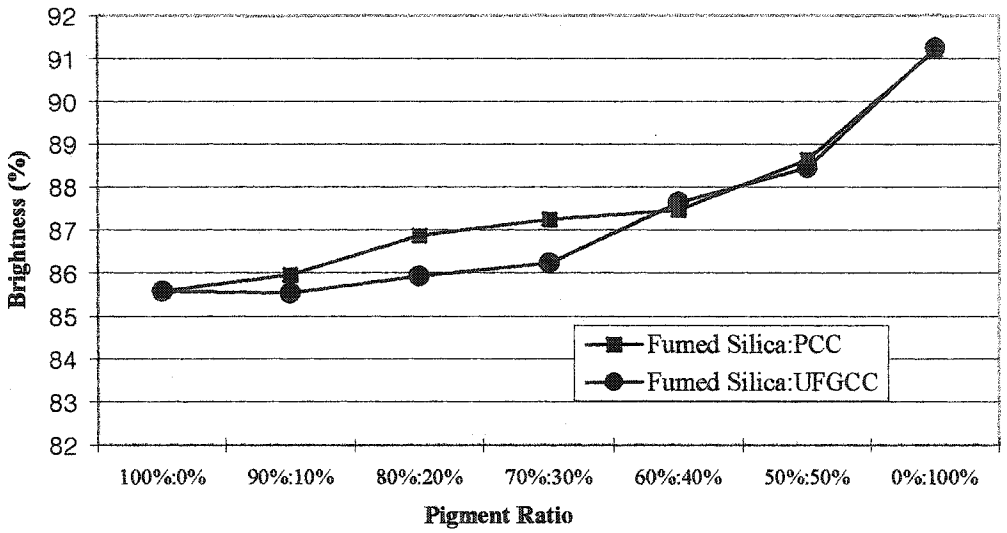

Figure 19. Brightness comparison of PCC and UFGCC coatings (Coat weight:10 gsm, Calendered samples, Pigment:Binder=7:1)

Figures 20 and 21 show the relationship between the glosses and roughness of each coating. From these figures, it is seen that the addition of PCC improved gloss due to the increase of refraction and smoothness, until 30% addition but after 40% addition of PCC, the gloss decreased. The results indicate that although the refractive index of the coating surface increased due to the addition of PCC, the surface roughness, microroughness, increased due to a change in packing order of the fumed silica and PCC. In the coating of fumed silica and UFGCC, the gloss decreased until a 30% addition of UFGCC was added. After this point, the gloss improved.

Figures 22 and 23 show how the permeability of the coating layers affected ink density. The coating layers with a more open pore structure (higher permeability) absorb the ink vehicle more quickly and help to fix ink pigment or dye on the surface. Since inkjet inks have negative charge, it is preferred that the coating layer have a

positive charge to fix the ink dye or pigment to the surface. However, addition of PCC and UFGCC caused the reduction of positive charge of coating layer in this experiment.

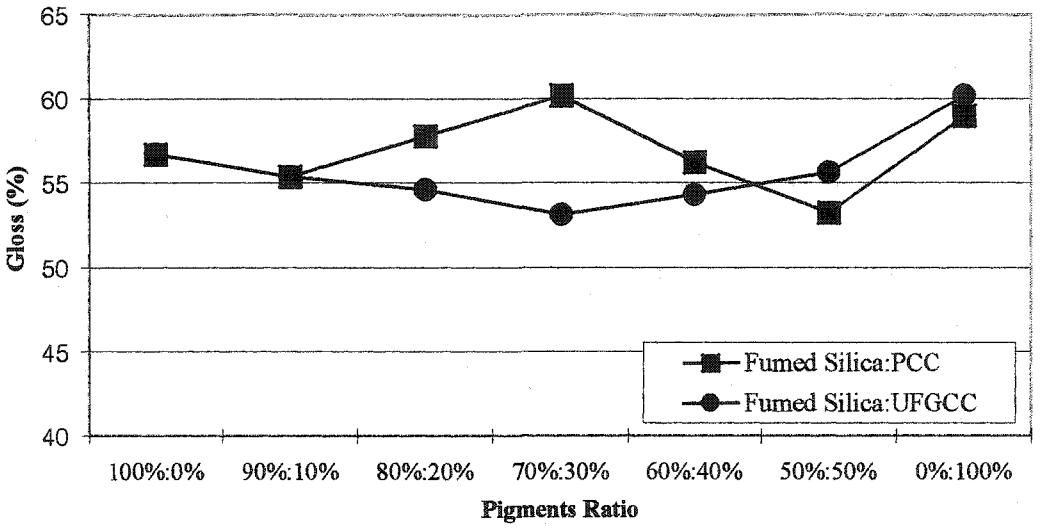

Figure 20. Gloss comparison of PCC and UFGCC coatings
(Coat weight:10 gsm, Calendered samples,Pigment:Binder=7:1)

Figures 24 and 25 show the relationship between ink gloss and paper gloss. Ink gloss decreased with paper gloss. Unlike the offset printing process, whereas the surface area of the substrate increases, ink gloss is reduced by the shrinkage of the ink film. For this printing process, the high surface energy of fumed silica does not cause shrinkage in the ink layer. Even the high surface energy of the coating layer can help ink dye to be fixed due to the fast-absorption of the ink vehicle.

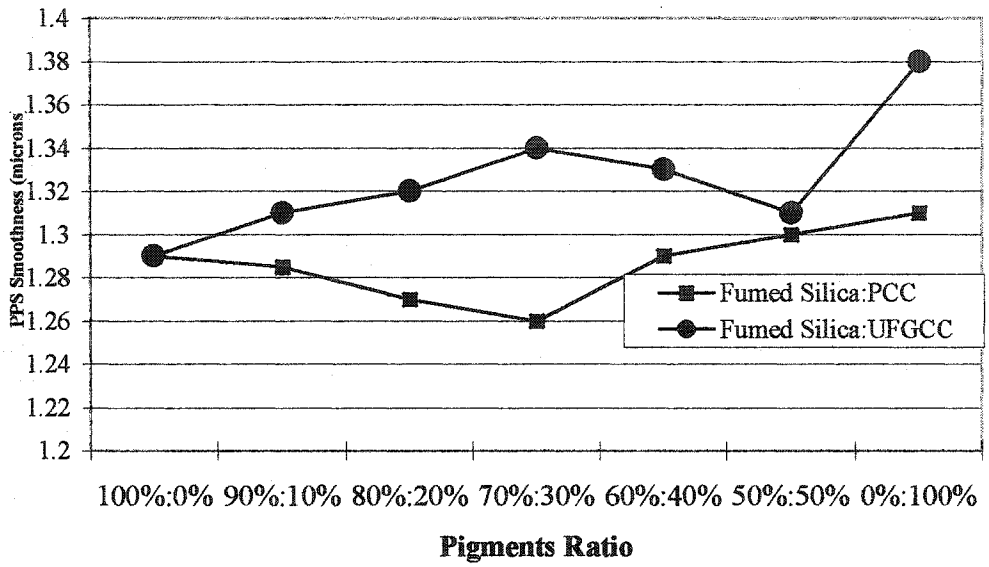

Figure 21. Roughness (PPS Smoothness) comparison of PCC and UFGCC coatings (Coat weight:10 gsm, Calendered samples, Pigment:Binder=7:1)

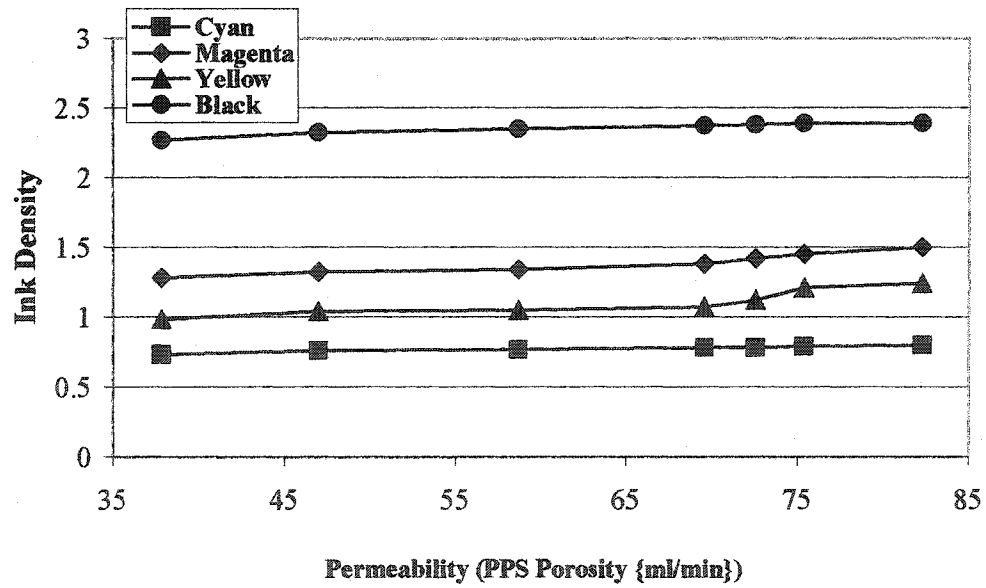

Figure 22. Porosity vs. ink density of fumed silica and PCC coatings (Coat weight:10 gsm, Calendered samples,Pigment:Binder=7:1)

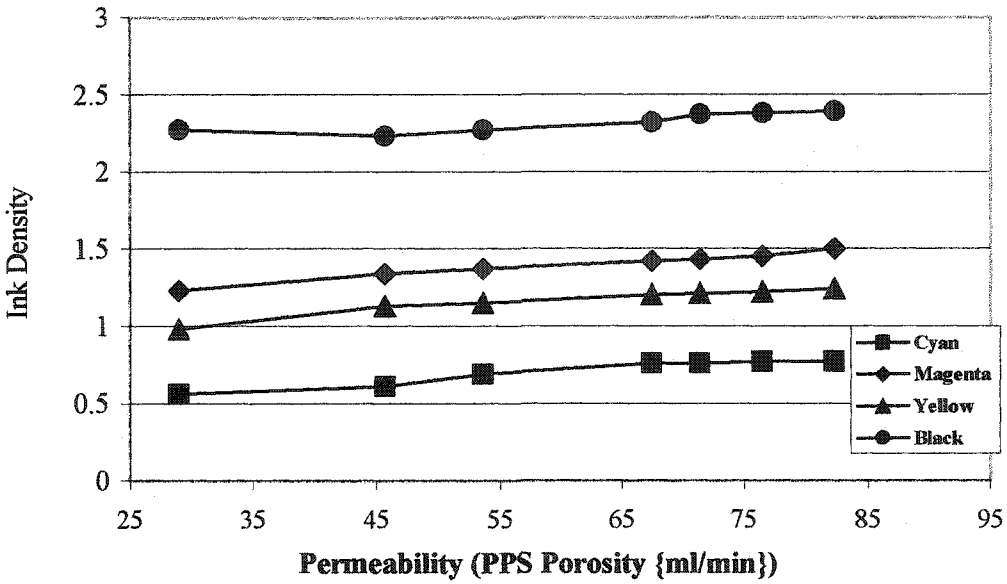

Figure 23. Porosity vs. ink density of fumed silica and UFGCC coatings
(Coat weight:10 gsm, Calendered samples,Pigment:Binder=7:1).

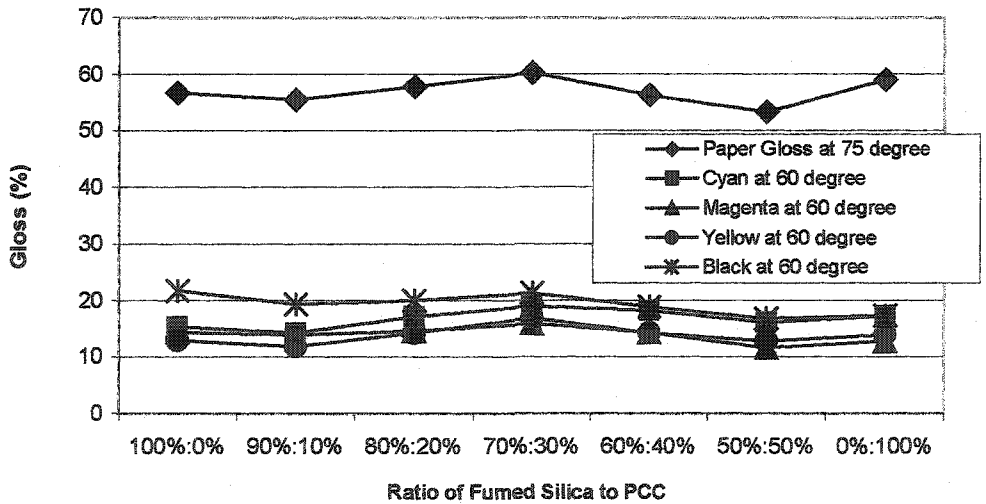

Figure 24. Gloss (75 degree) vs. ink gloss(60 degree) of fumed silica and PCC coatings
(Coat weight:10 gsm, Calendered samples,Pigment:Binder=7:1)

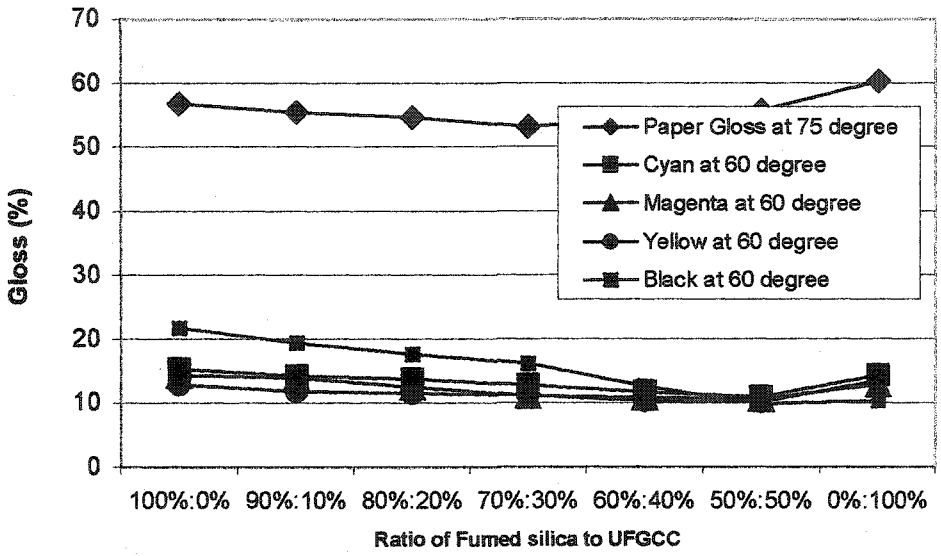

Figure 25. Gloss (75 degree) vs. ink gloss (60 degree) of fumed silica and UFGCC coatings
(Coat weight:10 gsm, Calendered amples,Pigment:Binder=7:1)

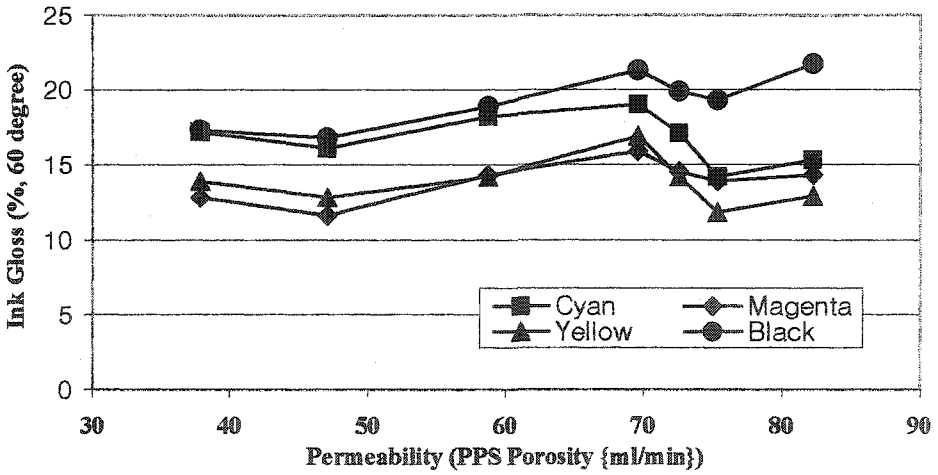

Figure 26. Ink gloss (60 degree) vs. permeability (PPS porosity) of fumed silica and PCC coatings
(Coat weight:10 gsm, Calendered samples, Pigment:Binder=7:1).

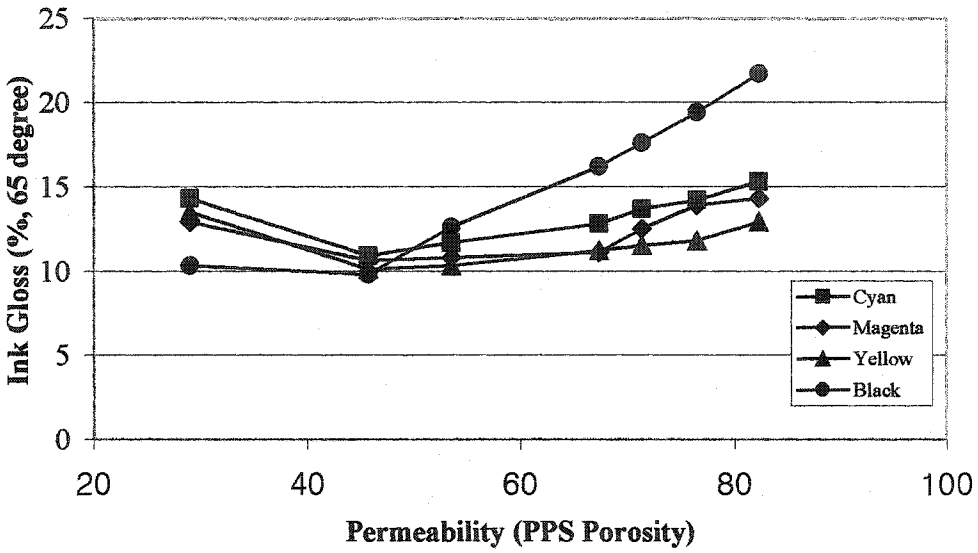

Figure 27. Ink gloss (60 degree) vs. permeability (PPS porosity)
of fumed silica and UFGCC coatings
(Coat weight:10 gsm, Calendered samples,Pigment:Binder=7:1).

Figures 26 and 27 show the relationship between permeability and ink gloss. Permeability did not affect the change of ink gloss. In the conventional printed of coated paper, the pore structure of the coating layer is able to change ink gloss[25]. However, in this study, ink gloss was affected by paper gloss more than by permeability.

Conclusion

This research indicates that brightness was influenced by the pigment type and the ratio of fumed silica and PCC and UFGCC. As the addition of PCC and UFGCC

increased, the brightness value increased. The brightness value of fumed silica and PCC coating was higher than that of fumed silica and UFGCC.

The addition of PCC improved gloss until 30% of PCC was added. The results indicate that although the refractive index of the coating surface increased due to the addition of PCC, the surface roughness, microroughness, increased due to a change in packing order of the fumed silica and PCC. In the coating of fumed silica and UFGCC, the gloss decreased until a 30% addition of UFGCC was added. After this point, the gloss improved.

The addition of PCC and UFGCC decreased the ink density but there are not big differences in this research. Permeability did not influence ink gloss. In the conventional printed of coated paper, the pore structure of the coating layer is able to change ink gloss. However, in this study, ink gloss was affected by paper gloss more than permeability.

References

1. Harrison, V. G. W., *Definition and measurement of Gloss*, The Printing and Allied Trades Research Association, 1945.

2. Lee, D. I., "A Fundamental Study on Gloss", *TAPPI Coating Conference*, 1974, pp.97-103.

3. Yoshifumi Limori, Terunisa Shimada, Hiraka, "Ink jet recording paper", U.S patent 5281467, p.1-4, (Jan 1994).

4. Lyne, M.B. and Aspler, J.S., "Paper for Ink-jet Printing," *TAPPI J.*, May 1985, p.106-110 (1985).

5. Taylor, D.H., "Specialty Media from High Quality Inkjet output," *5th Annual ink-jet printing workshop*, Cambridge, MA, March 1996.

6. Chapman, D.M., "Coating structure effects on inkjet print quality," *1997 Coating conference proceedings*, TAPPI press, p. 73-93, (1997).

7. Lee, Hyunkook, Joyce, Margaret K., Fleming, Paul D. and, Cameron, John , "Production of a Single Coated Glossy Inkjet Paper Using Conventional Coating and Calendering Methods", *Proceedings of the TAPPI Coating Conference*, May 2002.

8. Hyun-Kook Lee, M. K. Joyce, and Paul D. Fleming, "Influence of Pigment Particle Size and Packing Volume on Printability of Glossy Inkjet Paper Coatings", *Proceedings of the IS&T NIP19: International Conference on Digital Printing Technologies*, New Orleans, October 2003, pp613-618 and JIST, in press 2004.

9. Ramakrishnan, Raja, "Coating and Basesheet Influences on the Development of Gloss for Inkjet Papers Containing Fumed Metallic Oxides", Western Michigan University, MS thesis, 1999.

10. Chinmayanandam, T. K., *Phys. Rev.* **13**:96 (1919).

11. Casey, J. P., *Pulp and Paper*, John Wiley and Sons, Inc, Vol. **3**, 1981.

12. Hunter, R.S., "Method of Determining Gloss", *Journal of Research of the National Bureau of Standards*, V18, January 1937, pp.19-39.

13. Enomae, T., Hayano, S., and Takano, K., "Mechanisms of Print Gloss Development," 2000 *International Printing and Graphic Arts Conference*, October 2000.

14. Judd, D.B., and Wyszecki, G., *Color in Business, Science, and Industry*, John Wiley and Sons, Inc, 1963.

15. TAPPI Standard, T 480 Om-92.

16. Veronika Chovancova, Paul Howell, Paul D. Fleming III and Adam Rasmusson, "Printability of Different Epson Ink Jet Ink Sets", *Proceedings of the IS&T NIP20: International Conference on Digital Printing Technologies*, Salt Lake City, 2004.

17. Renmei Xu, Paul D. Fleming III and Alexandra Pekarovicova, "The Effect of Ink Jet Papers Roughness on Print Gloss and Ink Film Thickness" *Proceedings of the*

IS&T NIP20: International Conference on Digital Printing Technologies, Salt Lake City, 2004.

18. Cawthorne, James E., Joyce, Margaret and Fleming, Paul D., "Use of A Chemically Modified Clay as A Replacement for Silica in Matte Coated Inkjet Papers", *J. Coat. Tech*, **75**, No. 937, pp 75-81, Feb. 2003.

19. Boothby, C., "New technology drives global coating trends," *PIMA Papermaker*, May 1997, pp. 38-45.

20. Boylan, J.R., "Using polyvinyl alcohol in inkjet printing paper," *TAPPI J.*, **80**(1): 68 – 70, 1997.

21. Burak Aksoy, Margaret K. Joyce and Paul D. Fleming, "Comparative Study of Brightness/Whiteness Using Various Analytical Methods on Coated Papers Containing Colorants", *TAPPI Spring Technical Conf. & Trade Fair*, (Academic, Chicago, May 12-15, 2003).

22. Burak Aksoy, Paul D. Fleming and Margaret K. Joyce, "New Measures Of Whiteness That Correlate With Perceived Color Appearance", *Applied Optics*, in press.

23. Nakamura, K., "Recent Trends in Inkjet Printing Inks and Papers," *SPIE* Vol.**1912** Color Hard Copy and Graphic Arts II, 1993.

24. Lavery, A., and Provost, J., "Color-Media Interactions in Inkjet Printing", *IS&T's NIP 13: 1997 International Conference on Digital Printing Technologies*, 1997, pp. 437-442.

25. Donigian, D.W., "Inkjet Dye Fixation and Coating Pigments," *1998 TAPPI Coating/papermakers Conference*, 1998, pp.393-412. pp. 213-221.

26. Barker, L.J, de Pierne, O.S., and Wasser, R.B., "Image Bleed in Color Ink-Jet Printing of Plain Paper," *SPIE*, vol.2171, pp.121-125.

INFLUENCE OF SILICA AND ALUMINA OXIDE ON COATING STRUCTURE AND PRINT QUALITY OF INK JET PAPERS

Hyun-Kook Lee, Margaret K. Joyce, Paul D. Fleming, and James E. Cawthorne

Department of Paper Engineering, Chemical Engineering and Imaging

Center for Coating Development

Western Michigan University

Kalamazoo, Michigan 49008

Abstract

Advances in ink jet printing have resulted in a new generation of ink jet printers, which can print faster at wider widths, producing four-color images close to photographic quality. Ink jet printing papers must respond to these changes through quick ink absorption, minimizing ink bleeding and wicking, while retaining favorable ink optical density.

Amorphous and precipitated silica and silica gels, prepared by the acidification of a solution of sodium silicate, are commonly used in premium matte coated ink jet papers. Aqueous coatings for paper or paperboard applications use traditional coating pigments such as clay, calcium carbonate, and titanium dioxide. However, for matte coated ink jet papers, precipitated and gelled silica are used due to their unique morphological properties. The structure of these pigments provides an internal porosity and packing porosity that enables the rapid diffusion of liquid inks into the

coating layer. The rapid uptake of the ink immobilizes the anionic dyes at the surface of the coating. This accumulation of dye at the surface allows high optical print densities to be achieved. The particle size of precipitated and gelled silica is typically in the 3-16 μm range. Since particles of this size significantly reduce gloss, the use of these pigments in glossy ink jet media is hindered. Thus, they are primarily used in matte grades.

This study is focused on comparison of coatings using non-porous fumed silica, aluminum oxide, and precipitate silica in ink jet media. The coating process was not the cast coat process, but a blade coat process on a cylindrical lab coater (CLC). This research examines the contribution of pigment chemistry, functionality, and particle size on coating structure, and coating influences on ink jet print quality. The pigments used are commercially available and, because of this work, currently being used commercially.

Application Statement – This paper can help to guide coating formulators in the contribution of pigment characteristics to coating structure for matte coatings for ink jet printing that can be on machine coated.

Introduction

The quality of non-impact printing is improving because of improvements in technology that increase resolution and speed. This has resulted in adoption of color printers in the home and office. These trends are placing increasingly stringent

requirements on the paper coating to take advantage of the improved printing technology. To date, research in the area of paper coatings for ink jet printing has concentrated on examining the paper properties required for good print quality (1). The results of these studies have shown that good print quality depends very much on the structure and the surface properties of the dry coated paper.

To understand some of the demands placed on a coating during this printing process, a basic understanding of some of the typical ranges of ink and print properties is required. For a typical narrow-format, home/office ink-jet printer, the ink fluid contains 2-5 wt. % dye or pigment, 2-5 % surfactants and additives, 30 % humectant (ethylene glycol or diethanolamine), and 65% water. The important ink-fluid properties that contribute to the quality of the printed image are surface tension and viscosity (2).

Thus, because approximately 65 % of the desktop ink jet ink is water, media for ink jet paper must have the following properties (3);

1. Ink applied to the recording paper must be absorbed without running and must not smudge,
2. Ink dots formed on the paper must have high contrast and bright color tones,
3. Ink dots must be suitably described in the direction of the paper surface, the dots should be almost round with sharp edges, and
4. Media must have excellent smoothness and gloss so that sharp images and high resolutions can be obtained.

Preparing coating for ink jet paper is very different from paper for conventional printing. The coating for ink jet paper must absorb large volumes of water from ink drops. The ink has to be fixed on the surface of ink jet paper to avoid bleeding or smudging when the ink drop hits the substrate. The ink drop should move evenly in the lateral direction to produce a clear edge for contrast and image fidelity (4,5). Fumed, pyrogenic silica is produced by the flame hydrolysis of silica tetrachloride or tetrafluoride. The result is an aerosol of small primary particles typically 7-40 nm in diameter. These particles stick together by hydrogen bonds into aggregates, and the aggregates into micron-sized agglomerates. Porosity is created by virtue of the packing of the dense particles into secondary structures. These secondary particles are shear sensitive, thus shear can destroy the inherent porosity that gives them their inherent absorptivity (6).

Although precipitated silica is prepared by mixing sodium silicate and mineral acids, the reaction system is typically sheared during the silicate polymerization process. Because of the pH and temperature of the reaction system, which favor silicate dissolution and reprecipitation, the primary, non-porous particles grow in size to 5 to 100 nm. Because of the shear forces applied during the reaction, the developing network between these particles is continually broken down, and the primary particles are again only weakly bonded together, as in the case of fumed silica. Conceptually, fumed and precipitated-silica agglomerates resemble a cluster of grapes rather than the sponge structure of the silica gels. Gel-precipitate hybrids, or high structure factor precipitated silicas, are prepared by additional treatment with soluble silicates, and

this treatment encourages siloxane bonding between the primary particles. This method of secondary treatment for network development produces agglomerates that are still somewhat shear sensitive, and does not yield materials with as high of porosity as that which can be achieved in silica gels.

The affect of coating properties on ink jet print quality depends on the micro- and macro-porosity of the coating (7). Due to the large volume of water contained in the ink, it has been found that a coating capable of quickly absorbing and holding water, to set the ink quickly, is required for good print quality. Penetration of water into the basesheet results in fiber swelling, which can distort the image and thereby reduce the print quality. Undesirable cockling of the sheet can also occur. Conventional coatings, which are designed primarily for solvent-based liquid or paste inks, rather than water/dye holding ability, are largely inadequate for use in color ink-jet printing papers.

Ink density is an important quality control indicator in the printing process. Ink density impacts the final visual quality, color gamut, and color fidelity. The main factor identified with color density is the concentration of colorant in the ink. Other major factors determining ink densities are ink dot coverage on the coating surface and colorant concentration at the surface. In the interaction of the colorant with coated paper, electrostatic interactions play the key role in colorant-coated paper interactions. The nature of the anionic dyes and the oxides will determine the print quality of the ink jet printing, since electrostatic interactions of colorant with coated media occur between the anionic groups of dyes and the oxides. The binding energies

of the dyes are greatly increased by electrostatic interactions, resulting in a high binding strength (8-10).

Conventional coating media from conventional pigments such as kaolin, calcium carbonate, and titanium dioxide are primarily limited by their available void fraction for liquid uptake (0.2 to 0.4 μm) as well as the narrow pore diameters for fluid flow (0.02 to 0.04 μm). For example, special methods (8, 11) have to be applied to improve the water uptake, and therefore drying of ink jet inks, when using precipitated calcium carbonate (PCC) pigments in the coating. Thus, coating technologies using silica pigment and polyvinyl alcohol (PVOH) have been developed (7). Precipitated and gelled silica pigments are matte pigments, so they are not suitable for glossy inkjet grades.

Polyvinyl alcohol is produced by the hydrolysis of polyvinyl acetate (Figure 28). It can possess different physical and chemical properties due to varying polymerization of the intermediate polyvinyl acetate that affects the molecular weight of the polyvinyl alcohol (12,13). Other structural variables, which may also be manipulated during the manufacturing process, include branching, spatial orientation or tacticity, and the distribution of the hydroxyl and remaining acetate groups along the polymer backbone chain. Branching, which is low compared to cornstarch, may vary from one supplier to another. Sequencing of the residual acetate groups could, depending on the process, be used to prepare PVOH, in either block or random form. However, the structural variables that most significantly impact its use in paper coatings are the degree of hydrolysis and molecular weight.

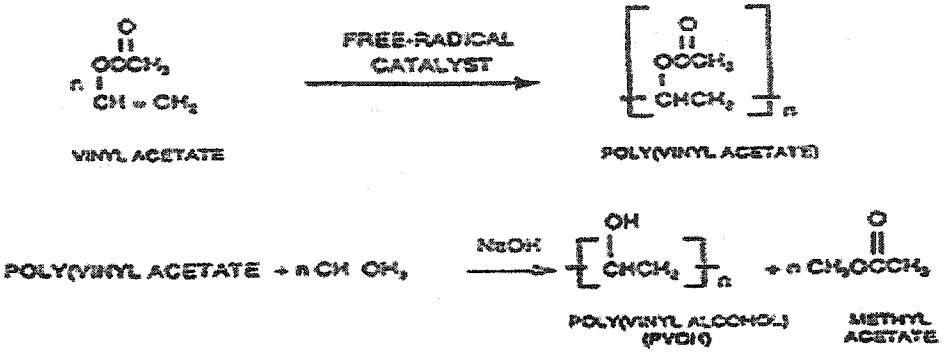

Figure 28. The chemistry of polyvinyl alcohol

Ink jet printing places demands on paper that are quite different from those required by conventional contact printing methods (3). Most inkjet printers require low viscosity and low solids ink to achieve proper jetting. Thus, to obtain images with sufficient optical densities, relatively large volumes of these inks are required. High liquid loading presents a peculiar problem to the design of an optimum ink jet coated paper.

Ink jet papers can be classified into four major categories, as shown in Table 8. Depending on the grade, the coating formulation, application process (air knife, pre-metering size press, rod, or blade), and coating, cost can vary substantially (7).

Table 8.The classification of the media

• Plain or surface-sized paper	Low cost, good monochrome text, poor color (limited coverage, poor gamut, high bleed, strike-through, cockle/curl)
• Coated matte paper	Higher cost, good color gamut, fast dry time, excellent resolution, 100% coverage
• Coated glossy paper	Very high cost, nanoporous, slow dry time,
• Cast coated paper and resin coated paper	Very high cost, highest gloss, photorealistic image

Objectives

In this study, two fumed silicas, alumina, and precipitated silica were used in ink jet coating formulations. Previously (8,9,14,15), coatings based on these pigments were shown to be applicable at high speed (650-1000 m/min) and good ink jet print quality can be obtained. Pigment particle size and packing are also very important (16) for such coatings.

Following these earlier results, an understanding of the contribution of coating properties on coating structure and print quality was sought.

The objectives of this research were:

(A). To study influence of fumed silicas, aluminum oxide and precipitate silica on optical properties of coated paper and printing properties.

(B). To study the surface properties of the coatings using dynamic contact angle measurements, and the porous structure of the coating using mercury porosimetry.

Experimental design

The base paper (basis weight: 75 g/m^2) was obtained from International Paper (Otis, Maine) for the CLC coating trials. The base paper was determined to be a neutrally sized paper with a Hercules Sizing value of 69 seconds (TAPPI standard test method T-530 pm-89). And brightness was 87.2%(TAPPI standard method T 452 om-92), gloss was 6.4% (TAPPI standard test T 480 OM-92) and roughness was 3.93 microns (TAPPI T555 pm-94).

Two fumed silicas (A and B) of varying surface areas, one aluminum oxide pigment with a surface area similar to pigment A, and precipitated silica were obtained. The physical properties of the pigments are shown in Table 9.

The binder used in the coating formulation was a partially hydrolyzed, low viscosity polyvinyl alcohol. This polyvinyl alcohol was chosen to optimize the coatings solids by minimizing the interaction between pigments and PVOH. Polyvinyl alcohols with a higher degree of hydrolysis are known to interact more strongly with silica pigments, thus limiting the coating solids that can be obtained. They are also less

hydrophilic; reducing the ink absorption properties of the coating, hence print quality. Solutions of polyvinyl alcohol were prepared at 32-33% solids by adding the required amount of dry PVOH powder to cold water under agitation and heating the mixture to 185 °F. The solution was held at this temperature for 35 - 40 minutes to assure complete dissolution and hydration of the PVOH. A defoamer was then added (Foam Master VF, Henkel). The solids content of the solution was measured using a CEM Labwave 9000 microwave moisture analyzer.

Table 9. The physical properties of pigments as supplied

Sample	Solids Content %	Color	Specific Gravity (25° C)	Surface Area (m^2/g)	Particle Size(μm)	pH
Aluminum Oxide	40%	White	1.40	55	0.160	3.8-4.2
Fumed Silica (A)	30%	White	1.20	90	0.225	10.0-10.3
Fumed Silica (B)	25%	White	1.20	170	0.135-0.155	9.0-10.0
Precipitated Silica	97% (powder)	White	2.10	250-280	2-3	6.5-7.5

The solution was cooled to 40 °F before adding the slurried pigments. The precipitated silica coating was prepared at a pigment to binder ratio of 1.75:1. The fumed alumina and silica coatings were prepared at 4:1under slow agitation. The higher surface area precipitated silica pigment required more binder for sufficient

adhesion and cohesion (Dusting was observed at lower binder addition). The coatings were mixed for 20 - 30 minutes and the pH and viscosity measured. The viscosities of the coatings were measured using a Brookfield RVT digital viscometer (#5 spindle @ 100 rpm).

The base papers were blade coated using a Cylindrical Laboratory Coater (CLC) at a speed of 610 m/min. Coatings were prepared using the two fumed silicas (A and B) of varying surface areas, an aluminum oxide and precipitated silica. Due to low pH (4.4) of the aluminum oxide coating formulation, the pH of the coating formulation was adjusted with 0.1% KOH. Table 10 shows the coating properties of each formulation. Four different coat weights were applied: 6 ± 1 g/m^2, 9 ± 1 g/m^2, 12 ± 1 g/m^2, and 15 ± 1 g/m^2.

The brightness, gloss, roughness, and air permeability (PPS porosity) of the papers were measured. The brightness of the papers was measured using Technidyne Brightness meter, TAPPI procedure T 452 om-92. Gloss was measured using a Hunter 75° gloss meter according to standard TAPPI procedure T 480 OM-92. The surface roughness and permeability of the sheets were measured using a Parker Print Surf (PPS) tester (TAPPI T555 pm-94).

The rate of liquid absorption of the papers was measured using a First 10 Angstrom Dynamic Contact Angle measuring device.

The samples were printed on an Epson Stylus Pro photo realistic ink jet printer, using a proprietary test print pattern created with Adobe software (8, 9,14-16). The print densities of the samples were then measured using an X-rite 408 densitometer.

The pore volume and pore size distribution of coated papers were measured using a Micromeritics Mercury Intrusion Porsimetry.

Table 10. Properties of coating formulations

Coating	pH	Solid Content (%)
Aluminum Oxide + PVOH	8.82	27.18
Fumed Silica(A) + PVOH	9.26	31.75
Fumed Silica(B) +PVOH	9.25	27.00
Precipitate Silica + PVOH	6.50	27.00

Results and discussion

Typically, small pigments and narrow size distribution pigments produce more gloss, due to the ability of the smaller pigments to fill the surface irregularities, providing a smoother surface with more compact air boundary surfaces (17). For uncalendered samples, the gloss of the precipitated silica coating was much less than of the fumed silica (A and B) and alumina coatings and the gloss of all increased with coat weight (Figure 29). This result indicates that although the precipitated silica and fumed silica particles have similar shapes, the precipitated the gloss silica coating surface has much lower gloss, due to the larger particles of precipitated silica. On the other hand, fine-particle size fumed silicas and alumina oxide tend to orient and pack

together tightly, producing a microsmooth surface. Figure 30 shows that the roughness (Parker Print Surf smoothness) of the precipitated silica coating was higher than that of the fumed silica (A and B) and alumina coatings.

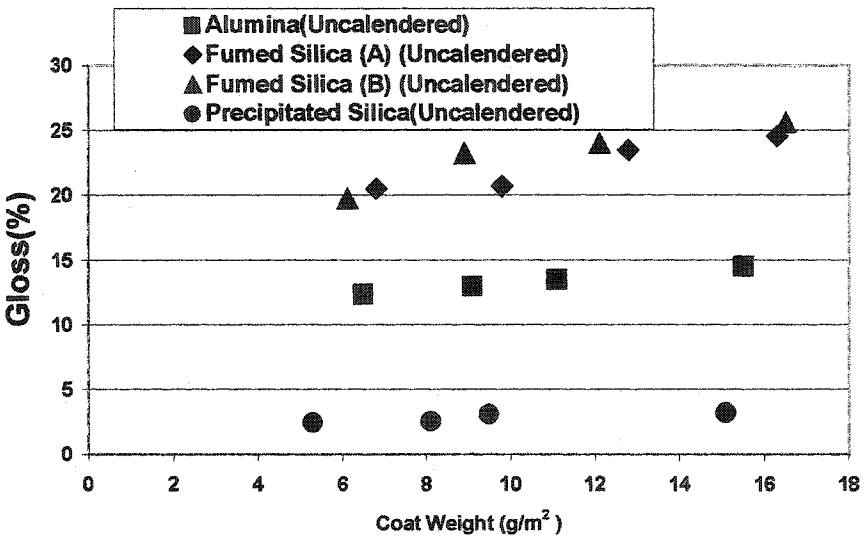

Figure 29. Influence of pigment on gloss

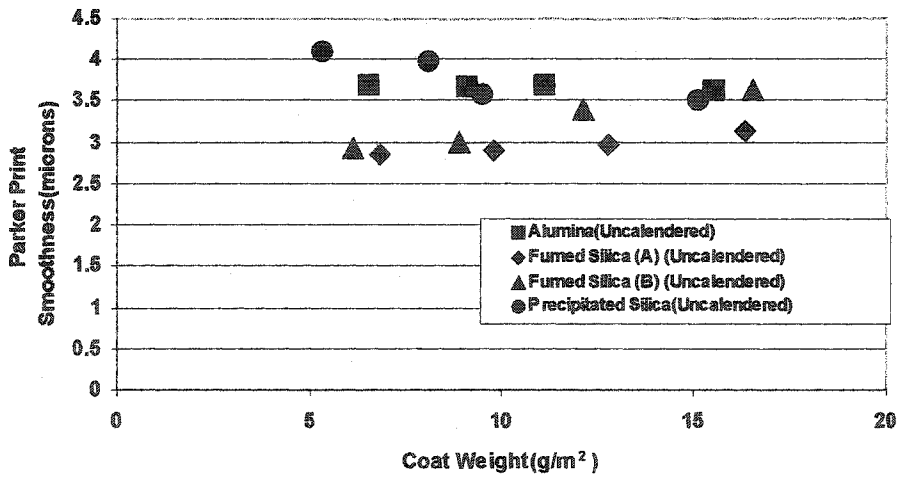

Figure 30. Influence of pigments on roughness.

Figure 31 shows the permeabilities (PPS porosities) of the coated papers as a function of coat weight and pigments type. It is evident that permeability increased with coat weight. The high permeability of these coatings is attributed to the clustered particle arrangement. As coat weight increases, the thickness of the coating layer also increases providing more passageways for air to flow. As a result, permeability increased. The permeability of precipitated silica coating was much higher than that of the fumed silica coatings and the aluminum oxide coating. The larger particles of precipitated silica increased the size of air voids between particles. Therefore, increased air voids impart more air- flow pathways.

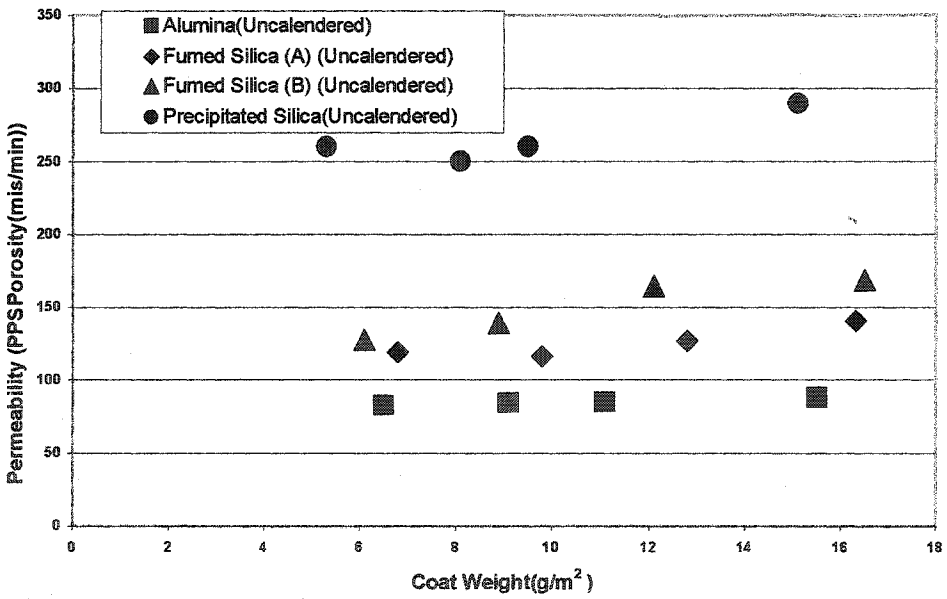

Figure 31. Influence of pigments on permeability (PPS porosity)

Initial contact angle measurements and printing studies were performed to determine if the rate of liquid absorption and print quality were adversely affected.

The initial contact angle of each sample was measured to estimate the rate of liquid absorption into the sheet and to study the influence of pigment type on the surface energy of the sheet. As seen in Figures 32, the initial contact angle decreased with increasing coat weight. This corresponds to the permeability results, which showed permeability also to increase with coat weight. Once again, the initial contact angle of the aluminum oxide coating was highest. The higher initial contact angles are believed to be caused by basesheet effects. The basesheet was highly sized (HST=120 s). As coat weight increases, the basesheet coverage increases and the available void spacing increases to promote wetting.

The coated papers were printed on an Epson Stylus Pro photo realistic ink jet printer. The ink densities of the printed samples are presented in Figures 33-34. For all samples, the black and magenta ink densities for the alumina samples were higher than those of the fumed silica coatings (A and B) and the precipitated silica samples.

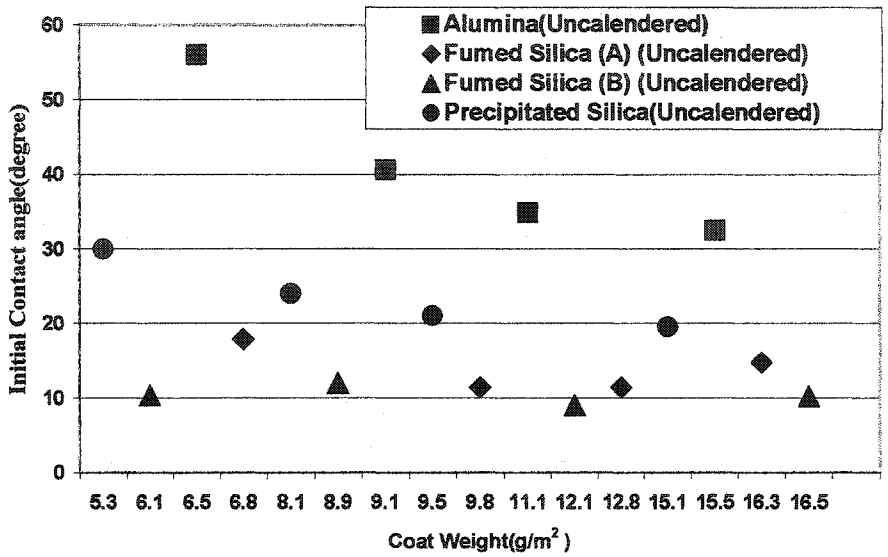

Figure 32. Influence of pigments on contact angle

Coat weight had little impact on the ink densities of all samples. For all samples, the density of the black ink was higher than the density of the magenta ink. The porosity of the coated layers was obtained using a Micromeritics Mercury Porsimeter. The pore size distributions, median pore diameters, and total intrusion volumes are shown in Figures 35. The precipitated silica samples had a wide pore size distribution curve because the larger particles of the precipitated silica made a wide porous structure in the coating layer. This is consistent with the permeability data.

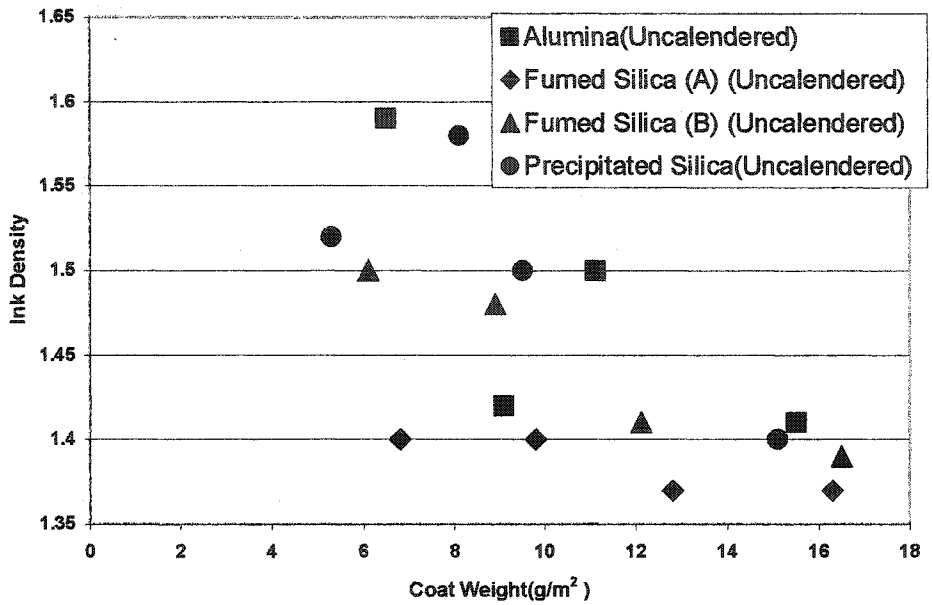

Figure 33. Influence of pigments on black ink density

Figures 36 and 37 show the influences of permeability on ink density for the black and magenta ink. They indicate that the permeability of the coating layer did not significantly affect ink density.

Likewise, Figures 38 and 39 show the effect of contact angle on ink density. From the Figure 38 and 39, both black and magenta ink densities of alumina oxide samples were higher than those of the silica samples. This can be explained, since the coating layers of alumina samples have higher cationic charges compared to the cationic charge of silica coating layers. It is attracted more strongly to the negatively charged dye of inkjet ink. This keeps the dyes nearer to the top of the coating surface, which produces higher optical print density (18). The differences of the pore structure probably play a role on the development of ink density, as well.

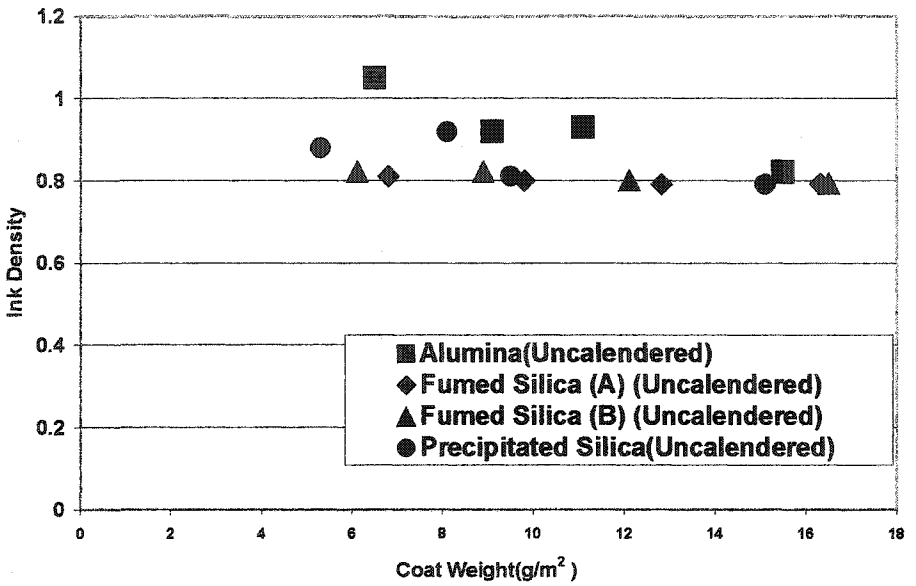

Figure 34. Influence of pigments on magenta ink density

Conclusion

The results obtained from this study indicate that the optical properties, such as gloss, were affected by pigment type and coat weight. The correlation between improvements in optical properties and smoothness indicate that the property improvements were due to an increase in surface coverage with coat weight. Permeability increased with coat weight.

The dry coating properties were also influenced by pigment type, particle size, and coat weight. It is believed that the low solids of the coatings prevent the smooth application of the coating, due to base sheet roughening by the absorption of coating water and shrinkage during drying.

Print quality, as measured by ink density, was strongly dependent on pigment type and correlated well with pore size distribution results. Coat weight did not significantly affect these properties. The difference in print quality between the two colors, black and magenta, indicates differences between the two inks and confirms the need to perform print studies on multiple printers with multiple colors. The permeability and liquid absorption do not significantly affect the ink density.

References

1. Kulmala, A., Paulapuro, H. and Oittinen, P., "Paper requirements for electrophotographic printing," IS&T's 10th International Congress on Advances in Non-Impact Printing Technologies, IS&T, Springfield VA, 1994, pp. 466 - 470.

2. Chapman, D.M., "Silica-Gel coatings for ink-jet media," Grace Davison (internal document), Baltimore, MD.

3. Yoshifumi Limori, Terunisa Shimada, Hiraka, U.S patent 5281467, p.1-4, (Jan 1994).

4. Lyne, M.B. and Aspler, J.S., "Paper for Ink-jet Printing," TAPPI J., May 1985, p.106-110 (1985).

5. Taylor, D.H., "Specialty Media from High Quality Inkjet output," 5th Annual ink-jet printing workshop, Cambridge, MA, March 1996.

6. Chapman, D.M., "Coating structure effects on inkjet print quality," 1997 Coating conference proceedings, TAPPI press, p. 73-93, (1997).

7. Withiam, M. C., "Silica Pigment Porosity Effects on Color Inkjet Printability", IS&T, NIP12, 12th International Congress on Advances in Non-Impact Printing Technologies, pp 409-417.

8. Donigian, D. W., Wernett, P. C., McFadden, M. G. and McKay, J. J., "Inkjet Dye Fixation and Coating Pigments", Proceedings of the 1998 TAPPI Coating/Papermakers Conference, May 4-6, New Orleans.

9. Cawthorne, E. James, "Use of a Chemically-Modified Clay as a replacement for Silica in Matte Coated Ink Jet Papers", Western Michigan University, MS thesis, 1999.

10. Cawthorne, James E., Joyce, Margaret and Fleming, Paul D., "Use of A Chemically Modified Clay as A Replacement for Silica in Matte Coated Ink Jet Papers", *J. Coat. Tech*, **75**, No. 937, pp 75-81, Feb. 2003.

11. Superka, A., and Janson, J. A. "Defining Image Quality", *Proceedings of the IS&T NIP16 Conference on Digital Printing Technologies*, 2000.

12. Boothby, C., "New technology drives global coating trends," PIMA Papermaker, May 1997, pp. 38-45.

13. Boylan, J.R. "Using polyvinyl alcohol in ink jet printing paper," TAPPI, 80(1): 68 – 70, 1997.

14. Lee, Hyunkook, "The influence of fumed metallic oxides on coating structure and their relationships to print quality", Western Michigan University, MS thesis 1998.

15. Lee, Hyunkook, Joyce, Margaret K., Fleming, Paul D. and, Cameron, John, "Production of a Single Coated Glossy Inkjet Paper Using Conventional Coating and Calendering Methods", *Proceedings of the TAPPI Coating Conference*, May 2002.

16. Lee, Hyunkook, Joyce, Margaret K. and Fleming, Paul D., "Influence of Pigment Particle Size and Packing Volume on Printability of Glossy Inkjet Paper Coatings", *Proceedings of the IS&T NIP19: International Conference on Digital Printing Technologies*, New Orleans, September 28-October 3, 2003.

17. Lee, D. I., "A Fundamental Study on Gloss", *TAPPI Coating Conference*, 1974, pp.97-103.

18. McFadden, M. G. and Donigan, D. W., "Effects of Coating Structure on Inkjet Printability, *1999 TAPPI Coating Conference*, pp169-177.

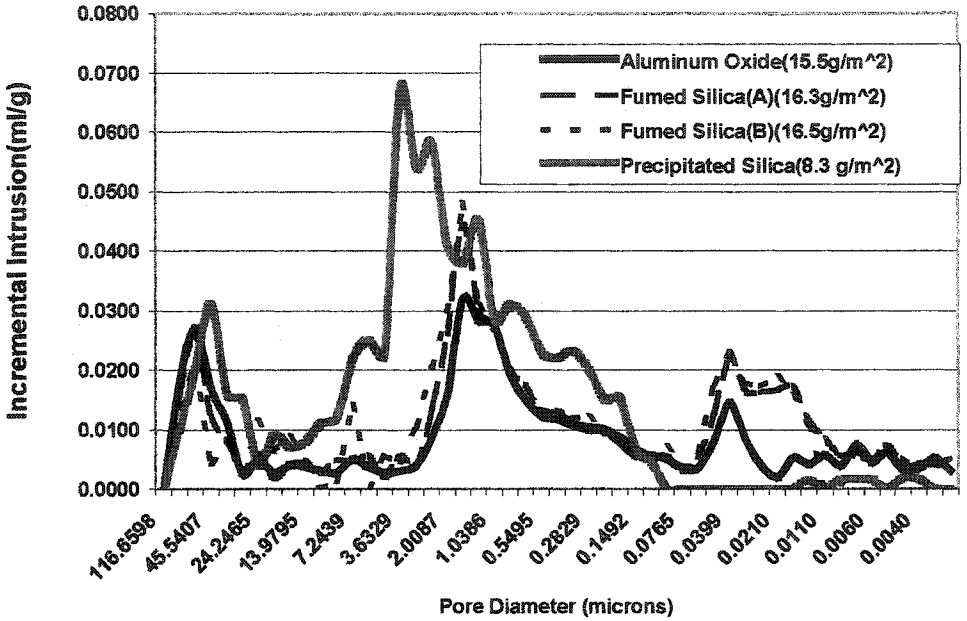

Figure 35. Influence of pigments on pore size distribution

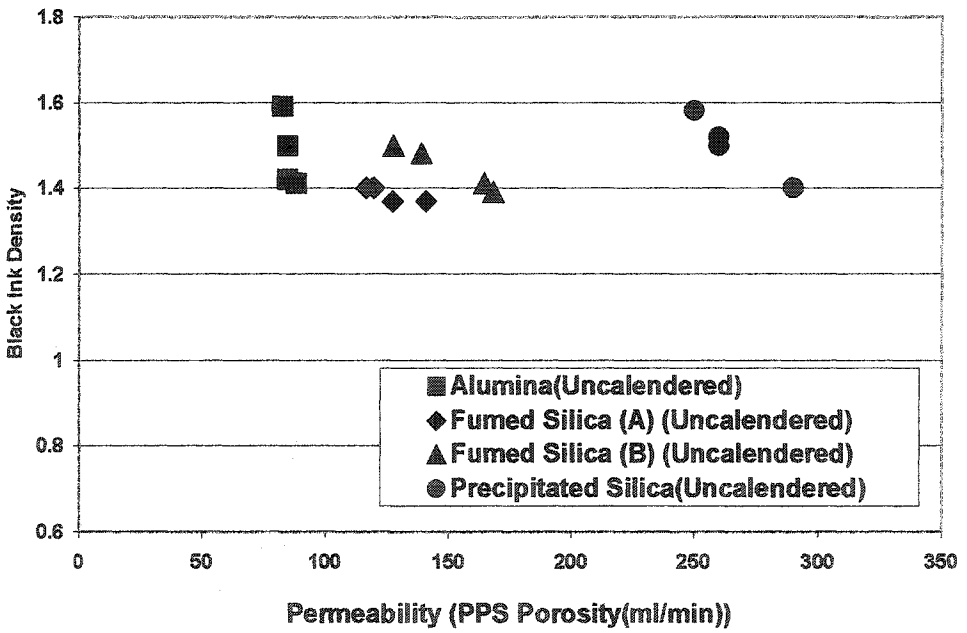

Figure 36. Permeability influences on black ink density

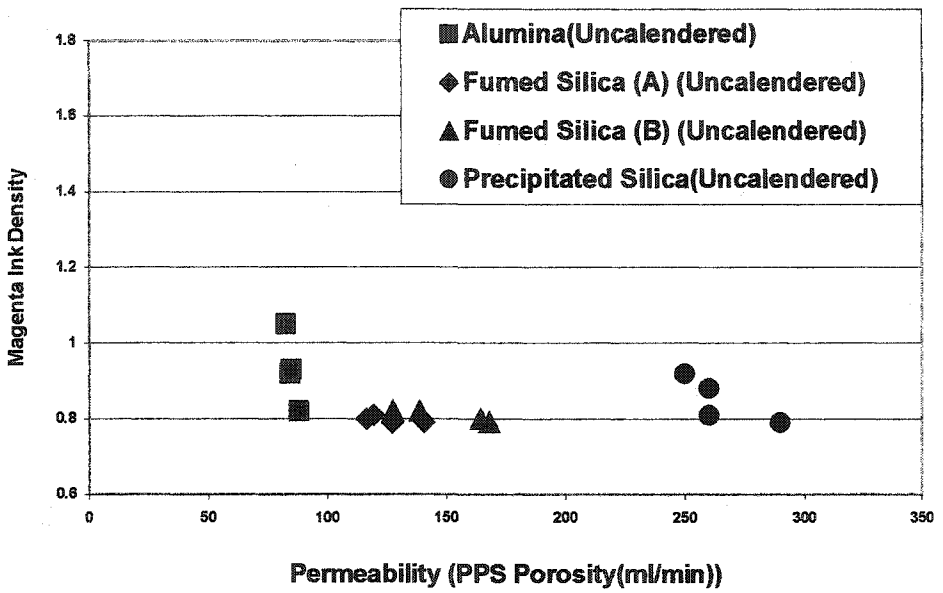

Figure 37. Permeability influences on magenta ink density

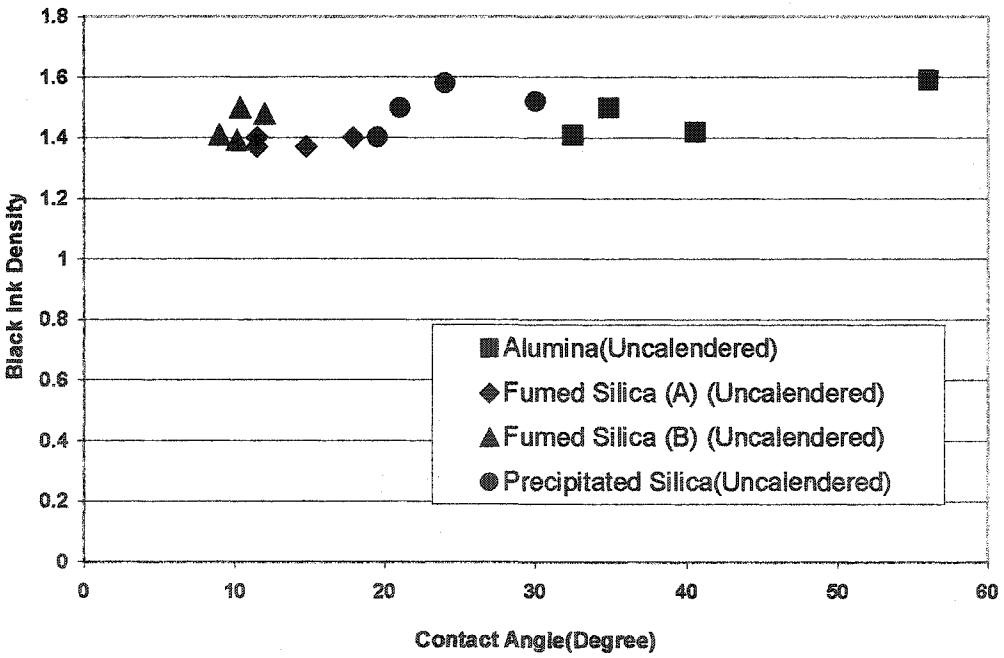

Figure 38. Initial contact angle influence on black ink density

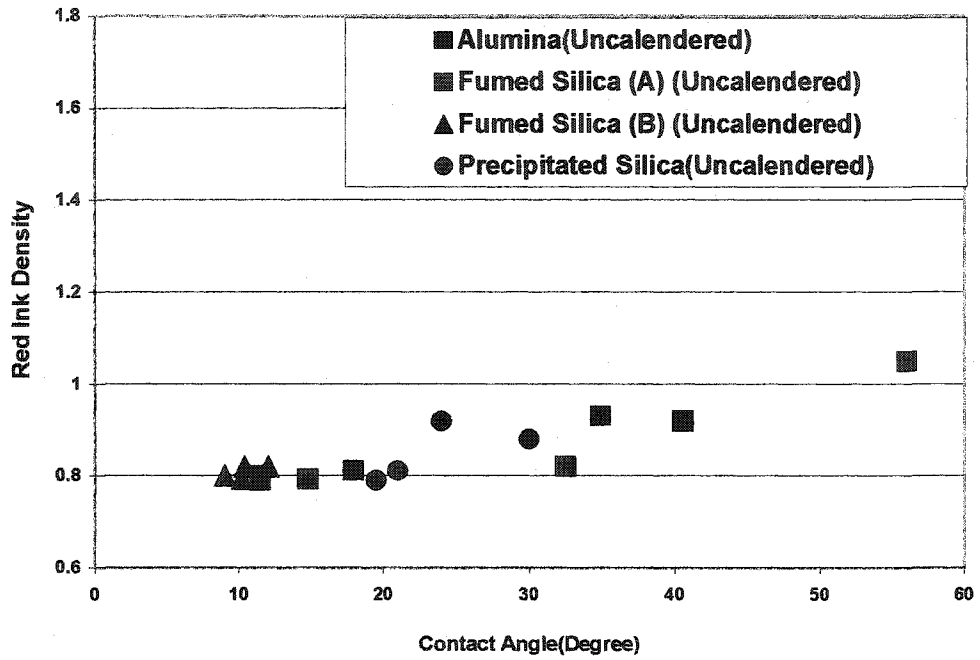

Figure 39. Initial contact angle influence on red ink density

PRODUCTION OF A SINGLE COATED GLOSSY INKJET PAPER USING CONVENTIONAL COATING AND CALENDERING METHODS

Hyun-Kook Lee, Margaret K. Joyce, Paul D. Fleming, and John H. Cameron

Western Michigan University

Department of Paper and Imaging Science and Engineering

Kalamazoo, Michigan 49008

Abstract

The unique structure of precipitated and gelled silicas provides an internal and packing porosity that enables the rapid diffusion of liquid inks into the coating layer. The rapid uptake of the ink immobilizes the anionic dyes at the surface of the coating, allowing high optical print densities to be achieved. However, precipitated and gelled silicas are primarily used in matte grades since the particle size of them is typically 3-16 μm range.

This study focused on the use of non-porous fumed silicas and alumina in glossy inkjet media. The coating process was a single coat blade application on a cylindrical lab coater (CLC) at speeds up to 920 m/min. The use of fumed alumina enabled gloss values of almost 70% to be achieved after 3 passes through a sheet fed soft nip calender at 60 °C and 123 kN/m. The work is significant because it demonstrates the ability to produce glossy inkjet coated papers by applying a single pigmented coating layer on a blade coater and finishing with a soft nip calender. The

research described herein examines the contribution of coating structure influences on inkjet print quality. The pigments used are commercially available and are currently being employed in this application.

Introduction

The quality of non-impact printing is improving as a consequence of increased resolution and the adoption of color printers in the home and office. These trends are placing increasingly stringent requirements on the paper coating. To date, research in the area of paper coatings for inkjet printing has concentrated on examining the paper properties required for good print quality (1). The results of these studies have shown that good print quality depends very much on the structure and the surface properties of the paper coating.

To understand some of the demands placed on a coating during this printing process, a basic understanding of some of the typical ranges of ink and print properties is required. For a typical narrow-format, home/office ink-jet printer, the ink fluid contains 2-5 wt. % colorant (dye or pigment), 2-5 % surfactants and additives, 30 % humectant (ethylene glycol or diethanolamine), and 65% water. The important ink-fluid parameters that contribute to the quality of the printed image are surface tension and viscosity (2).

For current generation printers, the effective resolution of the image (dots per inch or centimeter) is controlled by the dot size; for a 360 dpi image, an individual

dot should be approximately 100 microns in diameter, and for a 720 dpi image, the dot size should be approximately 50 microns. For these printers, the droplet volume varies from 150 pL (picoliters) to 40 pL. Since the diameter of liquid spheres of these volumes is considerably smaller than the respective diameters of the dots, it is clear that considerable radial spreading of the droplet typically occurs on the substrate immediately after droplet impact. The dependence of droplet spreading on ink properties (surface tension) as well as coating properties (surface tension, roughness, and porosity) is therefore very important to understand.

Ideally, the dot should be perfectly circular with a fixed diameter; this requires controlled gain, or spreading, of the ink droplet on impact. A typical coating thickness for matte-home/office media is roughly 20 microns. The volume of a cylinder of liquid that measures 60 microns in diameter and 20 microns in length is 56 pL. Since the droplet is 40 pL, the coating void fraction can be taken to be 0.6. Therefore, even one droplet can be considered to saturate this cylindrical volume fraction. Thus, it is clear that for full gamut color printing, which requires the juxtaposition of two or three droplets, the ability of the coating to handle the ink liquids and channel them away from the printing surface is essential. Furthermore, it is desirable for the colorants to be deposited on or near the surface, as penetration into the base sheet will lower print optical density.

The effect of coating properties on print quality has been shown to depend on the micro- and macro-porosity of the coating (3). Due to the large volume of water contained in the ink, it has been found that a coating capable of quickly absorbing and

holding water, to set the ink quickly, is required for good print quality. Penetration of water into the substrate results in fiber swelling which distorts the image, thus reducing the print quality. Undesirable cockling of the sheet can also occur. For these reasons, conventional coatings are largely inadequate for use in color ink-jet printing papers.

The coating media from conventional pigments such as kaolin, calcium carbonate, and titanium dioxide are not widely used for inkjet papers, primarily because of their available void fraction for liquid uptake as well as the narrow pore diameters for fluid flow (0.02 to 0.04 μm). Conventional pigments also require calendering to obtain their gloss and smoothness properties, which reduces the available void fraction for liquid uptake. So, for glossy inkjet papers, a dilemma exits as to how to simultaneously obtain gloss and maintain sufficient void fraction. Coating technologies using silica pigment and polyvinyl alcohol (PVOH) were developed to enable more void volume for liquid uptake. However, precipitated and gelled silica pigments are matte pigments, so they are not suitable for glossy inkjet grades.

Inkjet printing places demands on paper that are quite different from those required by conventional contact printing methods (4). Most inkjet printers require low viscosity and low solids ink to achieve proper jetting. Thus, to obtain images with sufficient optical densities, relatively large volumes of these inks are required. High liquid loading presents a peculiar problem to the design of an optimum inkjet coated paper.

Inkjet paper classifications

Inkjet papers can be classified into four major categories as shown in Table 11. Depending on the grade, the coating formulation, and application process (air knife, pre-metering size press, rod, or blade), cost can vary substantially (5,6).

Table 11. The classification of the media

Plain or surface-sized paper	Lowest cost, good monochrome text, poor color (limited coverage, poor gamut, high bleed, strike-through, cockle/curl)
Coated matte paper	High cost, good color gamut, fast dry time, excellent resolution, 100% coverage
Coated glossy paper	Higher cost, non-porous, slow dry time, slow dry, photorealistic image
Cast coated paper	Highest cost, highest gloss, photorealistic image, multiple coating layers, good waterfastness

Glossy inkjet papers are by far the best papers to use when photorealistic images are desired, better even than electrophotographic (laser). They best replicate silver halide photographs (6). They are currently made by one of three processes. One uses a double or triple coat process. Another coats a dense layer composed of a hydrophilic resin onto a plastic film or laminated paper (see Figure 1). This is called a resin-coated paper.

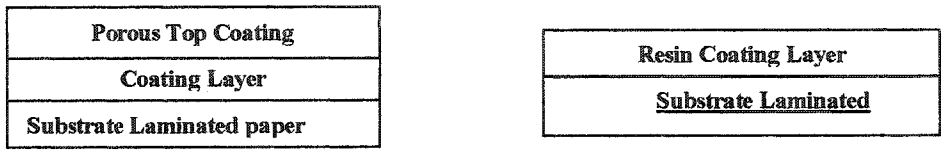

(a) (b)

Figure 40. (a) Cross section multicoated paper, and (b) film-substrate glossy based paper.

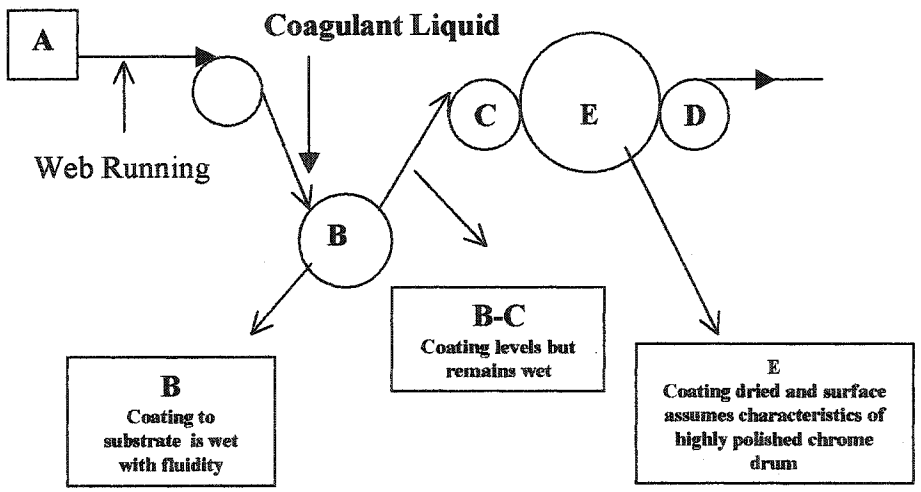

A: Coating Operation Part, B: Coagulant Roll, C: Forming Roll, D: Strip Off Roll, E: Heated Metal Drum with Specular Surface called "Cast Drum"

Figure 41. Schematic of the cast-coating process (adapted from reference 7)

The third process uses a cast coater to apply a special coating that produces a porous coating layer on a pre-coated paper substrate (7,8). The process for making cast coated papers is shown in Figure 2. The coagulation-method (cast) is specifically suitable for production of glossy inkjet papers due to the replication of the chrome cylinder. It is a highly specialized coater, limited in speed.

Objectives

In this study, two fumed silicas and one fumed alumina were used in the preparation of inkjet coating formulations. It was of special interest to determine if the use of the fumed silicas and alumina could provide the desired gloss and void fraction for liquid uptake required of high quality glossy inkjet papers. An understanding of the contribution of coating properties on coating gloss and print quality was sought.

The objectives of this research were:

(A) To study the influence of fumed silica and alumina on the optical properties and printing qualities of coated paper,(B) To compare the print quality between the fumed pigment coating samples and commercial coated inkjet samples, and (C) To study the surface properties of the coating using SEM (scanning electron microscopy), dynamic contact angle measurements, and the porous structure of the coating using mercury porosimetry between the fumed pigment coating samples and commercial samples.

Experimental design

Coating formulations were prepared from two fumed silicas of varying surface areas and one fumed alumina. The physical properties of the pigments used are shown in Table 12.

Table 12. Physical properties of pigments as supplied

Sample	Solids Content %	Color	Specific Gravity (g/cm^3, 25 °C)	Surface Area (m^2/g)	Mean Particle Size (μm)	pH
Fumed Alumina (FA)	40%	White	1.40	55	0.16	3.8-4.2
Fumed Silica A (FSA)	30%	White	1.20	90	0.225	10.0-10.3
Fumed Silica B (FSB)	25%	White	1.20	170	0.145	9.0-10.0

The binder used in the coating formulation was a partially hydrolyzed, low viscosity polyvinyl alcohol (PVOH). This polyvinyl alcohol was chosen to optimize the coatings solids by minimizing the interaction between pigments and PVOH.

Polyvinyl alcohols with a higher degree of hydrolysis are known to interact more strongly with silica pigments, thus limiting the coating solids content that can be obtained. The solution of PVOH was prepared at 32-33% solids by adding the required amount of dry PVOH powder to cold water under agitation and heating the mixture to 85 °C. The solution was held at this temperature for 35 - 40 minutes to assure complete dissolution and hydration of PVOH. A defoamer was then added. The solids content of the solution was measured using a CEM Labwave 9000 microwave moisture analyzer.

The PVOH solution was cooled to 25°C before addition to the slurried fumed pigments at a pigment to binder ratio of 4:1 (pigment: 100 parts and binder: 25 parts) under slow agitation. A pigment to binder ratio of 4:1 was selected based upon an extensive study, which showed this ratio to provide the near optimum gloss. The coatings were mixed for 20 - 30 minutes and the pH and viscosity were measured. The viscosities of the coatings were measured using a Brookfield RVT digital viscometer (#5 spindle @ 100 rpm, 25 °C).

The initial low pH (4.4) of the alumina coating formulation was increased with 0.1% KOH to raise the viscosity of the coating without the addition of a thickener. This was necessary to enable the desired coat weights to be achieved on the CLC coater. Table 3 shows the coating properties of each formulation as applied.

Table 13. Properties of coating formulations

Coating	Viscosity (cP)	pH	Solid Content (%)

FA + PVOH	1288	8.82	27.18
FSA + PVOH	536	9.26	31.75
FSB +PVOH	536	9.25	27.00

The 75 g/m^2 wood-free base paper was blade coated using a Cylindrical Laboratory Coater (CLC) at a speed of 610 m/min. Four different coat weights were applied: 6 ± 1 g/m^2, 9 ± 1 g/m^2, 12 ± 1 g/m^2, and 16 ± 1 g/m^2. The CLC samples were calendered through 3 nips at 123 kN/m and 60°C using a sheet fed hot-soft nip calender. Additional CLC runs were performed to assess the runnability of the coatings at higher speeds. The fumed alumina coating could be uniformly applied at speeds up to 920 m/min. However, the coating of the fumed silica (B) was limited to 610 m/min, because above this speed, undesirable streaks and spits were found and coat weight uniformity suffered.

The brightness, gloss, smoothness, and air permeability (PPS "porosity") of the coated papers were measured. The brightness of the coated papers was measured using a Technidyne Brightness meter, TAPPI procedure T 452 om-92. Gloss was measured using a Hunter 75° gloss meter according to standard TAPPI procedure T 480 OM-92. The surface smoothness and air permeability of the sheets were measured using a Parker Print Surf (PPS) tester (TAPPI T555 pm-94). The optical properties were analyzed using ANOVA table analysis.

The contact angles of water droplets on the calendered coating papers were measured using a First 10 Angstrom Dynamic Contact Angle measuring device. The calendered coated papers and commercial coated inkjet papers were printed on an Epson Stylus Pro photo realistic inkjet printer and a Hewlett-Packard 820C inkjet printer, using a proprietary test print pattern created with Adobe Photoshop and PageMaker. The ink density and ink gloss of the samples were then measured. The ink density was measured using an X-rite 408 densitometer. The ink gloss of the black ink and delta gloss were measured using a Gardener 60° Micro-Gloss meter. The fidelity of magenta dots was measured at 10% tone scale using a Hitachi HV-10 camera (Hitachi Denshi, Ltd, Japan). Image-Pro plus (version 3.0) was used for measuring the roundness.

The surface properties of the dry coating structure were characterized using a scanning electron microscope (SEM). The pore volume and pore size distribution of the coated papers were measured using a Micromeretics Mercury Intrusion Porsimeter.

Results and discussion

For the optical properties of the uncalendered samples, the highest brightness values were obtained for the fumed silica (A) coating. The brightness of all the samples increased with coat weight (Figure 42). The gloss of the fumed silica coatings (A and B) was higher than the gloss of the fumed alumina coating, prior to

calendering. As with brightness, the gloss of all the samples increased with coat weight.

The most significant optical property improvements with calendering were found in gloss and smoothness (Figures 43-44). The results indicate that the specular reflection of the alumina-coated surface is sufficient to provide gloss comparable to commercially coated glossy inkjet papers if the alignment of the particles and smoothness of the coating layer are improved by calendering. The 75 ^{0}gloss of the three commercial glossy inkjet papers ranged from 65-90%. The gloss values of the silica coatings were also increased significantly, but not as much as for the alumina coating. The differences in the gloss values before and after calendering and between the two silicas indicate a difference in the internal structure of the coating layers, which is attributed to the differences in their particle sizes. Typically, small pigments and a narrow pigment size distribution produce more gloss, due to the ability of the smaller pigments to fill the surface irregularities, providing a smoother surface with more compact air boundary surfaces. However, the opposite is found in this case. The gloss and smoothness of the larger particle fumed silica A was higher. The causes of these differences were revealed by the later inspection of the coating surfaces with a scanning electron microscope. Inspection of the surfaces of the two coatings revealed the presence of coating cracks in the fumed silica B sample (Figures 45-47). It is believed that the cracks are the results of binder shrinkage, a known polyvinyl alcohol/silica phenomenon. Due to the greater surface tension forces between the smaller particles of silica B during drying, more cracks are formed in its coating

layer, which detrimentally decreased its gloss. The difference between the gloss of the alumina and silica pigments of comparable size is the result of the difference in the refractive index of the two pigments (9). The refractive index of alumina is well known to be higher than the refractive index of silica (10).

Although calendering significantly improved the gloss of the coatings, calendering is not always desirable in this application, because it can have the negative effect of compressing the coating layer. Compression of the coating layer reduces the pore volume in the coating layer, adversely affecting the rate of liquid absorption (ink receptivity) and, consequently, can reduce print quality. As indicated in Figure 48, air permeability decreased with calendering.

Dynamic contact angle measurements and printing studies on the calendered samples were performed to determine if the rate of liquid absorption and print quality were adversely affected. The dynamic contact angle of each sample was measured and compared to three commercial inkjet papers, two glossy and one matte, to determine the rate of liquid absorption and to study the influence of pigment type on the surface tension of the sheet. As seen in Figures 49-51, the contact angles decreased with increasing coat weight. This corresponds to the air permeability results, which showed the air permeability to also decrease with coat weight (calendered samples). Comparison of these figures show the initial contact angle of the alumina coating to be higher than the silica pigments, indicating a greater interaction between the surface and test fluid (distilled water). The differences in surface interactivity with water were found to be even greater than the alumina, for

the commercial papers tested (Figure 52). This is not surprising since no cationic polymers or coating additives were added to our coatings and the presence of such additives would have a pronounced affect on the interactivity of the surface.

The dynamic contact angle measurements also show significant differences in the rate of liquid absorption between the commercial papers and coated calendered samples produced in this study. The fumed pigments were all more absorptive than the commercial samples. It was observed that these samples also dried faster after printing. The commercial papers were prone to ink setoff and had to be handled carefully after printing, while the fumed alumina and silica samples could be handled immediately. Tests to quantify the drying properties of the sheet were attempted, and resulted in the development of a new ink drying test method (11).

The ink density of the calendered samples and commercial samples are presented in Figures 53-58. The results for the Epson printer were quite different from those for the HP printer. For all calendered paper samples, the ink densities of the HP printed samples were higher than those of the Epson printed samples. For both printers, the ink density of the black ink was higher than the density of the cyan, magenta, or yellow inks. The differences between the ink densities of both fumed silica coated papers and commercially produced papers are small.

The black ink gloss of the HP printed samples was higher than that on the Epson printer samples (Figure 59-60). The ink gloss of the fumed silica (B) coated paper was higher than that of the other samples. Delta gloss is the difference between the ink gloss and the paper gloss. Positive or zero values of delta gloss indicate that

coating gloss is not lost when it contacts the ink. Table 4 shows delta gloss for the black ink. The delta gloss of fumed silica (A) and (B) samples had some positive values, indicating that they maintain or enhance their coating gloss when contacted by the ink. These results are quite different from the fumed alumina results, which are negative in value, indicating that the coating gloss is higher than the ink gloss. Comparison of the delta gloss values to the coating gloss values (not shown), measured at the same angle of incidence, show the loss in ink gloss for the alumina samples to range from +10 to -25% depending on the coat weight. The delta gloss of the commercially printed inkjet papers were almost negative ranging from +5 to -25% for the Epson printer and from +8 to -23% for the HP printer. Thus, the fumed silica and aluminum coated papers are better than or comparable to the commercial papers in ink gloss behavior.

The dot fidelity results for magenta dots are shown in Figures 61-63. Dot fidelity includes the area of dots and dot roundness (12). Roundness is one of the most important factors of print quality, because it represents the shape of the dot relative to a perfect circle. If the roundness is 1, it means the dots are perfect circles. Values of roundness greater than 1.0 actually indicate lack of roundness. Therefore, the closer the value of roundness is to 1, the better the quality of dots.

Table 14. Delta gloss of each sample (black)

[Epson Printer]

Fumed alumina		Fumed Silica(A)		Fumed Silica(B)	
Coat Weight (g/m^2)	Delta Gloss	Coat Weight (g/m^2)	Delta Gloss	Coat Weight (g/m^2)	Delta Gloss
6.5	-8.90	6.8	-3.08	6.1	-0.18
9.1	-9.30	9.8	-2.99	8.9	-0.68
11.1	-9.30	12.8	-3.13	12.1	0.52
15.5	-8.68	16.3	-2.20	16.5	0.86

[Hewlett Packard Printer]

Fumed alumina		Fumed Silica(A)		Fumed Silica(B)	
Coat Weight (g/m^2)	Delta Gloss	Coat Weight (g/m^2)	Delta Gloss	Coat Weight (g/m^2)	Delta Gloss
6.5	-9.12	6.8	-1.94	6.1	1.42
9.1	-8.73	9.8	-2.67	8.9	0.18
11.1	-9.56	12.8	-0.05	12.1	1.24
15.5	-8.90	16.3	1.23	16.5	1.34

The absolute area of a printed dot is important, because it represents the actual resolution of the printer, as opposed to the manufacturer's quoted resolution. The dot area should be as small as possible, while still being able to fill a solid area. The smallest space-filling dot has a diameter $\sqrt{2}$ times the spacing between dots (13). For example, the smallest diameter for a 300 dot per inch printer would be 120 μm. Any dots larger than this will only decrease the sharpness of the image without contributing significantly to the print density.

In essentially all of the cases, the roundness and dot diameter decrease with increasing coat weight (Figures 61-63). The dot diameters are all a factor of 2-3 larger than the smallest space-filling size discussed above (120 μm for the HP at 300 dots per inch and 50 μm for the Epson at 720 dots per inch).

The pore size distributions of the fumed silica (A and B) and fumed alumina produced papers are compared to that of commercial papers in Figures 64-66. The pore size distributions of the fumed pigments are much different from those of commercial papers. The incremental intrusion of the commercial glossy papers was different from that of fumed pigments samples because theirs pore structures consist of multiple coating layers.

Conclusion

The optical properties, brightness and gloss, were affected by pigment type and coat weight. The correlation between improvements in optical properties and

smoothness indicate that the property improvements were due to an increase in surface coverage with coat weight. Air permeability (PPS porosity) decreased with coat weight.

The substantial increase in gloss with calendering for the fumed pigments demonstrates that the particle sizes of the fumed pigments are sufficient to produce a high gloss inkjet coating.

Print quality, as measured by ink density, ink gloss, delta gloss, and roundness was strongly dependent on pigment type and correlated well with air permeability results. Coat weight did not significantly affect these properties. The difference in print quality between the two printers indicates differences between the two inking systems.

SEM photographs revealed the presence of coating cracks. Regardless of the pigment type, cracks were present. However, the cracks were larger for the pigment of smaller particle size, fumed silica B.

The mercury porsimetry data showed the pore size distribution of the two fumed silica samples were similar to one another, even though the particle sizes of the pigments were different. The pore size distribution of the alumina coating differed significantly from the silica coatings. The pore size distribution for both fumed pigments differed significantly from the commercial samples.

References

1. Kulmala, A., Paulapuro, H. and Oittinen, P., "Paper requirements for electrophotographic printing," IS&T NIP10, 10th International Congress on Advances in Non-Impact Printing Technologies, Springfield VA, 1994, pp. 466 - 470.

2. Chapman, D.M., "Silica-Gel coatings for ink-jet media," Grace Davison (internal document), Baltimore, MD.

3. Withiam, M. C., "Silica Pigment Porosity Effects on Color Inkjet Printability", IS&T, NIP12, 12th International Congress on Advances in Non-Impact Printing Technologies, pp 409-417.

4. Boothby, C., "New technology drives global coating trends," PIMA Papermaker, May 1997, pp. 38-45.

5. Boylan, J.R., "Using polyvinyl alcohol in inkjet printing paper," TAPPI, 80(1): 68 – 70, 1997.

6. Londo, Mike., "On-machine coating of inkjet paper possible with modified kaolin," Pulp and Paper, May 2000, pp. 37-43.

7. Omura, Tomonobu., Ueno, Takashi., and Limori, Yoshifumi., "Glossy inkjet media by cast-coating method", Proceeding of the 1998 Pan-Pacific and International Printing and Graphic Arts Conference, 1998, pp. 169-174.

8. Asano, Shinichi. *et al.*, U.S patent 5670242 (September 23, 1997).

9. Lee, D. I., " A Fundamental Study on Gloss", TAPPI Coating Conference, 1974, pp.97-103.

10. Dean, Trevor., "The Essential Guide to Aqueous Coating of Paper and Paperboard", PITA,1997, pp.3.1-3.66.
11. Thummala, Vinay., Joyce, Margaret and Fleming, P. D., "A Near Infrared Drying Technique for Measuring Inkjet Drying Time", In Preparation.

12. Sarafano, J. and Pekarovicova, A., "Factors Affecting Dot Fidelity in Solvent Based Publication Gravure", American Ink Maker, 77, 732-36 (1999).

13. Cawthorne, James., Fleming, Paul D., Mehta, Falguni, Halwawala, Saurabh and Joyce, Margaret, "Interpretation of Dot Area and Dot Shape based on Image Analysis", In Preparation.

Acknowledgement

We appreciate Wausau Paper Company (Otis, Maine) for supplying the base paper for this study.

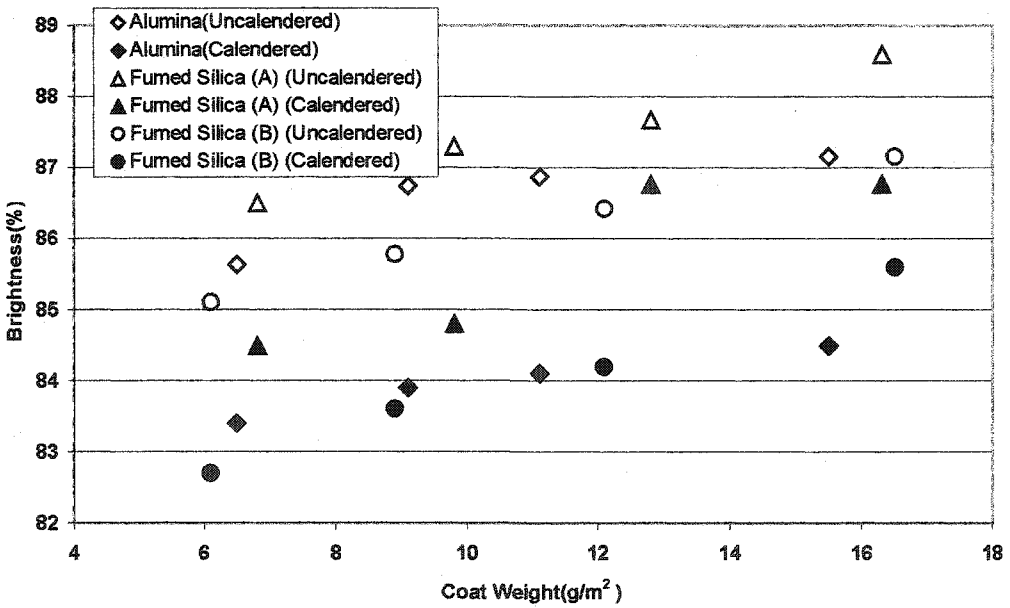

Figure 42. Influence of pigment on brightness

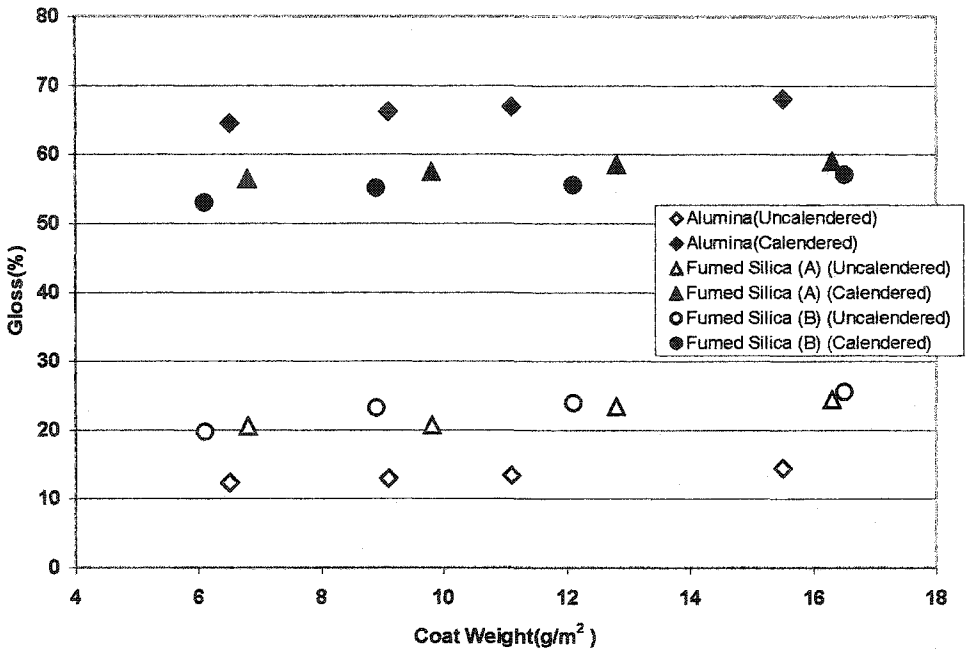

Figure 43. Influence of pigment on gloss

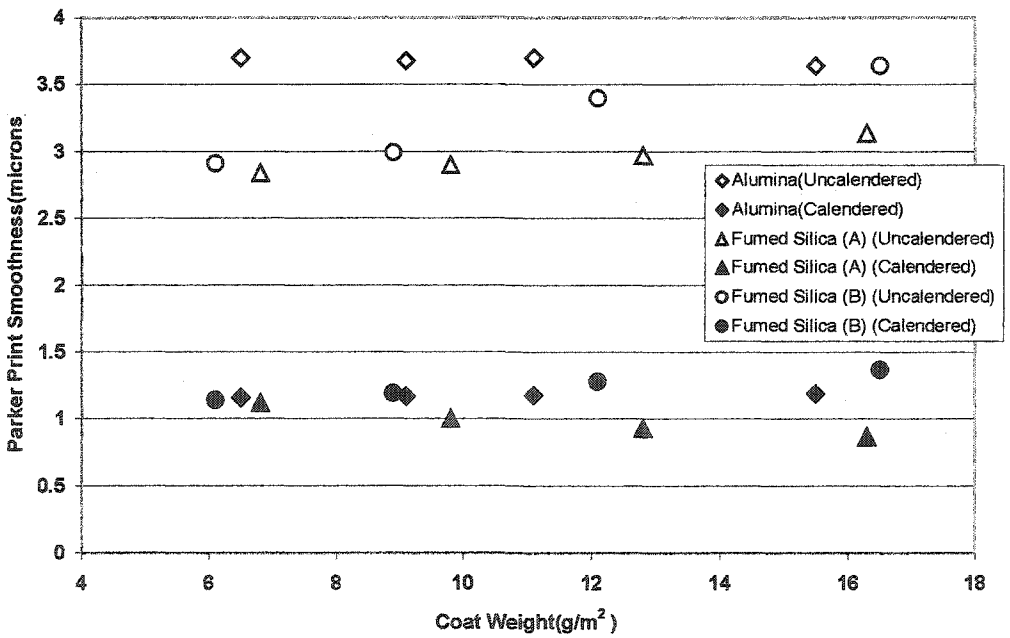

Figure 44. Influence of pigment on smoothness

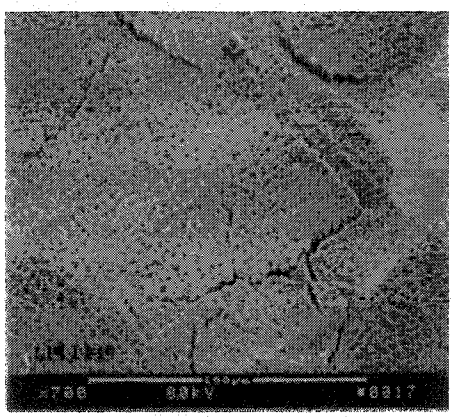

(700x magnifications)

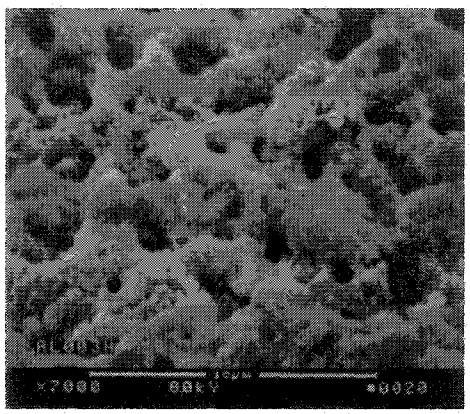

(7000x magnifications)

(Uncalendered Samples)

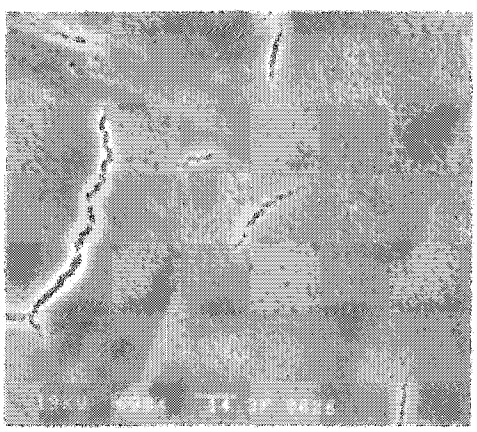

(700x magnifications)

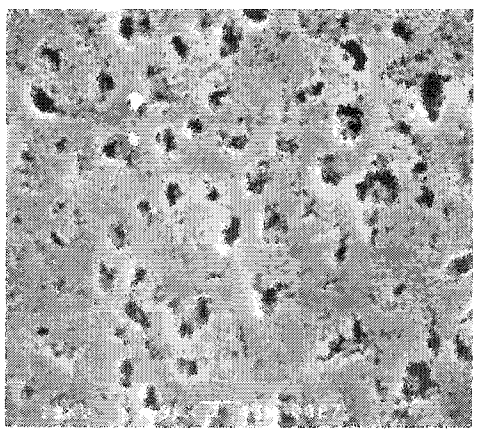

(7000x magnifications)

(Calendered Samples)

Figure 45. SEM pictures of alumina (Coat weight: 6 g/m^2)

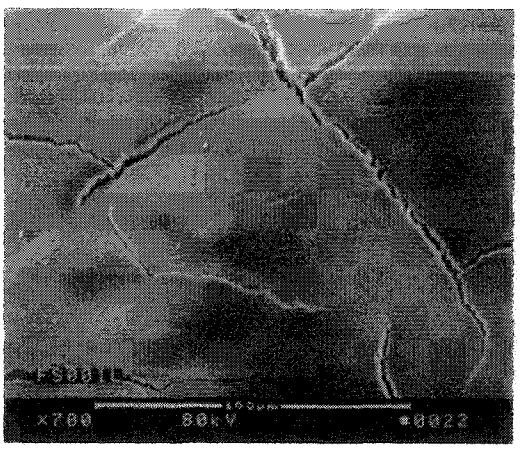

(700x magnifications)

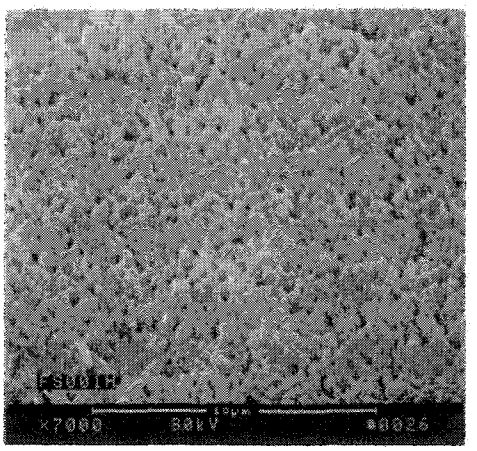

(7000x magnifications)

(Uncalendered Samples)

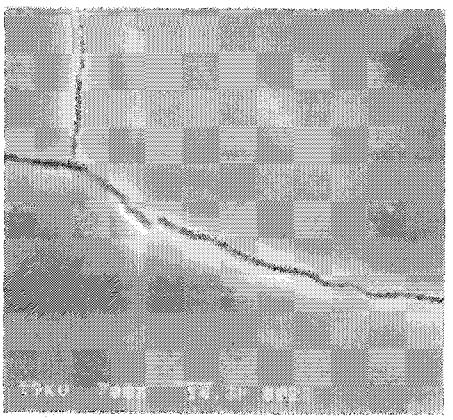

(700x magnifications)

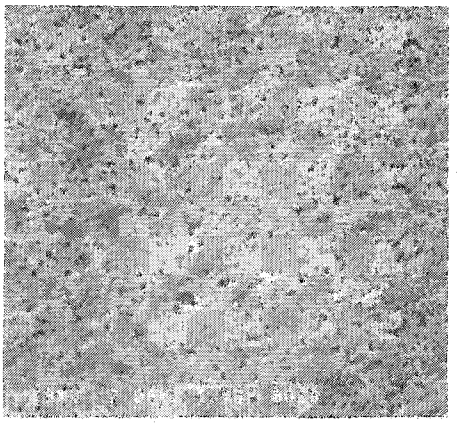

(7000x magnifications)

(Calendered Samples)

Figure 46. SEM pictures of fumed silica (A) (Coat weight: 6 g/m^2)

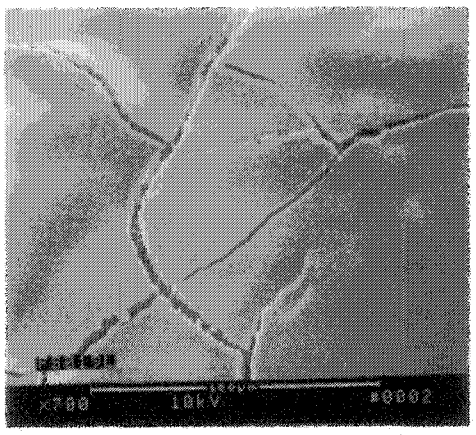

(700x magnifications)

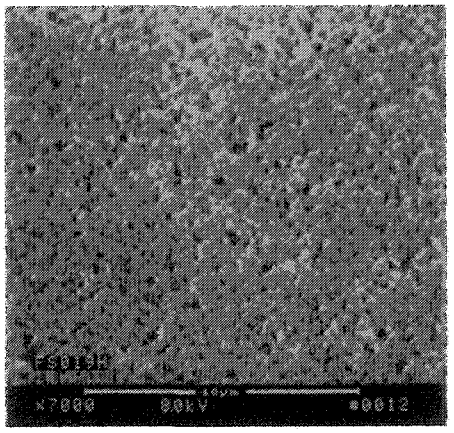

(7000x magnifications)

(Uncalendered Samples)

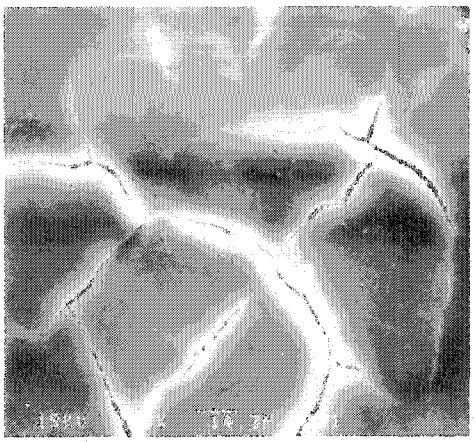

(700x magnifications)

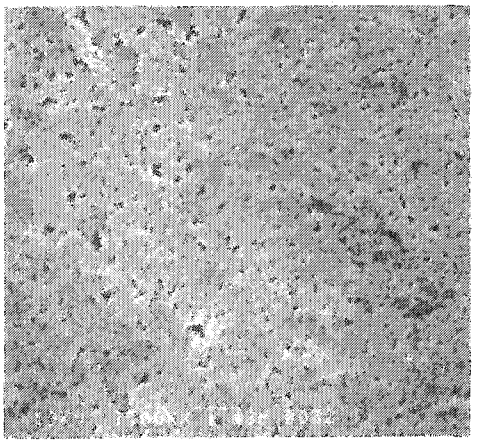

(7000x magnifications)

(Calendered Samples)

Figure 47. SEM pictures of fumed silica (B) (Coat weight: 6 g/m^2)

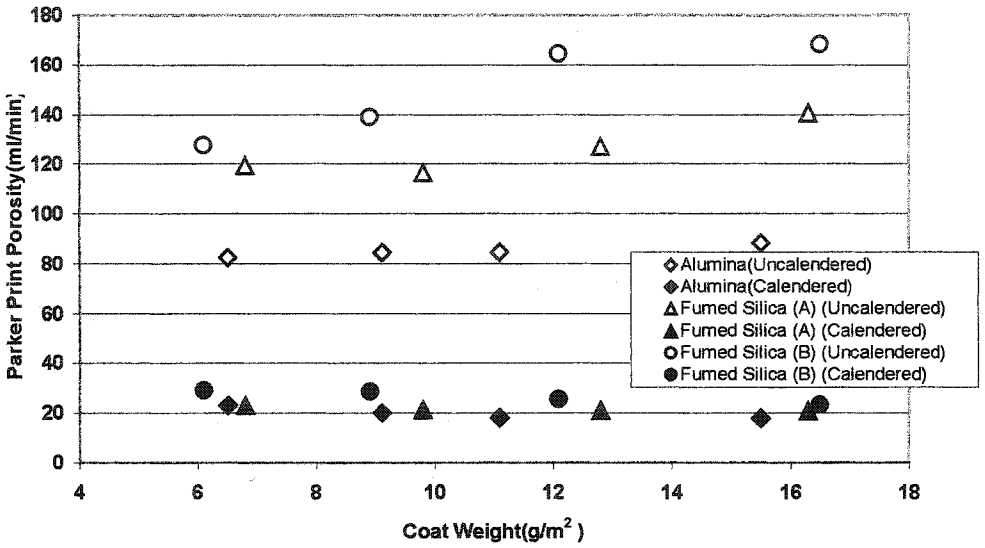

Figure 48. Influence of pigment on air permeability

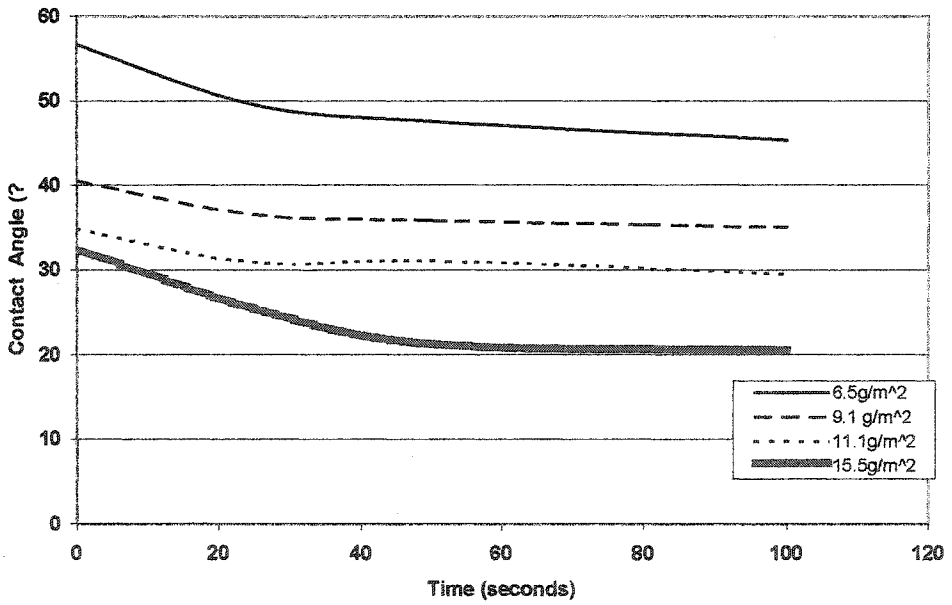

Figure 49. Contact angle of CLC coatings of alumina

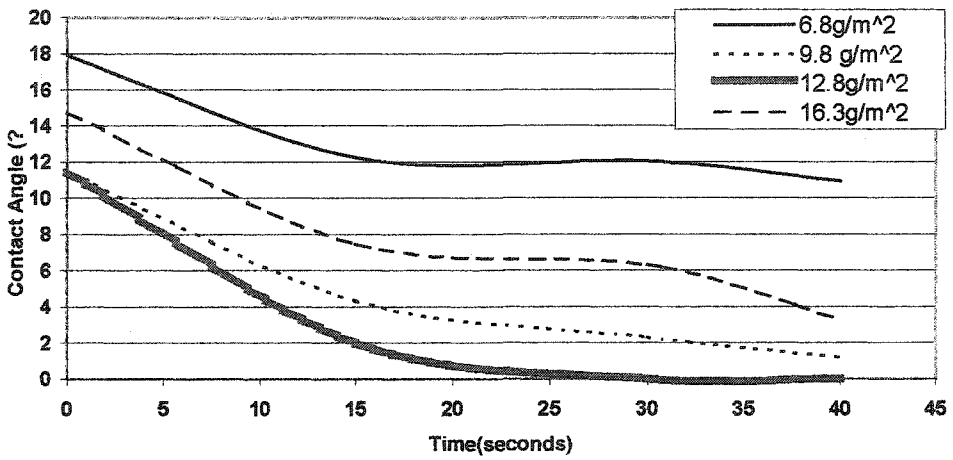

Figure 50. Contact angle of CLC coatings of fumed silica (A)

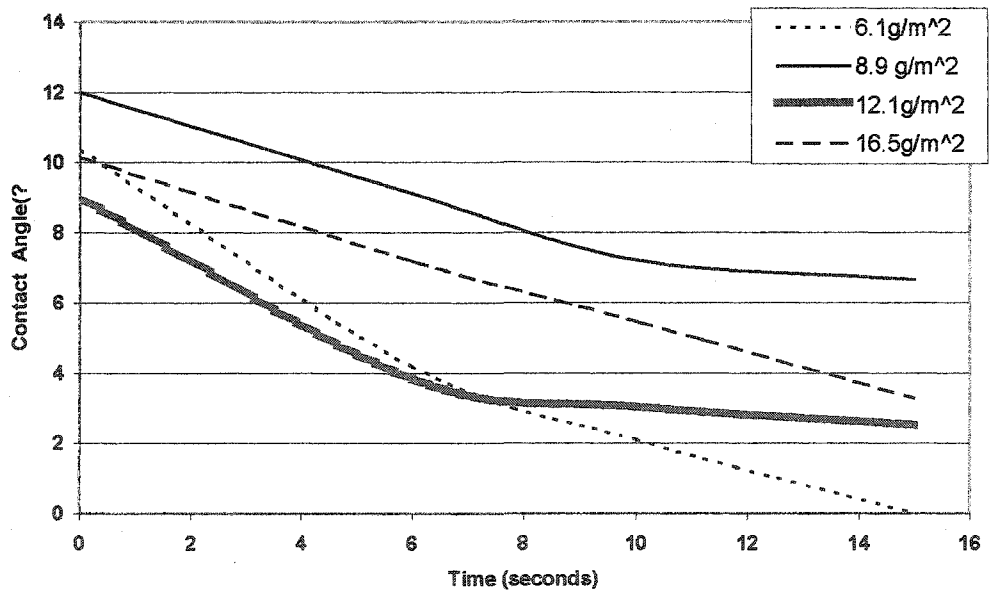

Figure 51. Contact angle of CLC coatings of fumed silica(B)

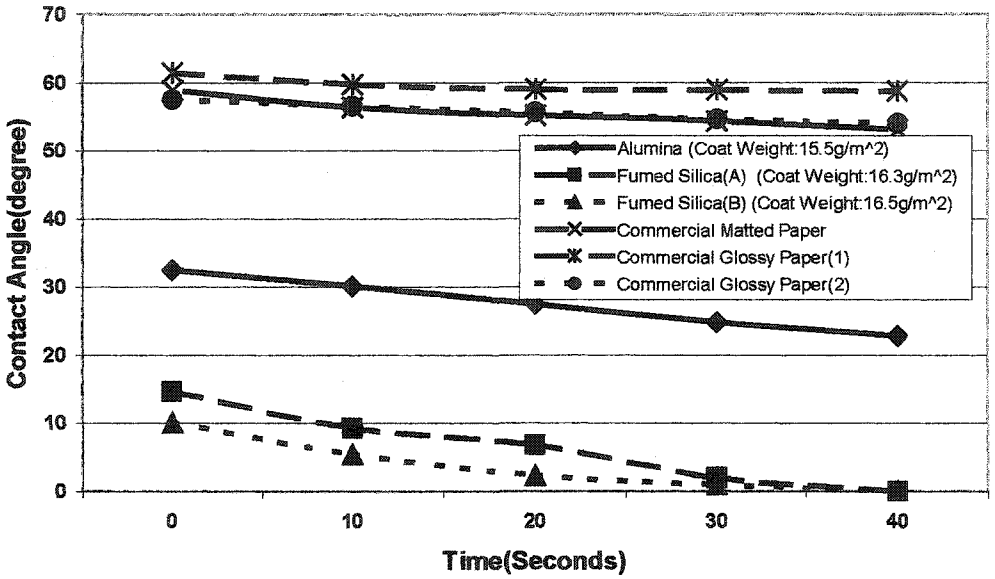

Figure 52. Contact angle comparison of fumed pigments and commercial papers

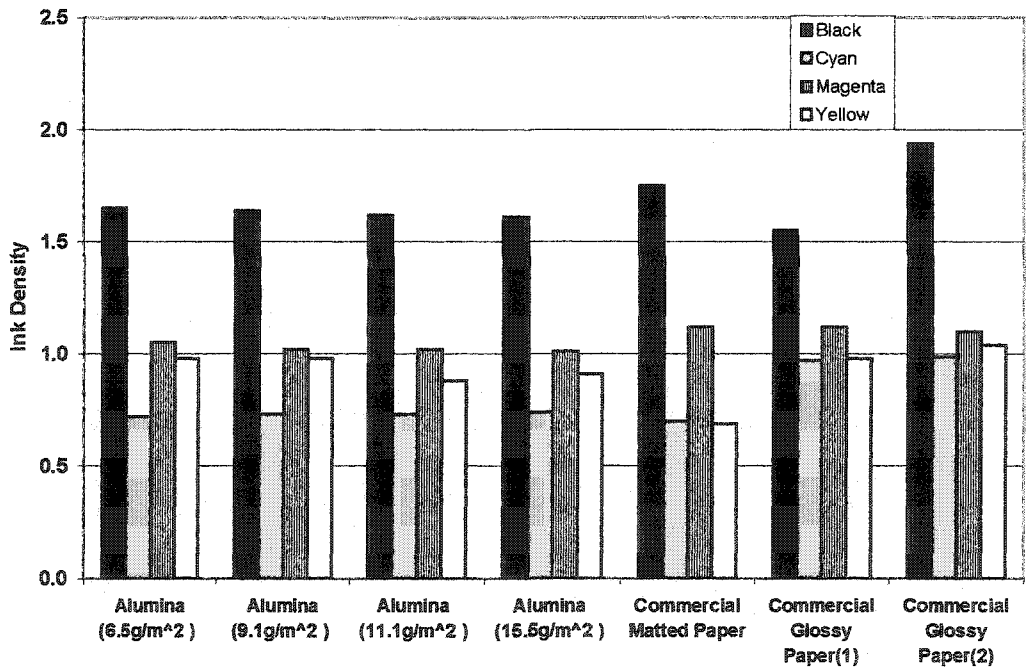

Figure 53. Ink density comparison of each sample (Epson printer)

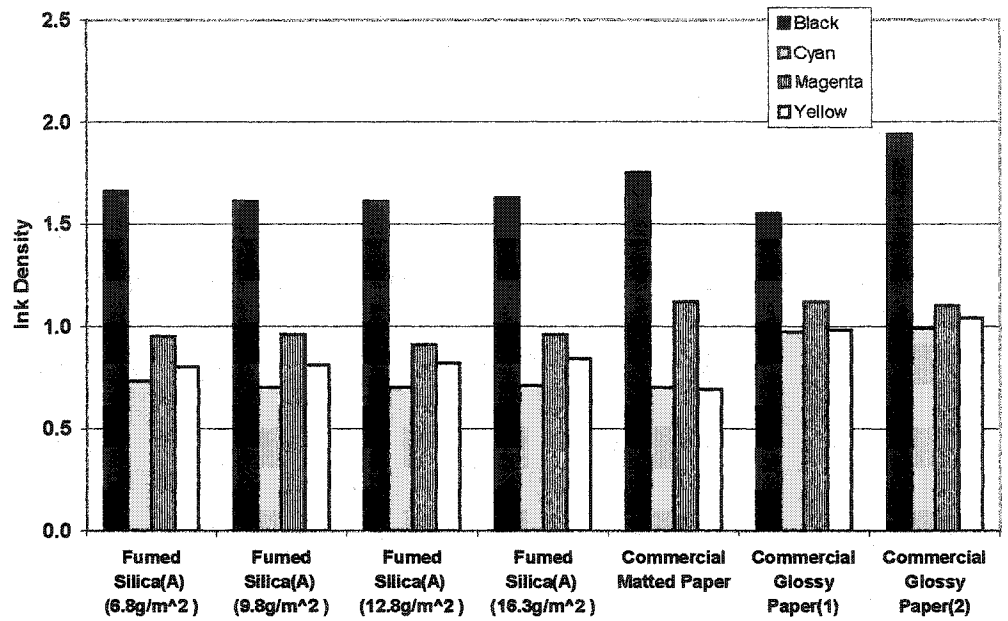

Figure 54. Ink density comparison of each sample (Epson printer)

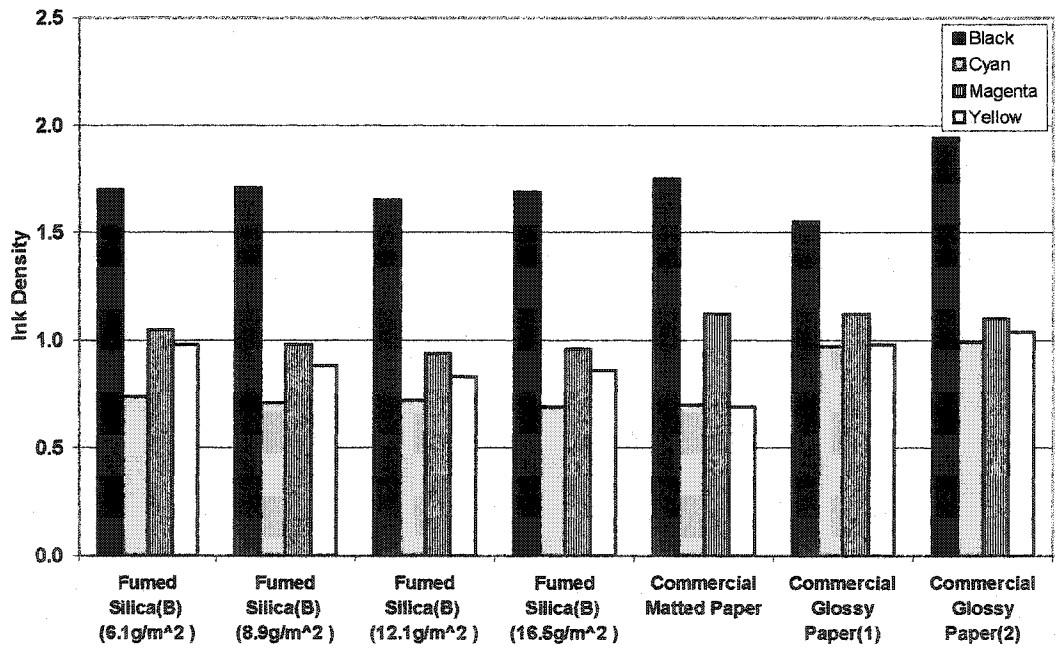

Figure 55. Ink density comparison of each sample (Epson printer)

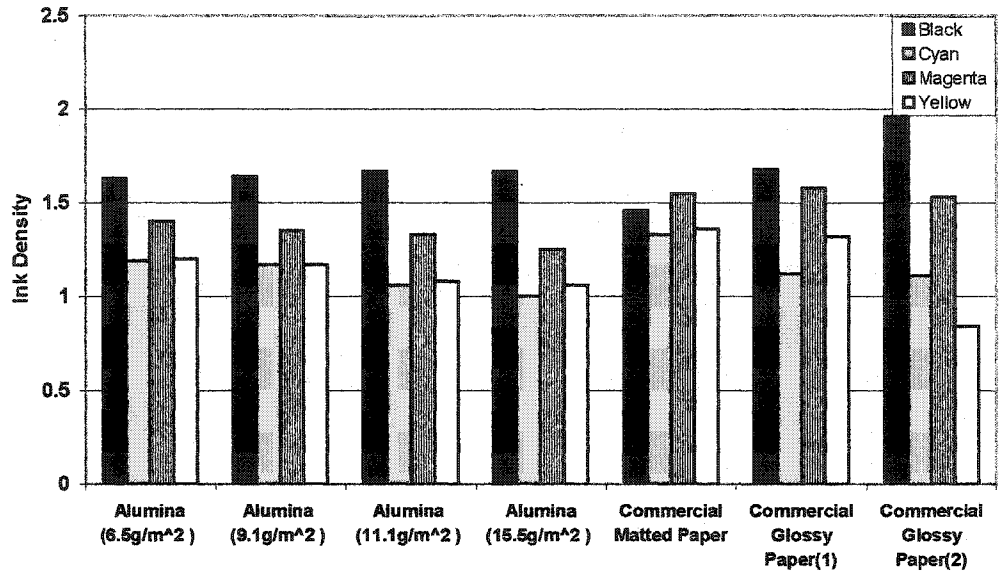

Figure 56. Ink density comparison of each sample (Hewlett Packard printer)

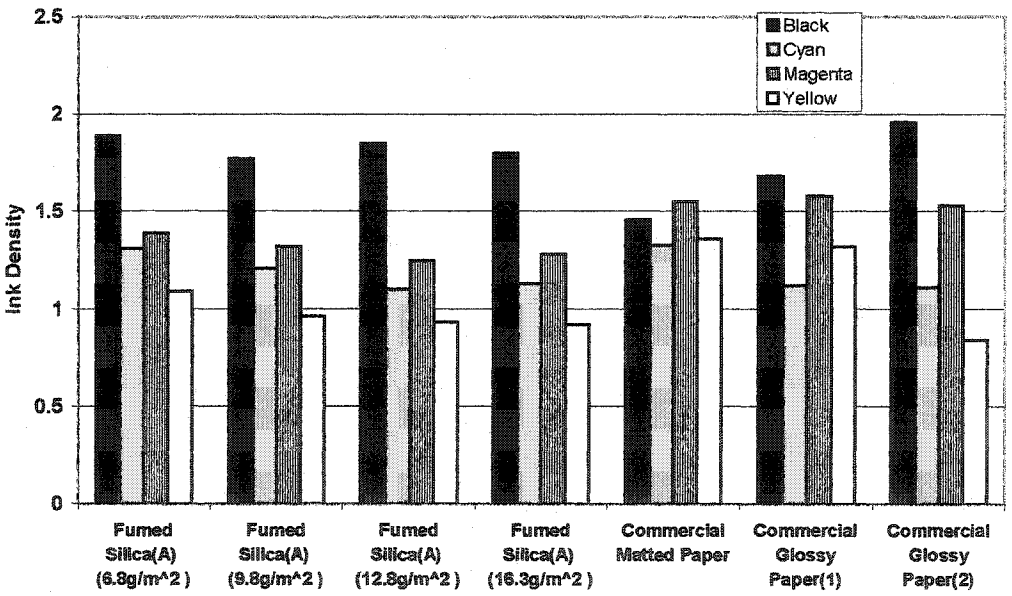

Figure 57. Ink density comparison of each sample (Hewlett Packard printer)

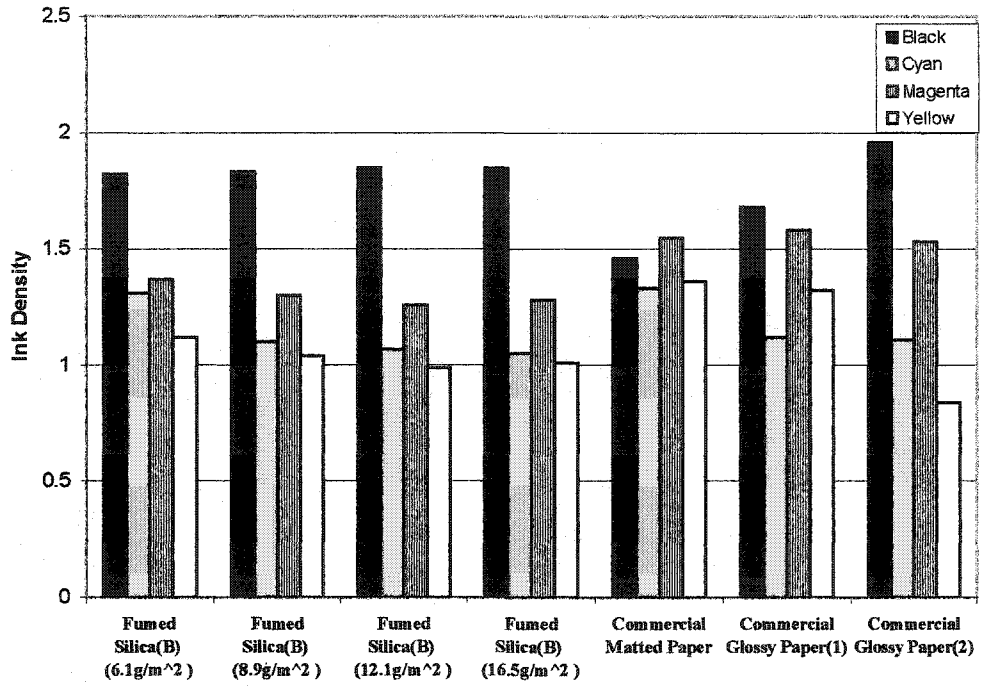

Figure 58. Ink density comparison of each sample
(Hewlett Packard printer)

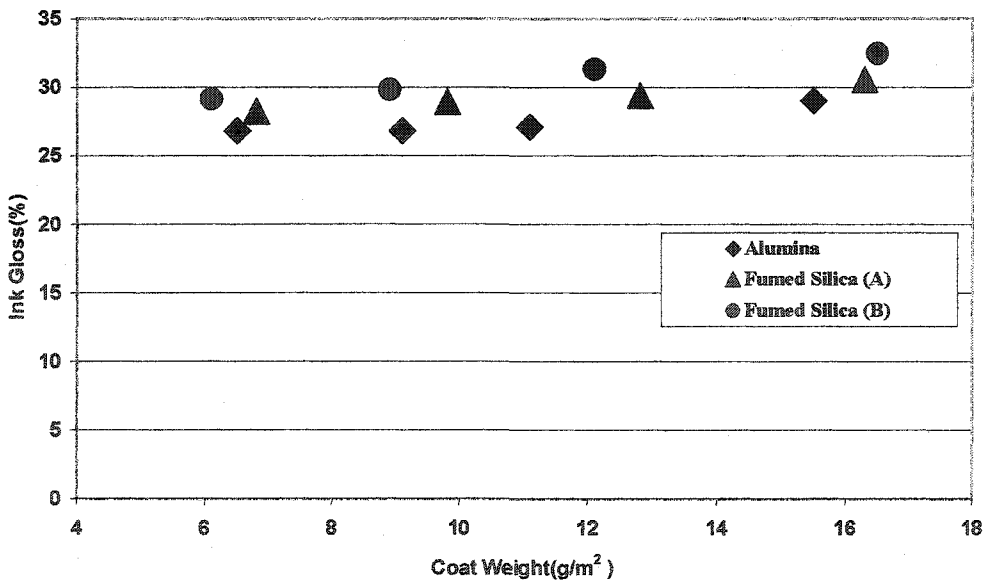

Figure 59. Ink gloss comparison of each sample
(Black, Epson printer)

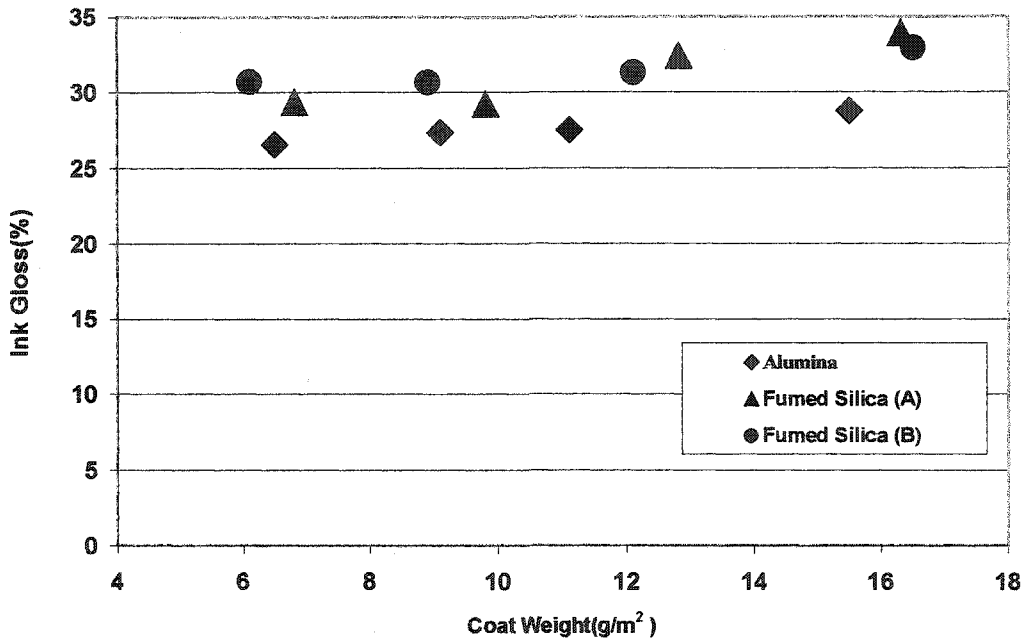

Figure 60. Ink gloss comparison of each sample
(Black, Hewlett Packard printer)

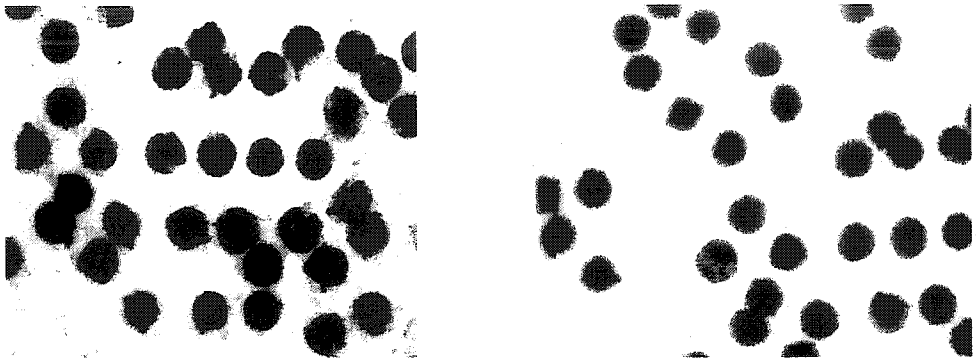

(Roundness=1.20, Standard deviation: 0.39) (Roundness=1.12, Standard deviation: 0.26)

(Diameter= 192 μ) (Diameter= 169 μ)

(A) Epson printing samples (Coat weight; left: 6.5 g/m^2, right: 15.5 g/m^2)

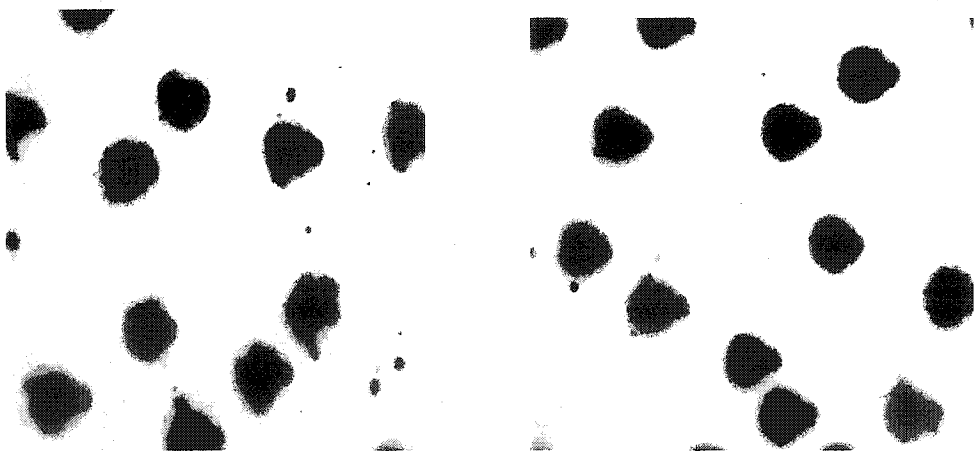

(Roundness=1.25, Standard deviation: 0.21) (Roundness=1.17, Standard deviation: 0.30)

(Diameter= 237 μ) (Diameter= 216 μ)

(B) Hewlett Packard printing samples (Coat weight; left: 6.5 g/m^2, right: 15.5 g/m^2)

Figure 61. Printing dots of alumina samples (Color: magenta)

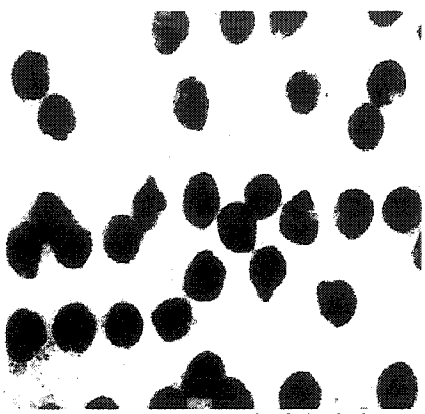

(Roundness=1.28, Standard deviation: 0.45)

(Diameter= 193 μ)

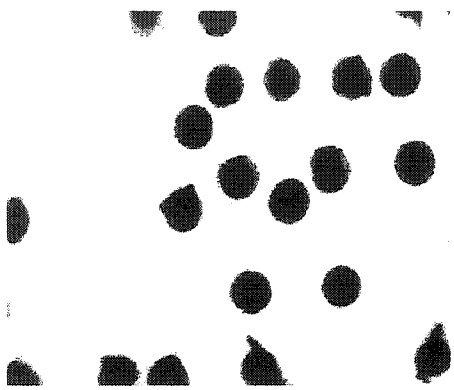

(Roundness=1.08, Standard deviation: 0.04)

(Diameter= 190 μ)

(A) Epson printing samples (Coat weight; left: 6.8 g/m^2, right: 16.3 g/m^2)

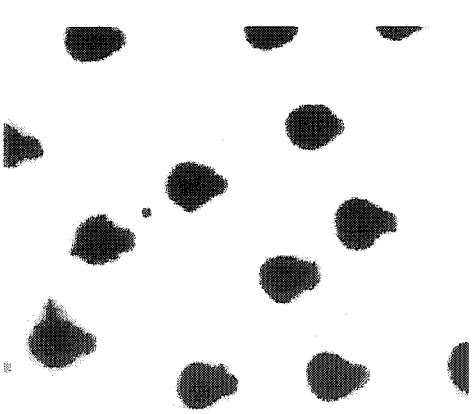

(Roundness=1.16, Standard deviation: 0.11)

(Diameter= 219 μ)

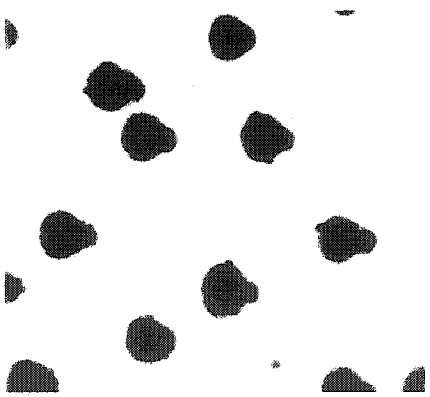

(Roundness=1.14, Standard deviation: 0.08)

(Diameter= 201 μ)

(B) Hewlett Packard printing samples (Coat weight; left: 6.8 g/m^2, right: 16.3 g/m^2)

Figure 62. Printing dots of fumed silica (A) samples (Color: magenta)

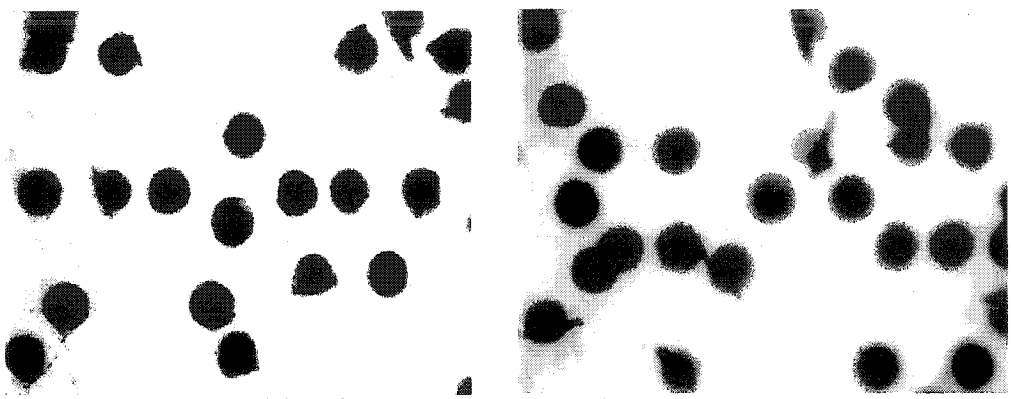

(Roundness=1.23, Standard deviation: 0.17) (Roundness=1.25, Standard deviation: 0.23)

(Diameter= 169 μ) (Diameter= 174 μ)

(A) Epson printing samples (Coat weight; left: 6.1 g/m^2, right: 16.5 g/m^2)

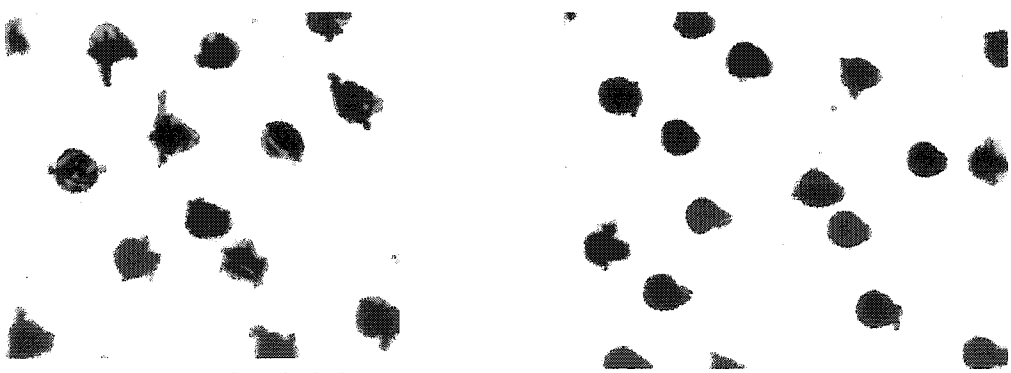

(Roundness=1.18, Standard deviation: 0.14) (Roundness=1.39, Standard deviation: 0.30)

(Diameter= 200 μ) (Diameter= 173 μ)

(B) Hewlett Packard printing samples (Coat weight; left: 6.1 g/m^2, right: 16.5 g/m^2)

Figure 63. Printing dots of fumed silica (B) samples(Color: magenta)

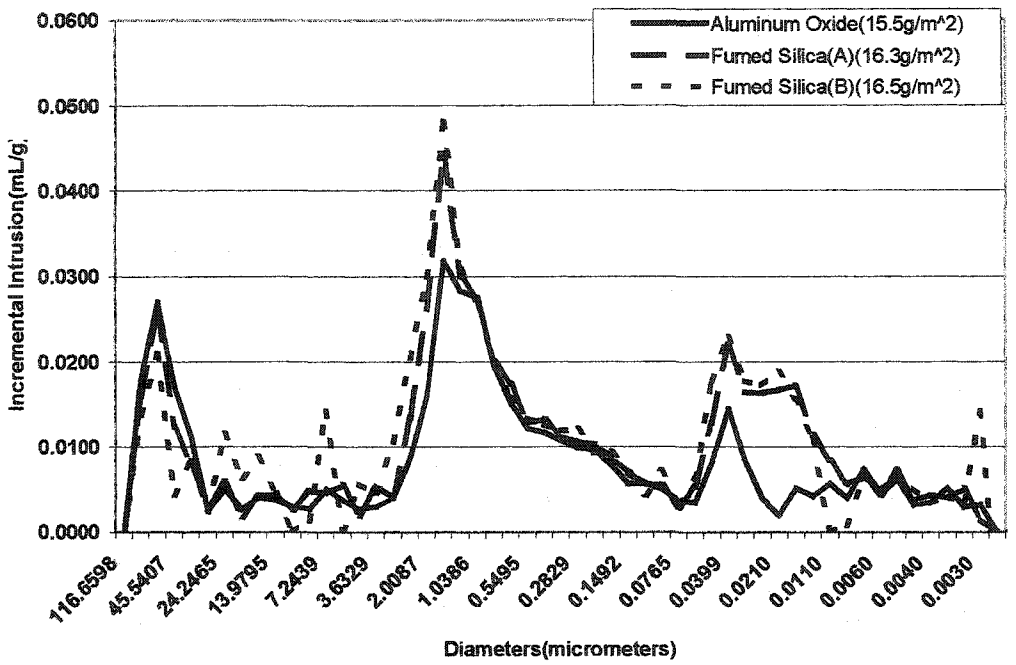

Figure 64. Pore size distribution of metallic oxides coatings by mercury intrusion porosimeter

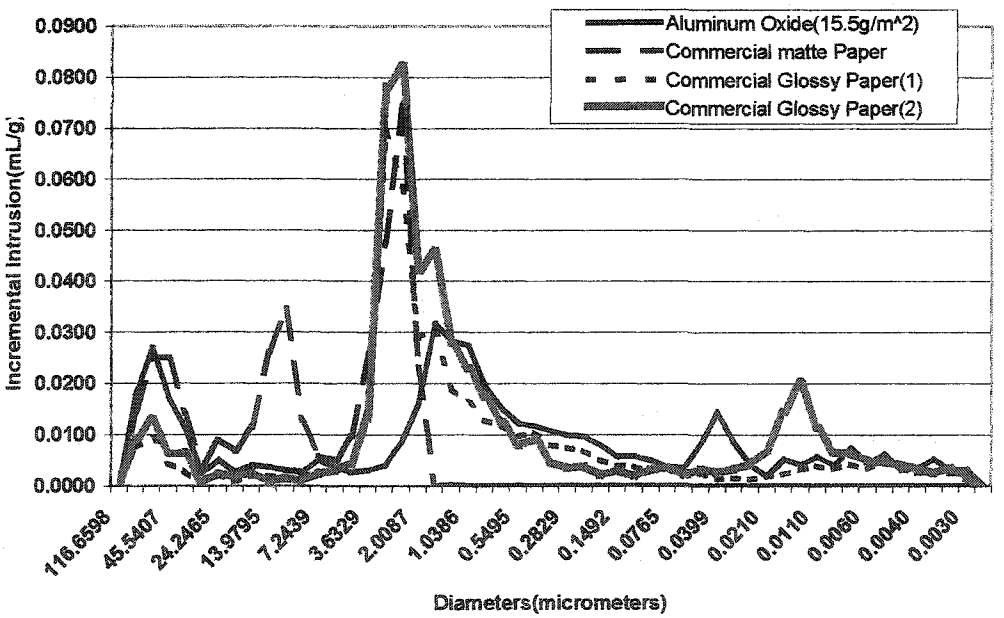

Figure 65. Pore size distribution of alumina and commercial papers by mercury intrusion porosimeter

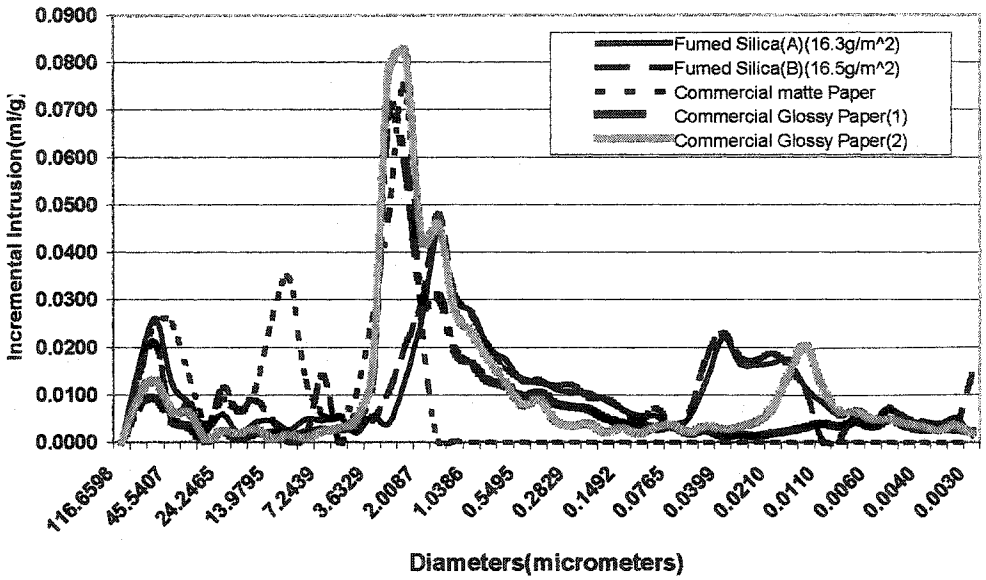

Figure 66. Pore size distribution of fumed silicas and commercial papers by mercury intrusion porosimeter

INFLUENCE OF PIGMENT PARTICLE SIZE AND PACKING VOLUME ON PRINTABILITY OF GLOSSY INKJET PAPER COATINGS – PART I

Hyun-Kook Lee, Margaret K. Joyce, and Paul D. Fleming

Department of Paper Engineering, Chemical Engineering and Imaging

Western Michigan University

Kalamazoo, Michigan 49008

Abstract

The optical properties and printability of inkjet coated papers are influenced by smoothness, surface chemistry and pore structure of the surface coating layer. To control these properties, the coating formulator must select the proper pigment(s) and binder(s), the two main components of any coating. For glossy inkjet papers, small particle, large surface area fumed silica and aluminum pigments have been shown to provide the desired properties for high quality glossy inkjet coated papers. However, their high cost and low make-down solids, in comparison to conventional pigments, has limited their use by the industry to these specialty grades.

The focus of this study was to determine if the costs and application solids of fumed silica and alumina coatings could be improved by extending the pigments with less expensive compatible pigments. The effects of the resultant change in packing volume and particle size distribution on the optical properties and printability were

determined. Blends capable of providing equal or better gloss and printability, at a reduced cost, were sought.

It was determined that up to 30 parts of the fumed silica and alumina could be replaced with less expensive compatible pigments, without significant loss to the optical and printing properties of the glossy inkjet paper.

Introduction

Inkjet printing has proven to be the first digital technology that has achieved an acceptable level of color quality at an affordable price for the majority of home/office end users [(1)]. As a result, there is a demand for inkjet media with intermediate and high gloss finishes, so that the inkjet printed image may resemble a photographic image. It is expected that as image quality improves and throughput speeds increase, inkjet printing will continue to expand into more printing markets and may begin to challenge electrophotography in many high-end applications. A key to meeting the needs of this evolving market is the development of coated inkjet media capable of providing the desired glossy image characteristics of photographic papers.

Another key optical property for photo quality papers is brightness. Brightness is important for print contrast. The higher the brightness, the higher the contrast between the paper and printed image, hence the "snappier" the image. For the paper industry, absolute brightness is defined as the reflectance of blue light peaking at a wavelength of 457 nm in terms of a perfectly reflecting, perfectly diffusing surface.

The brightness of pigment-coated paper is heavily dependent on the brightness of the raw stock. Therefore, the raw stock should have brightness as close as possible to that of the dried coating layer. The principal coating components that influence brightness are the pigments, binders, additives, and the relative proportion of each used in the coating formulation [2]. Optical brighteners [3-5] are commonly used in these grades. Papers with brightness values greater than 90, and as high as 100, are currently being marketed.

According to TAPPI standards [6], gloss is defined as the 75° spectral reflectance of light at λ = 550 nm. Based on this definition, coating gloss is optimized by increasing the refractivity of the coating layer, while minimizing the roughness of the coated surface layer.

The scattering coefficient is the fraction of light incident upon an infinitesimally thin layer of the material that is scattered backwards by that layer, divided by the basis weight of the layer. It is expressed in reciprocal basis weight units. Kubelka and Munk [7] provided a direct mathematical relationship between scattering absorption, and opacity.

The original theory of Kubelka and Munk was developed for light diffusing and absorbing infinitely wide colorant layers. Due to its simple use and to its acceptable prediction accuracy, this model is very popular in industrial applications. The concept is based on the simplified picture of two diffuse light fluxes through the layer, one proceeding downward and the other simultaneously upward [5,8,9].

Recent research in our laboratory by Lee et al [10,11] and Ramakrishan [12] showed that fumed metallic oxide pigments are capable of producing semi-gloss and high-gloss inkjet papers with acceptable print quality after calendering. In these works, it was found that the gloss of fumed alumina pigments was higher than fumed silica. An important finding of Ramakrishan's studies was that the gloss of the inkjet papers increased with an increase in silica particle size, which does not follow the findings for conventional pigments. The loss in gloss with reduction in silica particle size was attributed to the presence of coating cracks. The cracks were shown to result from drying stresses, which increased with an increase in silica surface area. Cracking was not present in the alumina coatings, resulting in the alumina coatings providing higher gloss values at equal coat weights.

Ink density is an important performance parameter in the printing process. Ink density impacts the final visual quality, color gamut, and color fidelity. The main factor identified with color density is the concentration of colorant in the ink. Other major factors determining ink density are ink dot coverage on the coating surface and colorant concentration at the surface. In the interaction of the colorant with coated paper, electrostatic interactions play the key role in colorant-coated paper interactions. The nature of the anionic dyes and the oxides will determine the print quality of the inkjet printing, since electrostatic interactions of colorant with coated media occur between the anionic groups of dyes and the oxides. The binding energies of the dyes are greatly increased by electrostatic interactions, resulting in a high binding strength [13,14].

Ink gloss depends on the smoothness of the substrates and the smoothness of the ink layer. Another factor contributing to the smoothness of the printed film is the amount of vehicle on the surface. If the pigment particles are completely covered by a level film of the vehicle, a good approximation to a mirror surface usually results irrespective of the smoothness of the substrates or of the ink [15]. However, the use of dyes rather than pigments in inkjet inks makes the former more relevant than the later.

Generally, optical properties and printing properties improve with increases in the coat weight, since increasing coating materials improve properties of the coated surface, For example, reflectance of light and ink absorption both increase with increased coat weight.

The objective of this research was to determine if less expensive compatible pigments could be blended with fumed alumina and silica pigments to yield coatings with equal or better glossing and printing properties. The influence of pigment blending on the packing volume of the coating was studied and the relationship between packing volume and inkjet print quality was determined.

Experimental design

Selected pigments were obtained from several pigment companies. Aluminum oxide (AO), fumed silica (FS), precipitated calcium carbonates (PCC), ultrafine ground calcium carbonate (UFGCC), alumina trihydrate (ATH), and baumite were

studied. The physical properties of the pigments and the ratio of the pigments used are shown in Table 1.

The binder used in the coating formulation was a partially hydrolyzed, low viscosity, polyvinyl alcohol (Airvol 203, Air Products Inc.). This polyvinyl alcohol was chosen to optimize the % coating solids by minimizing the interaction between pigments and PVOH and to promote the ink receptivity of the coating layer to the water based inkjet inks. Solutions of polyvinyl alcohol were prepared at 30% solids by adding the required amount of dry PVOH powder to cold-alkaline water (pH 9.0-10.0) under agitation and heating the mixture to 185°F. The solution was held at this temperature for 35-40 minutes to assure complete dissolution and hydration of the PVOH. A defoamer was then added (Foammaster VF, Henkel, Inc.). The solution was cooled to 40°F before adding the slurried pigments at a slow rate of agitation. The coatings were mixed for 30 minutes and the pH and viscosity measured. Coatings containing different fumed and conventional pigment ratios (50:50, 70:30, and 80:20, respectively) were prepared and draw downs made using various Mayer rods.

From this initial study, it was determined that PCC and UFGCC were the two most compatible pigments for blending with fumed silica due both their high pH requirements and high glossing properties. For the fumed alumina, baumite and alumina trihydrate performed best. It was also determined that substitution levels greater than 30 parts of these pigments into the coating, greatly diminished the gloss of the coatings, to where the coating gloss would not be acceptable for this commercial grade of inkjet paper. Based on these finding, the coatings for cylindrical

laboratory coating studies, CLC, application were prepared at a 70:30 ratio, a pigment-to-binder ratio of 7:1 and final solids of 30 ±1%.

Table 15. The physical properties of pigments as supplied

Sample	Solids Content	Color	Specific Gravity	pH	Refractive Index	Avg. Particle size (nm)
AO	40%	White	1.40	3.8-4.2	1.76	160
FS	30%	White	1.20	10.0-10.3	1.46	225
PCC	70%	White	2.72	9.0-10.0	1.58-1.63	544
UFGCC	75%	White	1.92	9.0-10.0	1.58	600
Baumite	30%	White	1.1-1.3	4.0-6.0 (5% sol)	1.65-1.66	200
ATH	65%	White	2.42	6.70	1.57	400

The coatings were applied to a 75 g/m^2 commercial base paper using a Cylindrical Laboratory blade coater at a speed of 2000 fpm. For each sample, the basepaper was pre-dried at 25% power for 10 s and post-dried at 100 % power for 60 s. Four different coat weights were applied: 6 g/m^2, 8 g/m^2, 10 g/m^2, and 12 g/m^2.

The brightness values of the papers were measured using the standard procedure [16] on a Technidyne Brightness meter. Gloss was measured using a Hunter 75° gloss meter according to the standard procedure [6].

The samples were printed on an Epson Stylus 900, Hewlett Packard 932C and

Canon S450 inkjet printers using a proprietary test print pattern created with Adobe software [10-13]. The printed images were bars of four solid colors (cyan, magenta, yellow, and black). The Epson 900 is a piezoelectric printer with a resolution of 1440 x 720dpi. The HP 932C is a thermal inkjet printer with a resolution of 2400 x 1200 dpi. The Canon S450 printer is thermal inkjet printer with a resolution of 1440 x 720 dpi. Print gloss was measured using a Gardener 60° Micro-Gloss meter. Print density was measured using a X-Rite 408 densitometer. Roundness was measured at 30% tone scale by using a Hitachi HV-10 camera and ImagePro Plus, version 3.0, was used for image detail analysis [10-13, 16].

Table 16. Ratio of pigments used.

Sample	Pigments	Parts	Viscosity* (cP)	pH
Sample A	Fumed silica	70	572	9.2
	UFGCC	30		
Sample B	Fumed silica	70	254	9.7
	PCC	30		
Sample C	Aluminum Oxide	70	984	5.9
	ATH	30		
Sample D	Aluminum Oxide	70	1766	6.9
	Baumite	30		
Sample E	Fumed Silica	100	72	9.8
Sample F	Aluminum Oxide	100	1231	8.1

*Viscosity=Brookfield viscosity, RPM:100, spinindle:#4

The coated samples were calendered on one side, through 3 nips at 123 kN/m and 60°C.

Results and discussion

The influence of coat weight and pigment type on brightness is shown in Figure 67. Both the coat weight and pigment type influenced the brightness of the coating. The addition of the calcium carbonate to the fumed silica improved the coating brightness. The addition of ATH increased the brightness of the fumed alumina. Comparison of the brightness data to calculated light scattering coefficient values for the data showed a strong correlation (See Figure 68).

The scattering coefficients of the coatings were calculated using the following equations [8]:

From the measurements of R_0 and $C_{0.89}$

$$a = 0.5(R_{0.89} + (R_0 - R_{0.89} + 0.89)/(0.89R_0)) \quad (1)$$

$$b = 0.5(1/R_\infty - R_\infty) \quad (3)$$

$$x = (1 - aR_0)/bR_0 \quad (4)$$

$$R_{0.89} = R_0 / C_{0.89} \quad (5)$$

$$R_\infty = a - (a-1)^{1/2} \quad (6)$$

$$sW = (0.5/b)[\ln(x+1)/(x-1)] \quad (7)$$

$$S = sW/W \quad (8)$$

$R_{0.89}$= reflectance of the layer which has behind it a surface with reflectance of 0.89.

R_0 = reflectance of the layer with ideal black background

$C_{0.89}$= $R_0/R_{0.89}$ = TAPPI opacity, as a fraction

sW = scattering power

W = basis weight

S = light scattering coefficient (LSC)

From the above equations, it is seen that brightness is influenced by the amount of light scattered and absorbed. Light is absorbed when colored matter is present. Scattering is influenced by the surface area of the pigments and the number of air-to–pigment interfaces due to the higher degree of refractivity between the two interfaces. Scattered light, to some extent, can mask the visual effect of colored impurities.

The addition of carbonate significantly increased the LSC of the silica coatings, improving the coating brightness and gloss (Figure 69). The addition of ATH to the fumed alumina coating resulted in a slight increase in the LSC with a corresponding increase in coating brightness. The increase in brightness with LSC value indicates that addition of the carbonates and ATH increases the air voids in the packing structure enabling more light to be scattered. This is consistent with Figure 70, which shows the influence of pigment addition on coating PPS porosity.

The results indicate that the addition of the larger pigments to the fumed silica coatings increased the porosity of the coating layer, enabling the coating to scatter more incident light. As a result, the brightness, gloss, and opacity (Figure 71) of the coatings increased. Unlike the fumed silica coatings, the LSC of fumed alumina coatings were not significantly changed by the addition of the ATH and baumite

pigments. The gloss of the fumed of alumina was the highest of all the samples tested. The addition of PCC to the fumed alumina enabled glosses comparable to the fumed alumina to be obtained.

Since gloss is a function of surface smoothness, the higher gloss could be indicating that fumed alumina (sample F) formed a smoother coat layer.

Chinmayanadam [18] has shown gloss to be a function of the refractive index and the wavelength of incident light, as well as the surface roughness:

$$\text{Gloss} = I/I_o = f(n,i)\ \exp[-(4\pi\sigma\cos(i)/\lambda)^2] \quad (9)$$

I and I_o are the specularly reflected and incident light intensities, f(n,I) is the Fresnel coefficient of specular reflection as a function of refractive index n and angle of incident light I, σ as the standard deviation of the surface roughness, and λ is the wavelength of incident light.

Application of this equation to the results indicate that the refractive index of sample F is sufficient to provide acceptable commercial glosses, if the proper alignment of the particles (in the case of platey pigments such as ATH) or smoothness of the coating layer is achieved. Small particles not only scatter more light, but better fill the microvoids within the coating and base paper, to provide higher smoothness than large and/or chunky particles. Although calendering improves smoothness, and hence gloss, it can have the negative effect of compressing the coating layer, adversely affecting the ink receptivity and consequently print quality of the paper.

The pore size distributions of the samples are shown in Figure 72. The LSC and Parker print porosity results for the fumed silica coatings correlate well to the Hg

porsimetry data. The results confirm that the addition of the needle shaped PCC (aragonite) with the grape-like silica clusters open the coating structure. The resultant structure was found to increase the print density and ink gloss of the samples (Figures 73-74). The results indicate that the new packing structure enables the ink dye to be fixed and dried closer to the coating surface. The ink density and gloss values of the fumed silica coatings were found to be higher than the fumed alumina coatings. In the case of ink density, the differences are probably not significant, the increased ink gloss for the silica samples is most likely due to the ink filling in the cracks known cracks in the silica based coatings [12-14]. This filling because these inks are either dye based or small pigment based [19,20] (~100nm for the HP black).

The dot roundness results for black dots are shown in Table 17. Roundness was defined in reference 17. Roundness near one is ideal because it indicates that he ink spreads uniformly, and thus is a measure of coating uniformity. If the roundness is 1, it means the dots are perfect circles. Values of roundness less than 1.0 indicate lack of roundness. Therefore, the closer the value of roundness is to 1, the better the quality of the dots.

From Table 17, most of the low coat weight samples have a smaller roundness values. That is to say, ink dots smeared on the coating layer because coating layers in the low coat weight is not able to hold ink dots well and coatings applied for the low coat weight samples didn't cover the substrate perfectly. The roundness values of Canon printer samples were better than the roughness values of HP and Epson printer samples.

Table 17. Dot roundness of samples

Canon S450

	Sample A	Sample B	Sample C	Sample D	Sample E	Sample F
6 g/m^2	.99	1.00	.97	.92	1.00	.95
8 g/m^2	1.00	1.00	.98	.89	1.00	.99
10 g/m^2	1.00	1.00	.96	.83	1.00	.99
12 g/m^2	.99	.99	.95	.80	1.00	1.00

HP 932C

	Sample A	Sample B	Sample C	Sample D	Sample E	Sample F
6 g/m^2	.93	.79	.83	.87	.96	.81
8 g/m^2	.90	.87	.85	.83	.96	.88
10 g/m^2	.85	.85	.88	.74	.92	.92
12 g/m^2	.99	.87	.85	.71	.97	.86

Epson Stylus Color 900

	Sample A	Sample B	Sample C	Sample D	Sample E	Sample F
6 g/m^2	.95	.99	.90	.80	.99	.91
8 g/m^2	.94	.98	.91	.79	1.00	.90
10 g/m^2	.97	1.00	.90	.81	.99	.92
12 g/m^2	.99	.90	.89	.69	.94	.86

Conclusion

The results obtained from this study indicate that the optical properties, brightness and gloss, were affected by pigment type and coat weight. Improvements in optical properties indicate that brightness improvements were due to an increase in scattering coefficient with large particle size and gloss improvements were due to increase in smoothness and refractive index.

The print properties were also influenced by pigment particle size and packing volume. Print qualities as measured by ink density and ink gloss were strongly dependent on pigment particle size and packing volume. Inks used in the printers influenced printing qualities.

Calendering improved the smoothness of the surfaces. Ink gloss and ink density consequently increased. And it is believed that the low solids of the coatings prevents the smooth application of the coating due to base sheet roughening by the absorption of coating water. Research is therefore needed to determine ways to control the penetration of the coating water into the base sheet. Base sheet sizing, coating solids, the application and formulation of a base coating, and coating rheology should be considered for topics of future studies.

From the results of these experiments, it is evident that the coatings of fumed metallic oxide and conventional pigments had as good optical properties and printing qualities as the coatings of fumed metallic oxides.

Acknowledgement

The authors wish to thank CABOT Corporation for supporting this research.

References

1. Mills, Ross N., "Inkjet printing – Past, Present and Future", *IS&T NIP10*, pp 410 – 413 (1994).

2. Casey, P. James, "Pigment Coating", *Pulp and Paper*, Chapter 22, Wiley, Inc., New York, NY, 1980, p.2181.

3. Aksoy, Burak, Joyce, Margaret K. and Fleming, Paul D., "Comparative Study of Brightness/Whiteness Using Various Analytical Methods on Coated Papers Containing Colorants", *Proceedings of the TAPPI Spring Technical Conference & Trade Fair*, Chicago, May 2003.

4. Bristow, J.A., *Advanced Printing Science & Technology*, 20: 193(1990).

5. "Measurement and Control of the Optical Properties of Paper", Second edition, Technidyne corporation, p.7.5-7.6, 1996.

6. TAPPI Standard, T480 m51.

7. Kubelka, P. and Munk, P., "Ein beitrag zur optik der farbanstrich", *Z. Tech Phys.* **12**:593-601, 1931.

8. TAPPI Standard, T1214 sp98

9. Mourad, S., Emmel, P., Simon, K., and Hersch, R. D., " Extending Kubelka-Munk's theory with Lateral Light Scattering", *IS&T NIP 17*: pp469-473 2001.

10. Lee, Hyunkook, "The influence of fumed metallic oxides on coating structure and their relationships to print quality", Western Michigan University, MS thesis 1998.

11. Lee, Hyunkook, Joyce, Margaret K. Fleming, Paul D. and, Cameron, John , "Production of a Single Coated Glossy Inkjet Paper Using Conventional Coating and Calendering Methods", *Proceedings of the TAPPI Coating Conference*, May 2002 and TAPPI J. in press..

12. Ramakrishnan, Raja, "Coating and Basesheet Influences on the Development of Gloss for Inkjet Papers Containing Fumed Metallic Oxides." Western Michigan University, MS thesis, 1999.

13. Cawthorne, E. James, " Use of a Chemically-Modified Clay as a replacement for Silica in Matte Coated Inkjet Papers." Western Michigan University, MS thesis, 1999.

14. Cawthorne, James E. , Joyce, Margaret and Fleming, Paul D., "Use of A Chemically Modified Clay as A Replacement for Silica in Matte Coated Inkjet Papers", *J. Coat. Tech,* 75, No. 937, pp 75-81, Feb. 2003.

15. Fetso, M. Jacqueline and Zettlemoyer, C. Albert., "Factors Affecting Printing Gloss and Uniformity", TAPPI Journal, August 1962, p.667-681.

16. TAPPI procedure T 452 om-92.

17. Fleming, Paul D., Cawthorne, James E., Mehta, Falguni, Halwawala, Saurabh, and Joyce, Margaret K., "Interpretation of Dot Area and Dot Shape based on Image Analysis", *IS&T NIP18* pp 474-477 2002, JIST Sept.-Oct. 2003.

18. Chinmayanandam, T. K., Phys. Rev. 13:96 (1919).

19. Frimova, A., "Particle Size Analysis of Commercial Printing Inks and Their Press Stability and Printability", MS Thesis, Western Michigan University, April 2003.

20. Frimova, Andrea, Pekarovicova, Alexandra, Fleming, Paul D., "Particle Size of Printing Inks; Stability, Colorimetry and Printability", In Preparation.

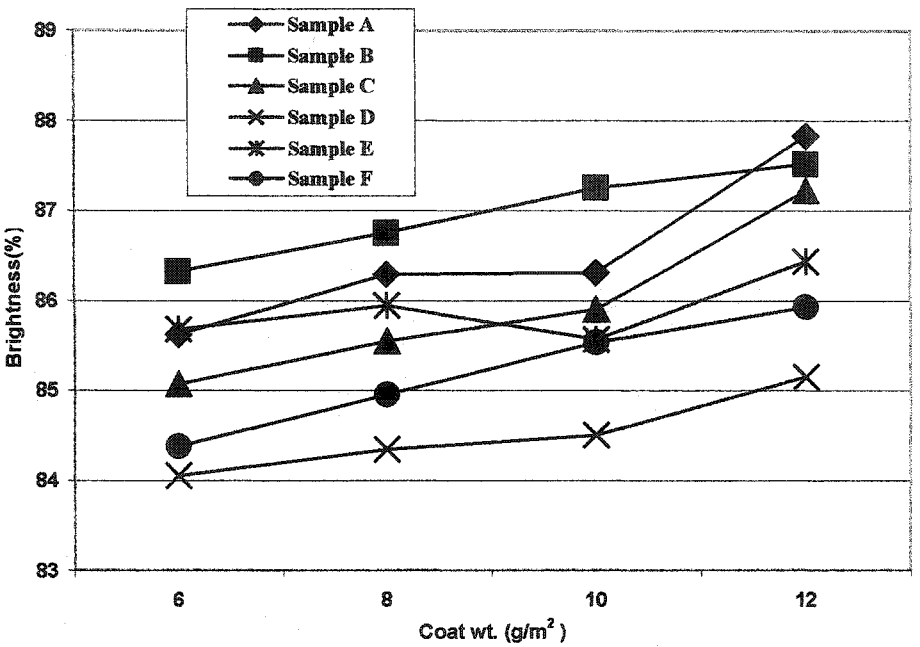

Figure 67. Brightness comparison of each coating formulation (Calender)

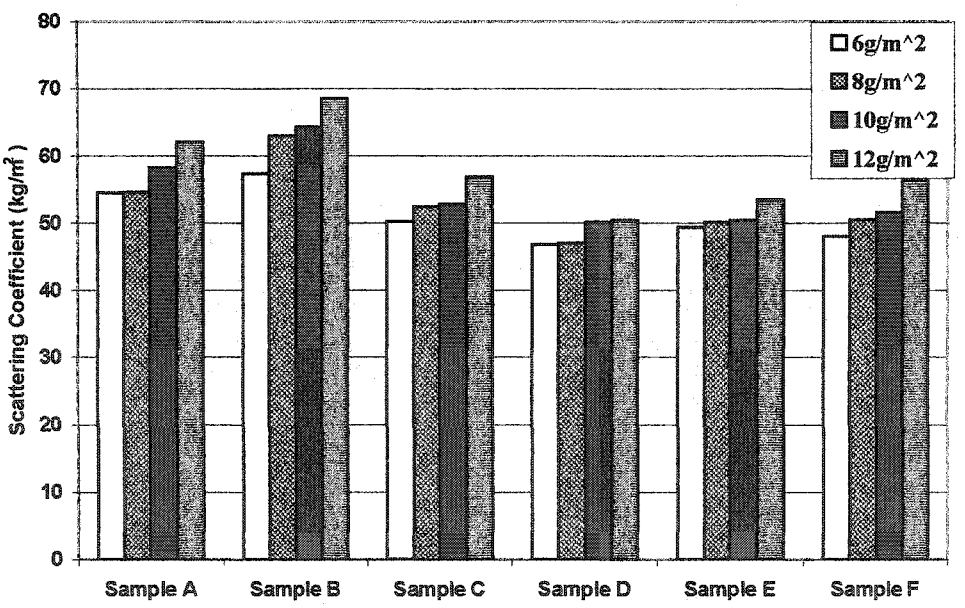

Figure 68. Influence of scattering coefficient on coat weight (Calender)

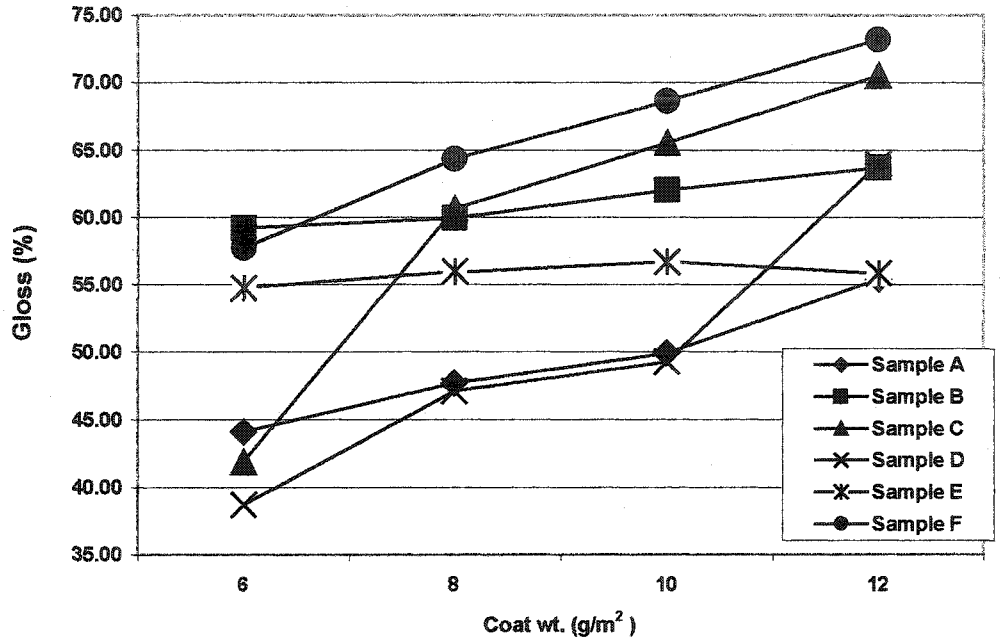

Figure 69. Gloss comparison of each coating formulations (Calender)

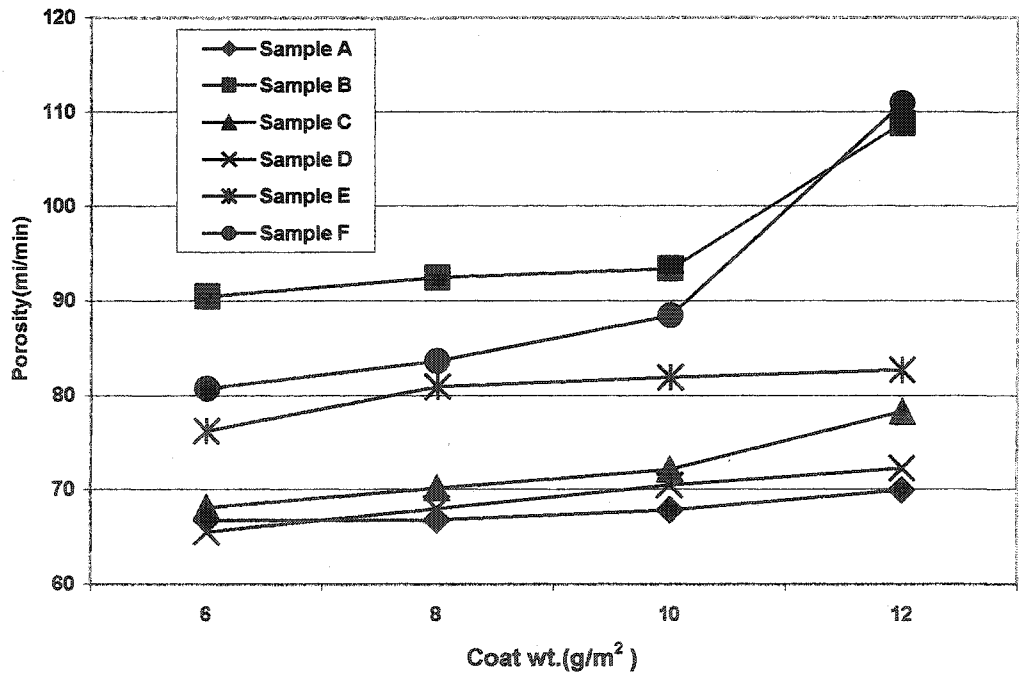

Figure 70. Porosity comparison of each coating formulation

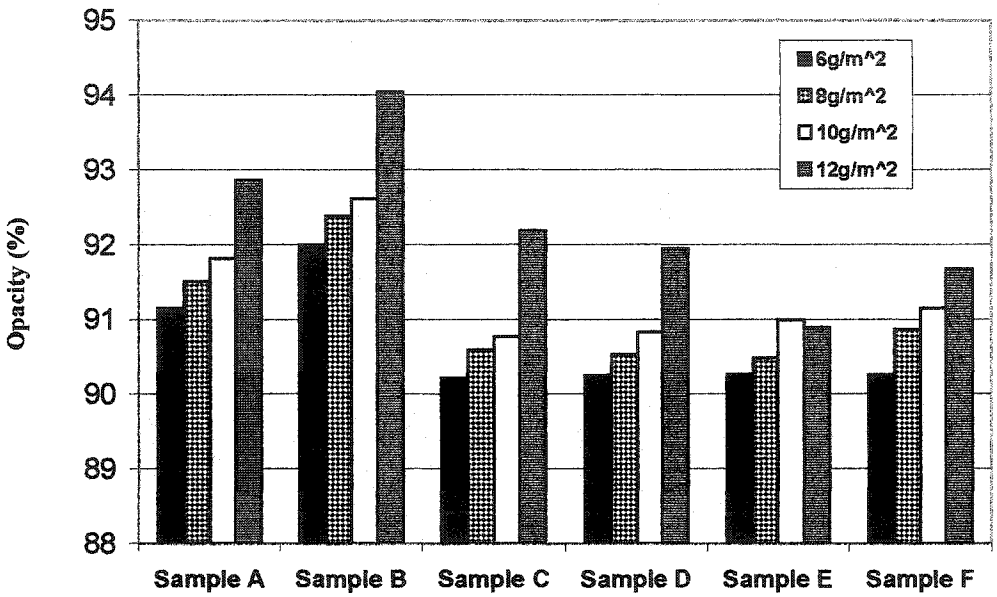

Figure 71. Opacity comparison of each coating formulation (Calender)

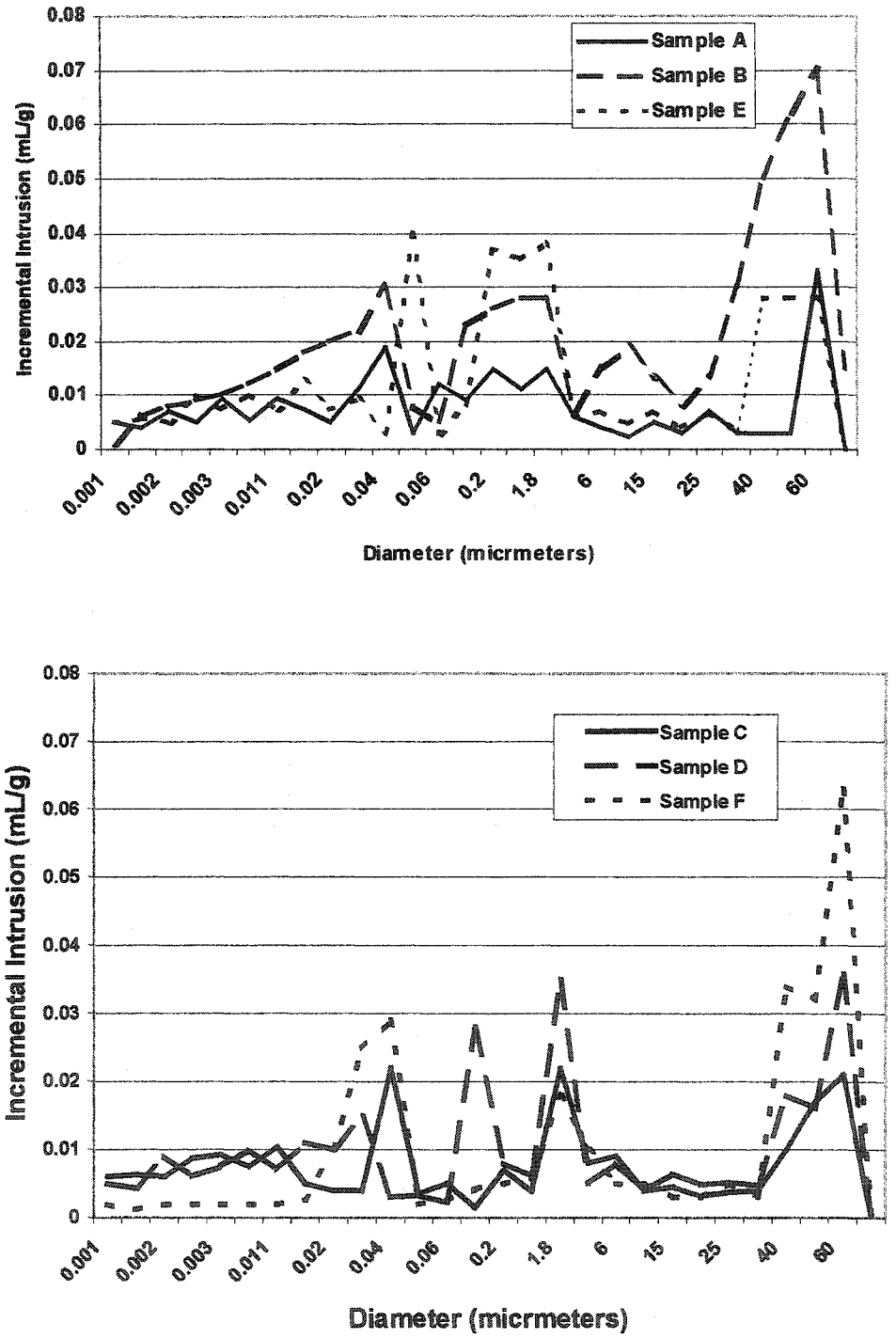

Figure 72. Pore size distribution by mercury intrusion porosimeter (Coat weight: 12 g/m^2)

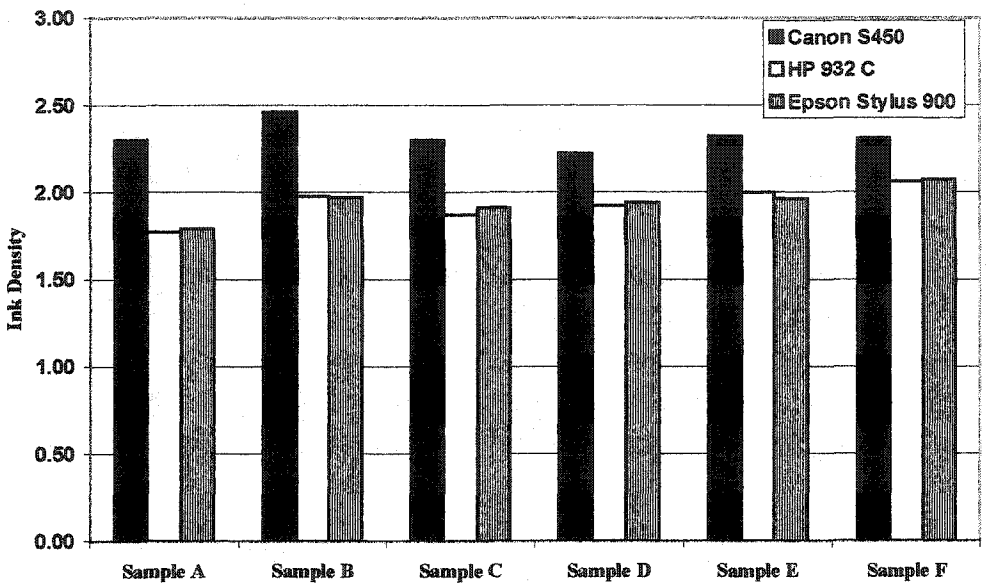

Figure 73. Ink density comparison of each coating formulations
(Coat wt. : 12 g/m^2, Color: black)

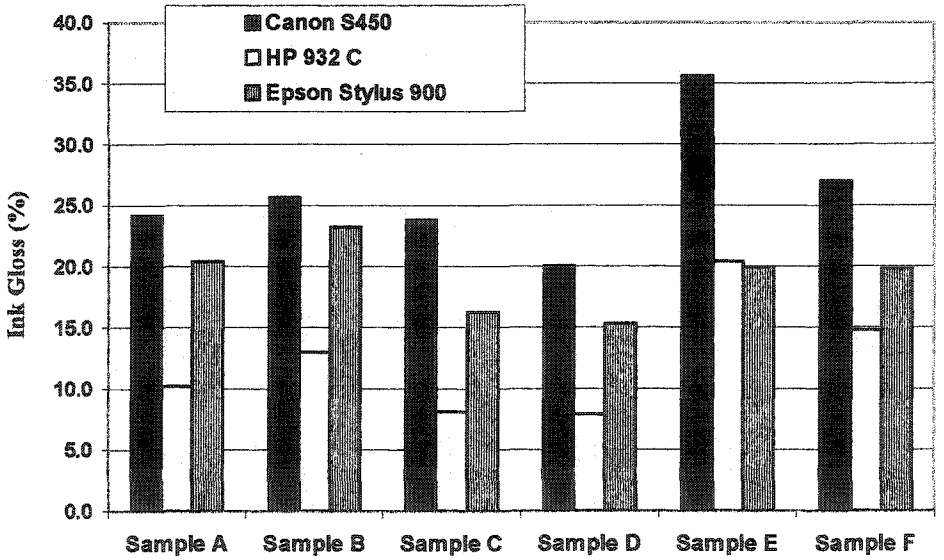

Figure 74. Ink gloss comparison of each coating formulations
(Coat wt.: 12 g/m^2, Color: black)

Appendix

1. Printing dots of sample A (Coat weight: 12 g/m^2, Color: black)

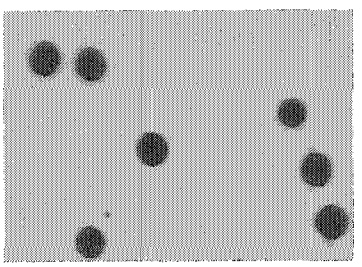

Canon S450

Roundness: 1.01

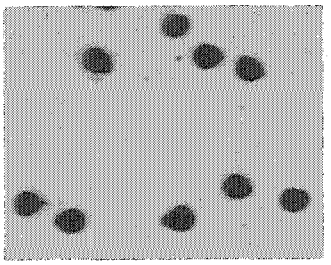

HP 932

Roundness: 1.01

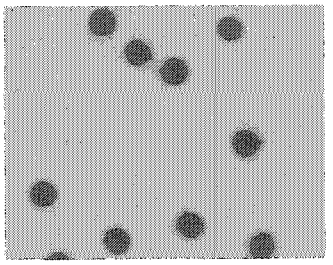

Epson Stylus 900

Roundness: 1.01

2. Printing dots of sample B (Coat weight: 12 g/m^2, Color: black)

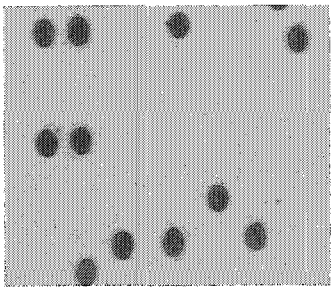

Canon S450

Roundness: 1.01

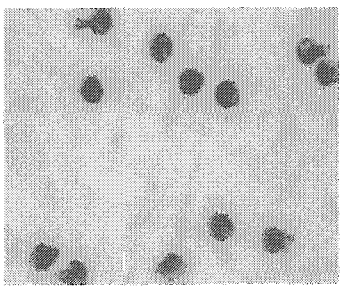

HP 932

Roundness: 1.15

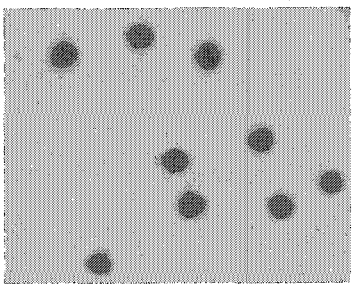

Epson Stylus 900

Roundness: 1.11

3. Printing dots of sample C (Coat weight: 12 g/m^2, Color: black)

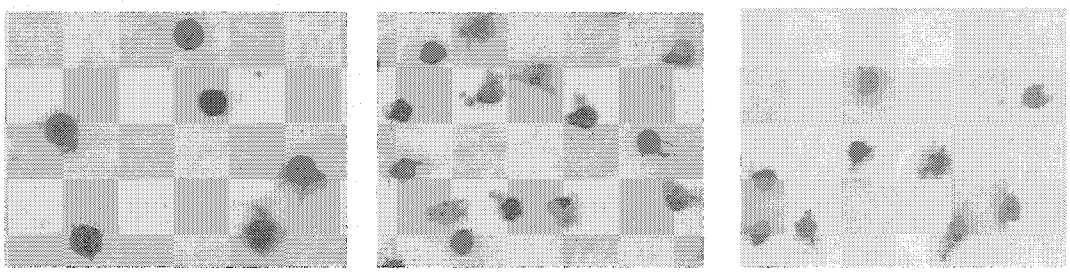

Canon S450 HP 932 Epson Stylus 900

Roundness: 1.25 Roundness: 1.41 Roundness: 1.45

4. Printing dots of sample E (Coat weight: 12 g/m^2, Color: black)

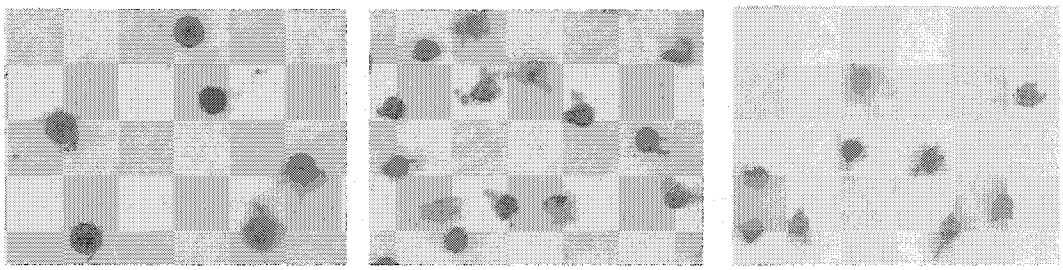

Canon S450 HP 932 Epson Stylus 900

Roundness: 1.25 Roundness: 1.41 Roundness: 1.45

5. Printing dots of sample E (Coat weight: 12 g/m^2, Color: black)

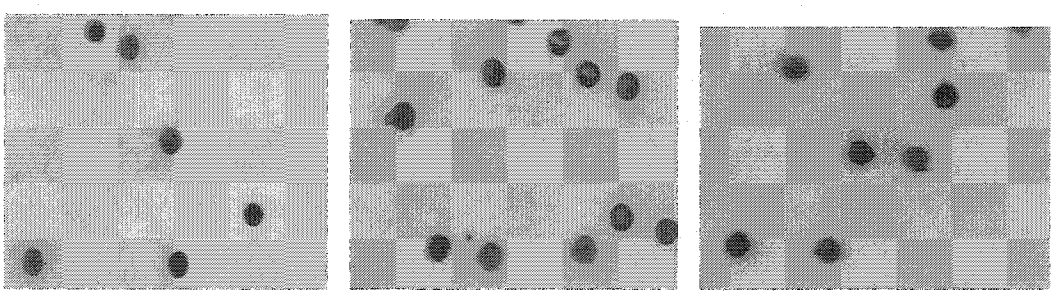

Canon S450 HP 932 Epson Stylus 900

Roundness: 1.00 Roundness: 1.03 Roundness: 1.06

6. Printing dots of sample F (Coat weight: 12 g/m^2, Color: black)

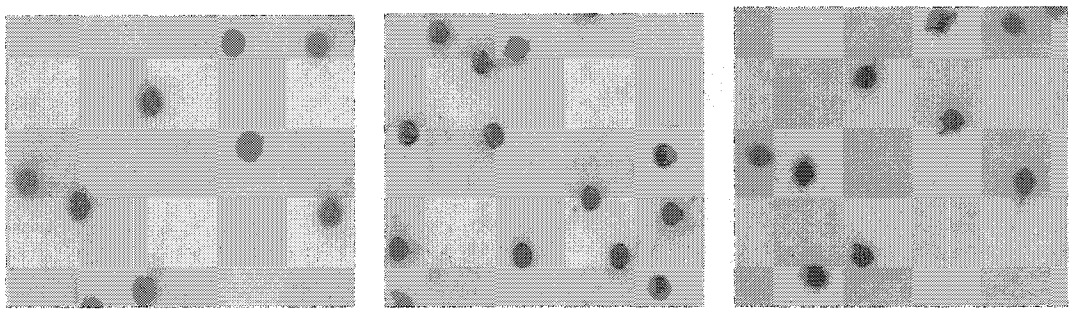

Canon S450

Roundness: 1.00

HP 932

Roundness: 1.16

Epson Stylus 900

Roundness: 1.16

INFLUENCE OF PIGMENT PARTICLE SIZE AND PIGMENT RATIO ON PRINTABILITY OF GLOSSY INKJET PAPER COATINGS– PART II

Hyun-Kook Lee, Margaret K. Joyce, and Paul D. Fleming

Center for Coating Development and Center for Ink and Printability

Department of Paper Engineering, Chemical Engineering and Imaging

Western Michigan University

Kalamazoo, Michigan 49008

Abstract

Product development activity in the area of inkjet printing papers has accelerated greatly to meet the rapidly growing market for inkjet printing. Advancements in inkjet printing technology have also placed new demands on the paper substrate, due to faster printing rates, greater resolution through decreased drop volumes, and better colorants added to the ink.

For glossy ink jet papers, small particle, large surface area fumed silica and aluminum pigments have been shown to provide the desired properties for high quality glossy ink jet coated papers. However, their high cost and low make-down solids in comparison to conventional pigments, has limited their use by the industry to these specialty grades.

In previous research, it was seen that the presence of coating cracks increased the microroughness of the papers coated with silica-based formulations, thereby reducing

the gloss of the silica-based coatings. Coating cracks were not observed for the alumina coated papers. To minimize the shrinkage of coating layer, coating solids greater than 30% solids should be targeted to reduce the difference between application solids and the coating's immobilization solids point. Since the immobilization solids point is the point at which the free drainage of coating water to the basesheet ceases, raising the application solids will reduce the amount of free water lost to the basesheet upon its application and metering and hence reduce the incidence of cracks.

The focus of this study was to determine if the costs can be reduced and application solids could be increased by extending the pigments with less expensive compatible pigments. The effects of the resultant change in packing volume and particle size distribution on the optical properties and printability were determined. It was determined that up to 50 parts of the fumed silica and up to 30 parts of fumed alumina can be replaced with less expensive compatible pigments, without significant loss to the optical and printing properties of the glossy inkjet paper.

Introduction

Inkjet printing has proven to be the first digital technology that has achieved an acceptable level of color quality at an affordable price for the large number of home/office end users [1]. As a result, there is a demand for inkjet media with intermediate and high gloss finishes, so that the inkjet printed image may resemble a

photographic image. It is expected that as image quality improves and throughputs increase, inkjet printing will continue to expand into more printing markets and may begin to challenge electrophotography [2] in many high-end applications. A key to meeting the needs of this evolving market is the development of coated inkjet media capable of providing the desired glossy image characteristics of photographic papers.

Another key optical property for photo quality papers is brightness. Brightness is important for print contrast. The higher the brightness, the higher is the contrast between the paper and printed image, and hence the "snappier" is the image. For the paper industry, brightness is defined as the reflectance of blue light peaking at a wavelength of 457 nm in terms of a perfectly reflecting, perfectly diffusing surface. The brightness of pigment-coated paper is heavily dependent on the brightness of the raw stock. Therefore, the raw stock should have brightness as close as possible to that of the dried coating layer. The principal coating components that influence brightness are the pigments, binders, additives, and the relative proportion of each used in the coating formulation [3]. Optical brighteners [4-8] are commonly used in these grades. Papers with brightness values greater than 90, and as high as 100, are currently being marketed.

Recently, attention has been shifted from brightness to "whiteness" as the key optical property of printing papers [6-10]. This discussion is beyond the scope of this paper, but is discussed extensively in references 6-10. Suffice it to say, high whiteness papers usually have high brightness and vice versa.

According to TAPPI standards [11], gloss is defined as the 75° spectral reflectance of light at λ = 550 nm. Based on this definition, coating gloss is optimized by increasing the refractivity of the coating layer, while minimizing the roughness of the coated surface layer. On the other hand, print gloss is usually measured at a 60° angle [12]. Nevertheless, paper and print gloss at both 60 and 75° are important in interpreting the printability of ink jet papers [13]. In general, smooth glossy and bright white paper provides good distinctness of image, contrast and quality appearance.

The scattering coefficient is the fraction of light incident upon an infinitesimally thin layer of the material that is scattered backwards by that layer, divided by the basis weight of the layer. It is expressed in reciprocal basis weight units. Kubelka and Munk [14] provided a direct mathematical relationship between scattering absorption, and opacity.

The original theory of Kubelka and Munk was developed for light diffusing and absorbing infinitely wide colorant layers. Due to its simple use and to its acceptable prediction accuracy, this model is very popular in industrial applications. The concept is based on the simplified picture of two diffuse light fluxes through the layer, one proceeding downward and the other simultaneously upward [5,15,16].

Recent research in our laboratory, by Lee et al [17,18] and Ramakrishan [19], showed that fumed metallic oxide pigments are capable of producing semi-gloss and high-gloss inkjet papers with acceptable print quality after calendering. In these works, it was found that the gloss of fumed alumina pigments was higher than fumed silica. An important finding of Ramakrishan's studies was that the gloss of the inkjet papers

increased with an increase in silica particle size, which does not follow the findings for conventional pigments. The loss in gloss with reduction in silica particle size was attributed to the increased presence of coating cracks with decreasing particle size. The cracks were shown to result from drying stresses, which increased with an increase in silica surface area. Cracking was not present in the alumina coatings, resulting in the alumina coatings providing higher gloss values at equal coat weights.

Ink density is an important quality control indicator in the printing process. Ink density impacts the final visual quality, color gamut, and color fidelity. The main factor identified with color density is the concentration of colorant in the ink. Other major factors determining ink density are ink dot coverage on the coating surface and colorant concentration at the surface. In the interaction of the colorant with coated paper, electrostatic interactions play the key role in colorant-coated paper interactions. The nature of the anionic dyes and the oxides will determine the print quality of the inkjet printing, since electrostatic interactions of colorant with coated media occur between the anionic groups of dyes and the oxides. The binding energies of the dyes are greatly increased by electrostatic interactions, resulting in a high binding strength [20,21]

Ink gloss depends on the smoothness of the substrates and the smoothness of the ink layer [13]. Another factor contributing to the smoothness of the printed film is the amount of vehicle on the surface. If the pigment particles are completely covered by a level film of the vehicle, a good approximation to a mirror surface usually results irrespective of the smoothness of the substrates or of the ink [22]. However, the use of

dyes rather than pigments in most inkjet inks makes the former more relevant than the latter. Comparison of ink gloss for dye and pigmented ink jet inks is given elsewhere [13].

Generally, optical properties and printing properties improve with increases in the coat weight, since increasing the amount of coating materials improves properties of the coated surface. For example, reflectance of light and ink absorption both increase with increased coat weight.

The objective of this research was to determine if less expensive compatible pigments could be blended with fumed alumina and silica pigments to yield coatings with equal or better gloss and printability. The influence of pigment blending on the packing volume of the coating was studied and the relationship between packing volume and inkjet print quality was determined.

Experimental design

The basis weight of the base paper was 75 g/m^2 with 120 seconds for the Hercules sizing test (HST) value. The roughness (Parker PrintSurf "smoothness") of the base paper was 3.93 μm. Selected pigments were obtained from several pigment companies. Aluminum oxide (AO), fumed silica (FS), precipitated calcium carbonate (PCC, from Imerys, Opti-Cal-Gloss), ultrafine ground calcium carbonate (UFGCC, from Imerys Carbital 95), alumina trihydrate (ATH, from GAC chemical corp., GenBrite), and baumite (from Condea Vista Company, Disperal Dispersion 20/30)

were studied. The physical properties of the pigments and the solids content of the pigments used are shown in Table 18.

Table 18. The physical properties of pigments as supplied

Sample	Solids Content	Color	Specific Gravity	pH	Refractive Index	Avg. Particle size (nm)
AO	40%	White	1.40	3.8-4.2	1.76	160
FS	30%	White	1.20	10.0-10.3	1.46	225
PCC	70%	White	2.72	9.0-10.0	1.58-1.63	544
UFGCC	75%	White	1.92	9.0-10.0	1.58	600
Baumite	30%	White	1.1-1.3	4.0-6.0 (5% sol)	1.65-1.66	200
ATH	65%	White	2.42	6.70	1.57	400

The binder used in the coating formulation was a partially hydrolyzed, low viscosity, polyvinyl alcohol (Airvol 203, Air Products Inc.). This polyvinyl alcohol (PVOH) was chosen to increase the % coating solids by reducing the interaction between pigments and PVOH and to promote the ink receptivity of the coating layer to the water based inkjet inks. Solutions of polyvinyl alcohol were prepared at 30% solids by adding the required amount of dry PVOH powder to cold-alkaline water (pH 9.0-10.0) under agitation and heating the mixture to 185°F. The solution was held at this temperature for 35-40 minutes to assure complete dissolution and hydration of the PVOH. A defoamer was then added (Foammaster VF, Henkel, Inc.). The solution

was cooled to 40°F before adding the slurried pigments at a slow rate of agitation. The coatings were mixed for 30 minutes and the pH and viscosity measured. It is important that this order of mixing is employed for the Alumina based coatings, because raising the pH of the alumina based slurries will cause gelation of dissolved aluminum ions and consequent agglomeration of pigment particles. This would greatly increase the effective particle size and viscosity, making the coating not runnable. Letting the pH adjust itself while in the presence of PVOH limits these effects. Coatings containing different fumed and conventional pigment ratios (50:50, 70:30, and 80:20, respectively) were prepared and drawdowns were made using various Mayer rods.

From this screening study, it was determined that PCC and UFGCC were the two most compatible pigments for blending with fumed silica, due to both their high pH requirements and high glossing properties. For the fumed alumina, baumite and alumina trihydrate performed best. It was also determined that substitution levels greater than 30 parts of these pigments into the coating, greatly diminished the gloss of the coatings, to where the coating gloss (<55%) would not be acceptable for this commercial grade of inkjet paper. Based on these finding, the coatings for cylindrical laboratory coating studies, (CLC), applications were prepared at 70:30 and 50:50 ratios, a pigment-to-binder ratio of 7:1 and final solids of 30 $\pm$1%.

The coatings were applied to a 75 g/m^2 commercial base paper using a Cylindrical Laboratory blade coater at a speed of 2000 fpm. For each sample, the basepaper was

pre-dried at 25% power for 10 s and post-dried at 100 % power for 60 s. Four different coat weights were applied: 6 g/m^2, 8 g/m^2, 10 g/m^2, and 12 g/m^2.

The brightness values of the papers were measured using the standard procedure [23] on a Technidyne Brightness meter. Gloss was measured using a Hunter 75° gloss meter according to the standard procedure [11].

The samples were printed on an Epson Stylus 900, Hewlett Packard 932C and Canon S450 inkjet printers, using a proprietary test print pattern created with Adobe software [17-21]. The printed images were bars of four solid colors (cyan, magenta, yellow, and black). The Epson 900 is a piezoelectric printer with a resolution of 1440 x 720dpi. The HP 932C is a thermal inkjet printer with a resolution of 2400 x 1200 dpi. The Canon S450 printer is thermal inkjet printer with a resolution of 1440 x 720 dpi. Print gloss was measured using a Gardener 60° Micro-Gloss meter. Print density was measured using an X-Rite 408 densitometer. Roundness was measured at the 30% tone scale by using a Hitachi HV-10 camera and ImagePro Plus, version 3.0, for image detail analysis [17-21, 24]. The coated samples were calendered on one side, through 3 nips at 123 kN/m and 60 °C.

Table 19. Ratio of pigments used.

Sample	Pigments	Parts	Viscosity* (cP)	pH
FSU	Fumed silica/UFGCC	70:30	572	9.2
FSU1	Fumed silica/UFGCC	50:50	704	8.94
FSP	Fumed silica/ PCC	70:30	254	9.7
FSP1	Fumed silica/PCC	50:50	608	9.05
FS	Fumed Silica	100	72	9.8
AOA	Aluminum Oxide/ATH	70:30	984	5.9
AOA1	Aluminum Oxide/ATH	50:50	1370	4.90
AOB	Aluminum Oxide/Baumite	70:30	1766	6.9
AOB1	Aluminum Oxide/Baumite	50:50	1130	4.2
AO	Aluminum Oxide	100	1231	8.1

*Viscosity=Brookfield viscosity, 100 RPM, spinindle:#4

Results and discussion

The influence of coat weight and pigment type on brightness is shown in Figure 75. Both the coat weight and pigment type influenced the brightness of the coating. The addition of the calcium carbonate to the fumed silica improved the coating brightness. The addition of ATH increased the brightness of the fumed alumina. Comparison of the brightness data to calculated light scattering coefficient values for the data showed a strong correlation (See Figure 76).

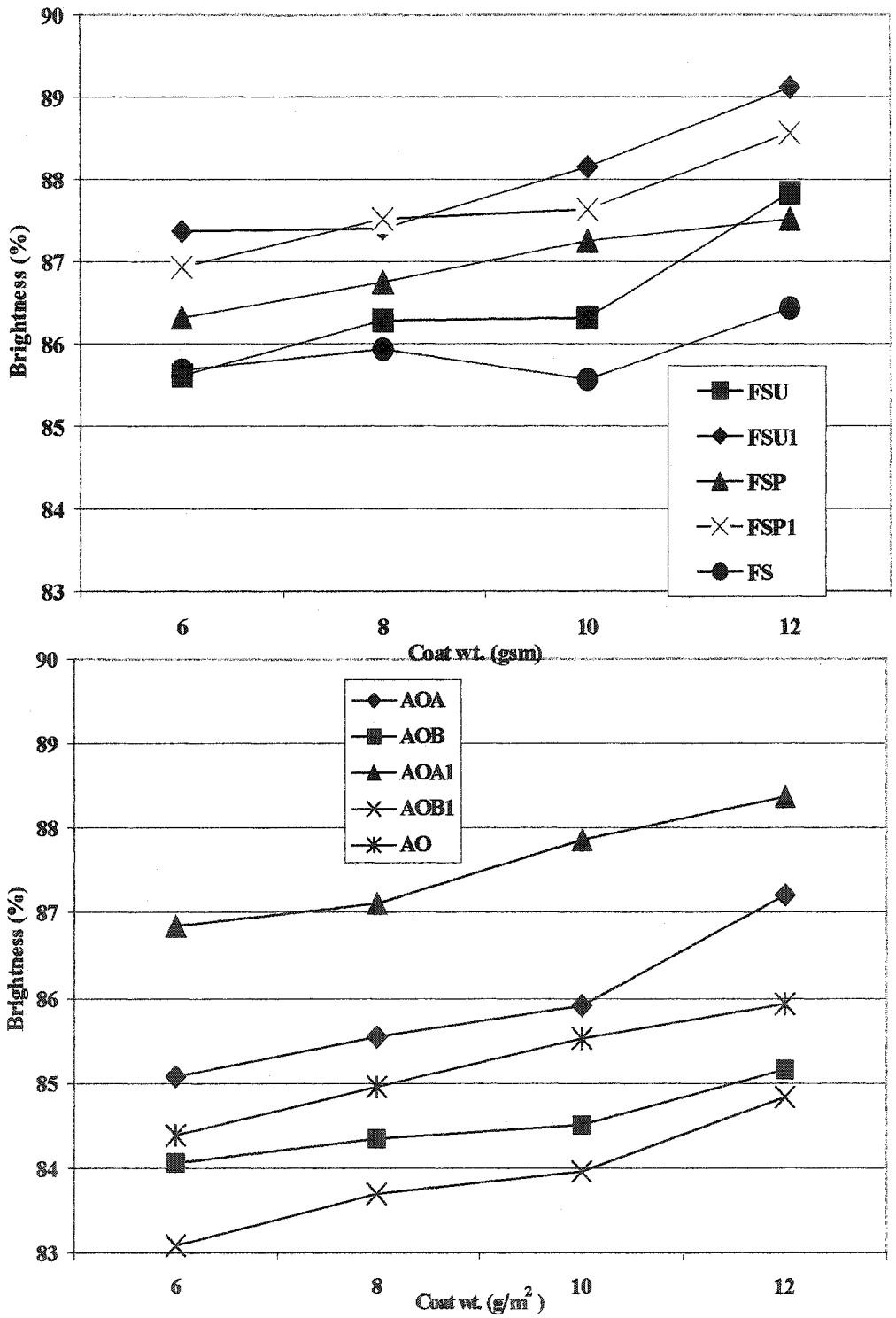

Figure 75. Brightness values for blended samples as a function of coat weight.

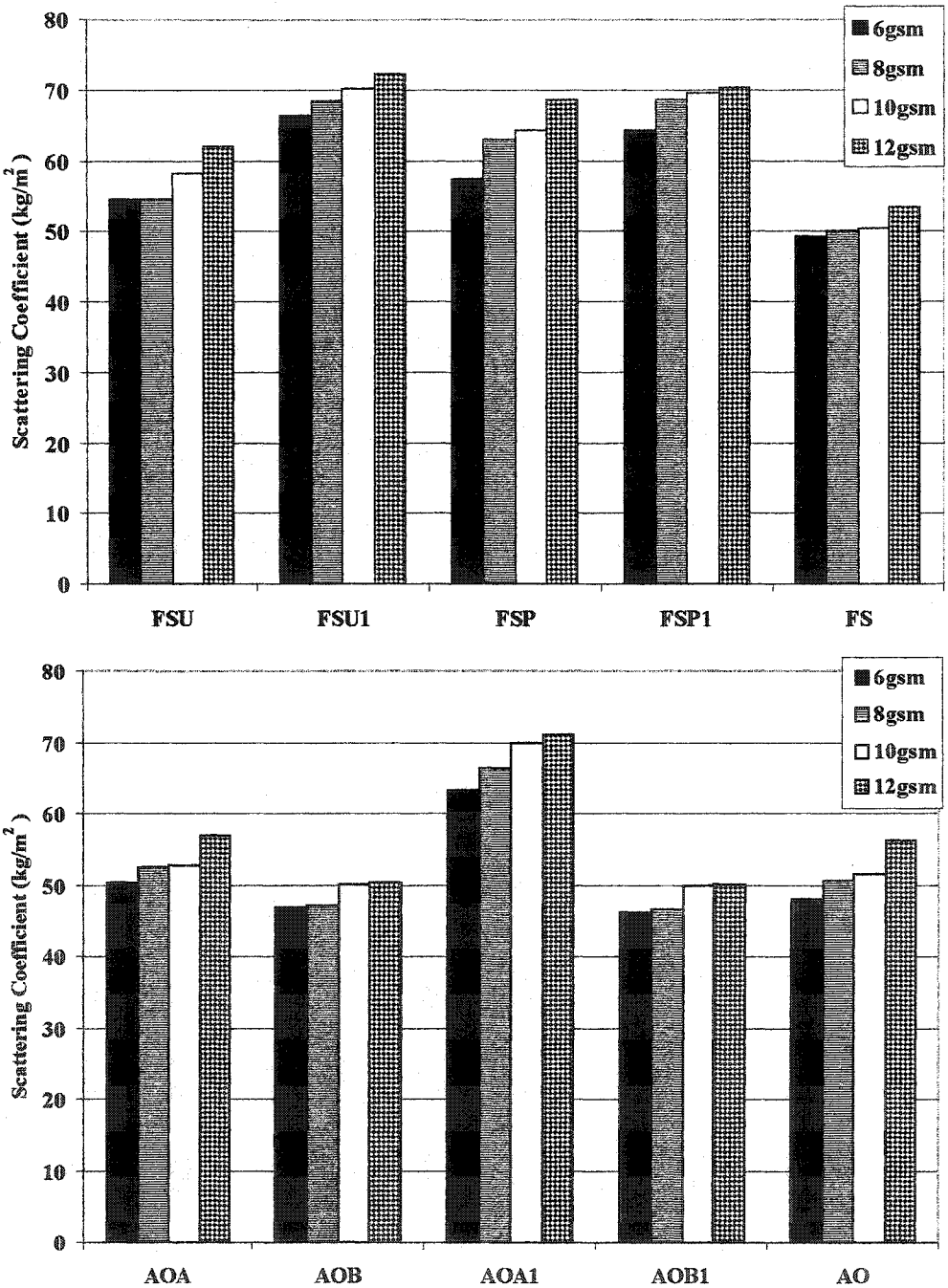

Figure 76. Scattering coefficient as a function of coat weight.

The scattering coefficients of the coatings were calculated using the equations [15] below. From the measurements of R_0 and $C_{0.89}$

$$a = 0.5(R_{0.89} + (R_0 - R_{0.89} + 0.89)/(0.89R_0)) \quad (1)$$

$$b = 0.5(1/R_\infty - R_\infty) \quad (2)$$

$$x = (1 - aR_0)/bR_0 \quad (3)$$

$$R_{0.89} = R_0 / C_{0.89} \quad (4)$$

$$R_\infty = a - (a-1)^{1/2} \quad (5)$$

$$s_W = (0.5/b)[\ln(x+1)/(x-1)] \quad (6)$$

$$S = s_W/W \quad (7)$$

$R_{0.89}$ = reflectance of the layer which has behind it a surface with reflectance of 0.89.

R_0 = reflectance of the layer with ideal black background

$C_{0.89}$ = $R_0/R_{0.89}$ = TAPPI opacity, as a fraction

s_W = scattering power

W = basis weight

S = light scattering coefficient (LSC)

R_∞ = reflectance of infinitely thick paper sample.

From the above equations, it is seen that brightness is influenced by the amount of light scattered and absorbed. Light is absorbed when colored matter is present. Scattering is influenced by the surface area of the pigments and the number of air-to-

pigment interfaces due to the higher degree of refractivity between the two interfaces. Scattered light, to some extent, can mask the visual effect of colored impurities.

The addition of carbonate significantly increased the LSC of the silica coatings, improving the coating brightness and gloss (Figure 77). The addition of ATH to the fumed alumina coating resulted in a slight increase in the LSC with a corresponding increase in coating brightness. The increase in brightness with LSC value indicates that addition of the carbonates and ATH increases the air voids in the packing structure enabling more light to be scattered. This is consistent with Figure 78, which shows the influence of pigment addition on coating permeability, as indicated by PPS porosity.

The results indicate that the addition of the larger pigments to the fumed silica coatings increased the permeability of the coating layer, enabling the coating to scatter more of the incident light. As a result, the brightness, gloss, and opacity (Figure 79) of the coatings increased. Unlike the fumed silica coatings, the LSC of fumed alumina coatings were not significantly changed by the addition of the ATH and baumite pigments. The gloss of the fumed alumina was the highest of all the samples tested. However, the addition of ATH and baumite to the fumed alumina enabled glosses almost that of the fumed alumina alone to be obtained.

Since gloss is a function of surface smoothness, the higher gloss could be indicating that fumed alumina (sample F) formed a smoother coat layer. Chinmayanadam [19] has shown gloss to be a function of the refractive index and the wavelength of incident light, as well as the surface roughness:

$$\text{Gloss} = I/I_o = f(n,i)\exp[-(4\pi\sigma\cos(i)/\lambda)^2] \qquad (8)$$

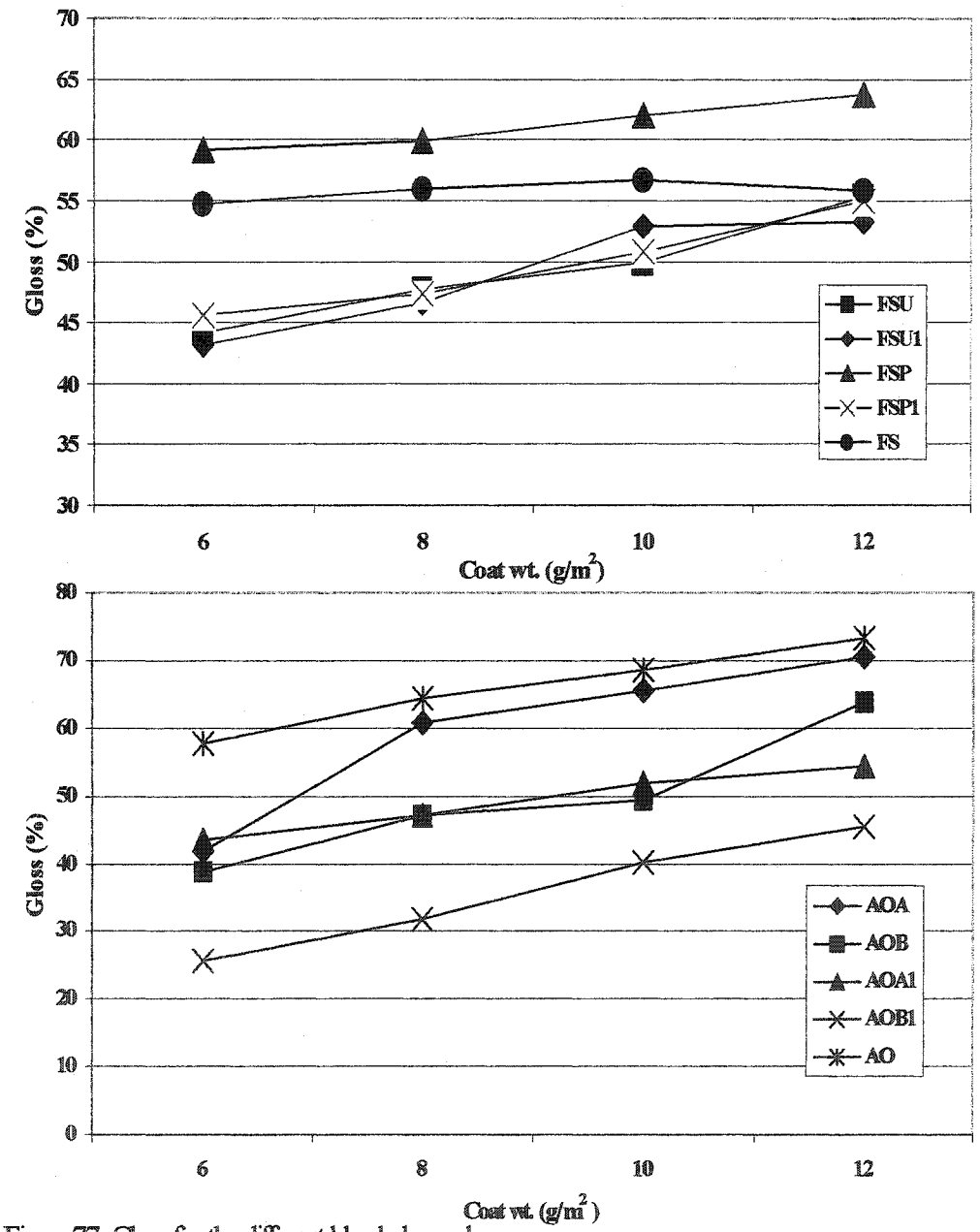

Figure 77. Gloss for the different blended samples.

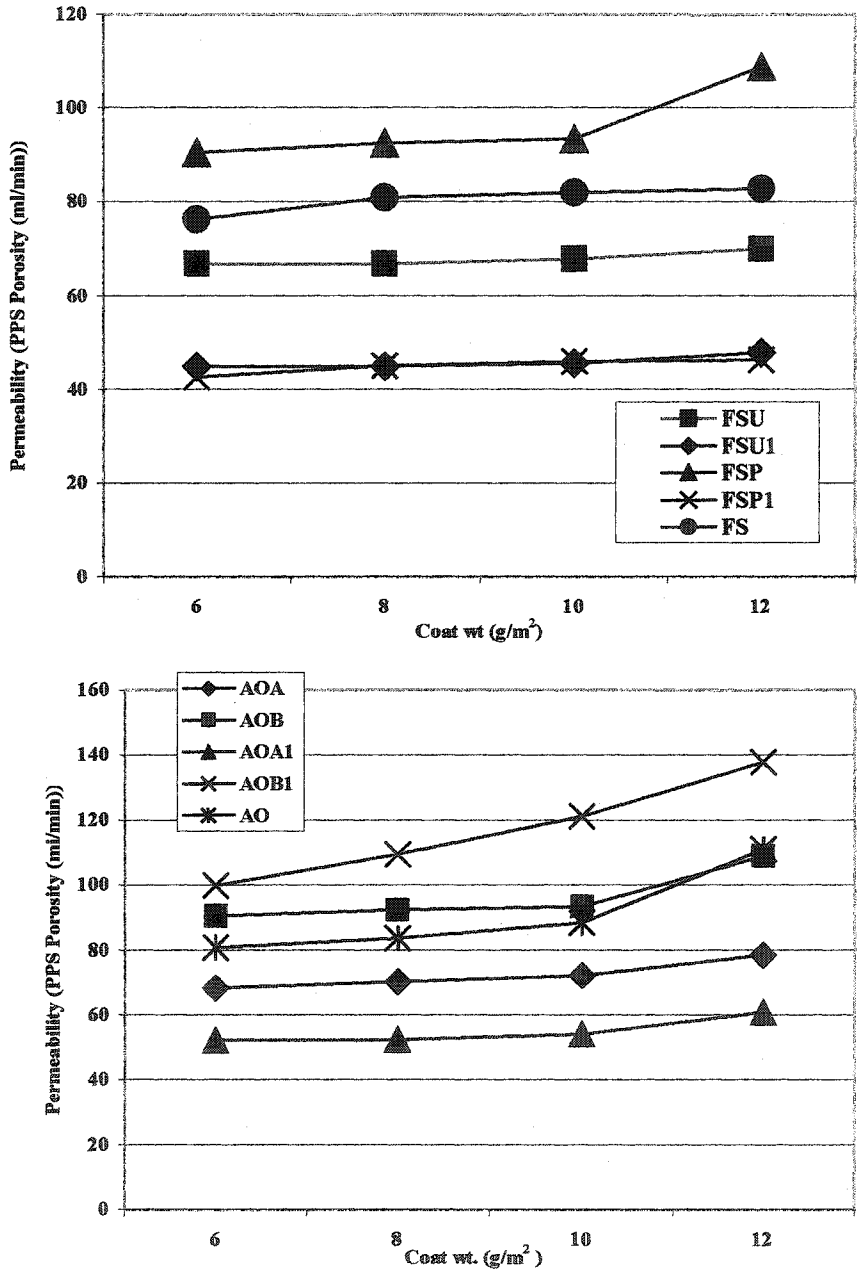

Figure 78. Permeability (PPS porosity) comparison of blended samples.

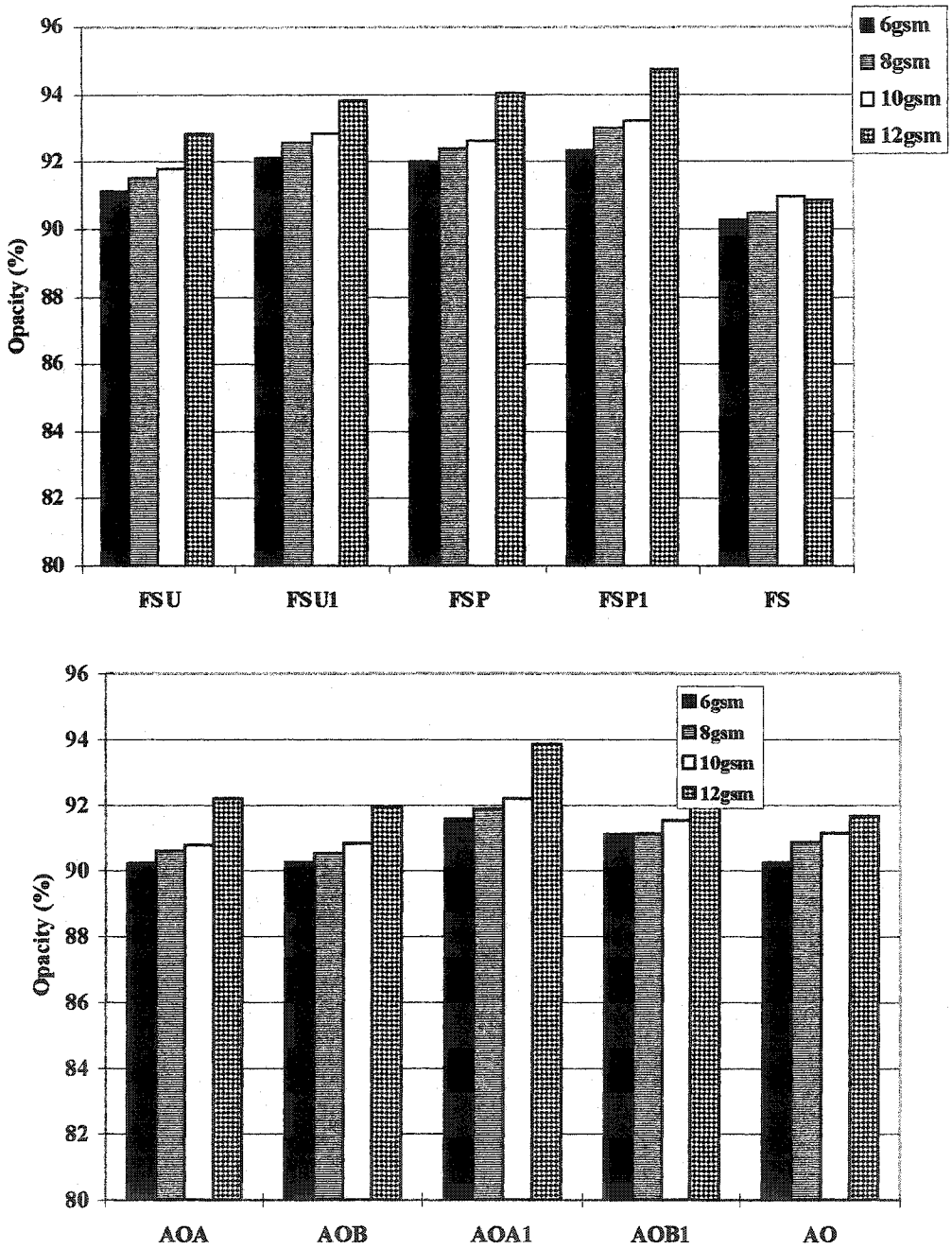

Figure 79. Opacity comparison of each coating formulation.

I and I_o are the specularly reflected and incident light intensities, f(n,i) is the Fresnel coefficient of specular reflection as a function of refractive index n and angle of incident light i, σ is the roughness (standard deviation of the surface profile) and λ is the wavelength of incident light.

Application of this equation to the results indicates that the refractive index of sample F is sufficient to provide acceptable commercial glosses (> 55%), if the proper alignment of the particles (in the case of platey pigments such as ATH) or smoothness of the coating layer is achieved. Small particles not only scatter more light, but better fill the microvoids within the coating and base paper, to provide higher smoothness than large and/or chunky particles.

Although calendering improves smoothness, and hence gloss, it can have the negative effect of compressing the coating layer, adversely affecting the ink receptivity and consequently print quality of the paper.

The pore size distributions of the samples are shown in Figure 80. The LSC and permeability results for the fumed silica coatings correlate well with the Hg porsimetry data. The pore data confirm that the addition of the needle shaped PCC (aragonite) with the grape-like silica clusters open the coating structure for the 70:30 samples, but the needles are probably filling the holes for the 50:50 samples. The Canon ink density values (Figure 81) are higher for the PCC blends versus the silica alone, but the HP and Epson values are lower. The 60° ink gloss (Figure 82) shows mixed dependence on PCC addition but the Δ ink gloss (60° ink gloss minus 60° paper gloss, shown in Figure 83) are generally worse for PCC addition. On the other

hand, blending of UFGCC with the silica leads to systematic reduction in permeability. The ink density values for the UFGCC samples are comparable to those for silica alone. However the gloss and Δ gloss values are slightly worse for the UFGCC samples.

The negative (for all but FS with Canon ink) Δ gloss values in Figure 83 are typical of dye based inks [13]. Pigmented ink jet inks generally improve the Δ gloss values to less negative, or even positive in some cases [13], probably due to packing of ink pigment particles with coating pigment particles.

These results indicate that the new packing structures may enable the ink dye to be fixed and dried closer to the coating surface. The ink density and gloss values of the fumed silica coatings were found to be higher than the fumed alumina coatings. In the case of ink density, these differences are probably not significant.

The increased ink gloss for the silica samples is most likely due to the ink filling in the known cracks in the silica-based coatings as discussed previously [17-20]. This filling occurs, most likely, because these inks are either dye based or small pigment based [13,26-28].

The dot roundness results for black dots are shown in Table 20. Roundness was defined in reference 18. Roundness near one is ideal because it indicates that he ink spreads uniformly, and thus is a measure of coating uniformity. If the roundness is 1, it means the dots are perfect circles. Values of roundness less than 1.0 indicate lack of roundness.

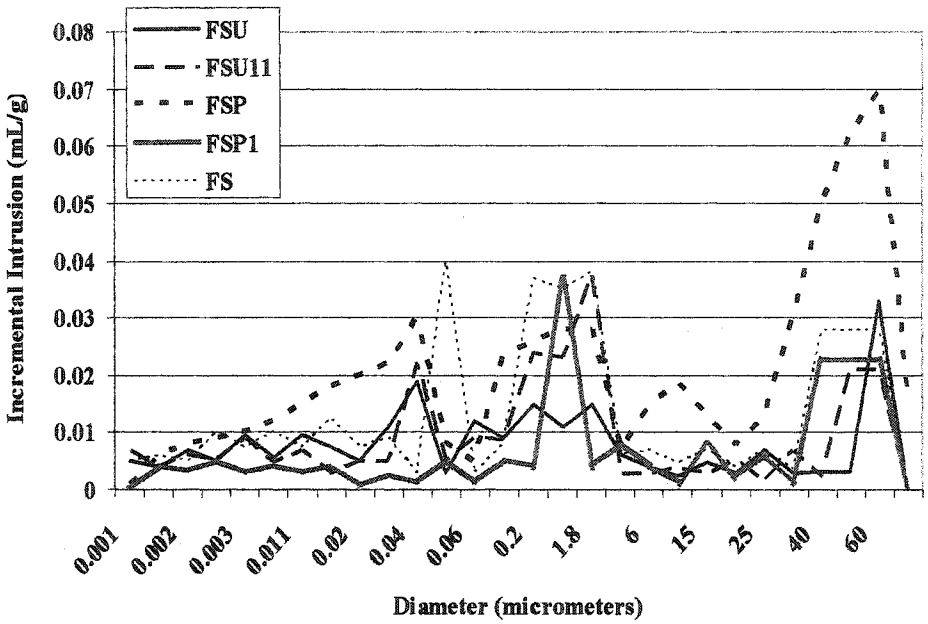

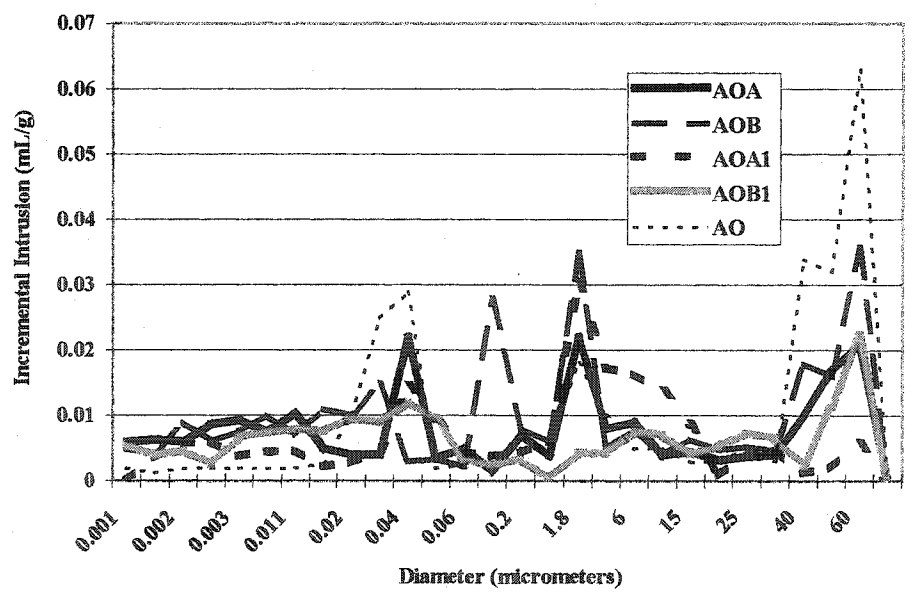

Figure 80 . Pore size distribution by mercury intrusion porosimeter
(Coat wt.: 12g/m^2, calendered samples).

The dot roundness results for black dots are shown in Table 20. Roundness was defined in reference 18. Roundness near one is ideal because it indicates that he ink spreads uniformly, and thus is a measure of coating uniformity. If the roundness is 1, it means the dots are perfect circles. Values of roundness less than 1.0 indicate lack of roundness. Therefore, the closer the value of roundness is to 1, the better the quality of the dots. Rounder dots can have a dramatic effect on Distinctness of Image, or visual perception of the image.

From Table 20, most of the low coat weight samples have a smaller roundness values. That is to say, ink dots smeared on the coating layer because coating layers in the low coat weight is not able to hold ink dots well and coatings applied for the low coat weight samples didn't cover the substrate perfectly. The roundness values of the Canon printer samples were better than the roughness values of HP and Epson printer samples.

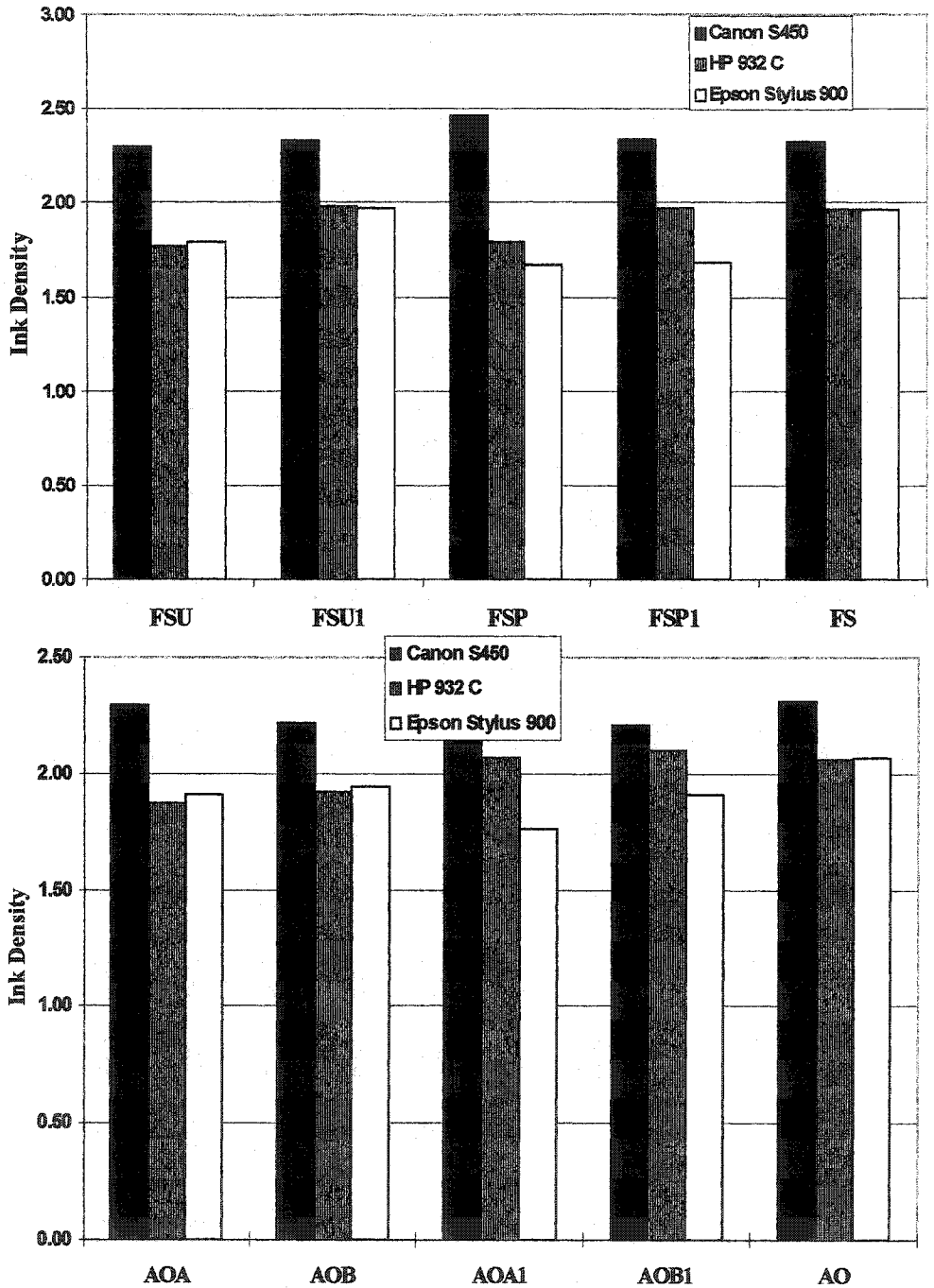

Figure 81. Ink density comparison of coating formulations
(Color: black, coat wt. : 12 g/m^2)

Table 20. Dot roundness of samples

Canon S450

Coat weight	FSU	FSU1	FSP	FSP1	FS	AOA	AOA1	AOB	AOB1	FA
6 g/m^2	.99	.97	1.00	1.00	1.00	.97	.97	.92	.89	.95
8 g/m^2	1.00	.97	1.00	.99	1.00	.98	.97	.89	.82	.99
10 g/m^2	1.00	.98	1.00	.99	1.00	.96	.98	.83	.78	.99
12 g/m^2	.99	.98	.99	1.00	1.00	.95	.98	.80	.75	1.00

HP 932C

Coat weight	FSU	FSU1	FSP	FSP1	FS	AOA	AOA1	AOB	AOB1	FA
6 g/m^2	.93	.88	.79	.79	.96	.83	.75	.78	.75	.95
8 g/m^2	.90	.89	.87	.82	.96	.85	.75	.78	.75	.99
10 g/m^2	.85	.92	.85	.84	.92	.88	.78	.73	.78	.99
12 g/m^2	.99	.93	.87	.85	.97	.85	.79	.70	.79	1.00

Epson Stylus Color 900

Coat weight	FSU	FSU1	FSP	FSP1	FS	AOA	AOA1	AOB	AOB1	FA
6 g/m^2	.95	.96	.99	.96	.99	.90	.90	.80	.78	.95
8 g/m^2	.94	.96	.98	.95	1.00	.91	.90	.79	.77	.99
10 g/m^2	.97	.97	1.00	.96	.99	.90	.93	.81	.79	.99
12 g/m^2	.99	.97	.90	.96	.94	.89	.95	.69	.82	1.00

Conclusion

The results obtained from this research indicate that the optical properties, brightness and gloss, were affected by pigment type and coat weight. Improvements in optical properties indicate that brightness improvements were due to an increase in scattering coefficient with large particle size and gloss improvements were due to increase in smoothness and refractive index.

The print properties were also influenced by pigment particle size and packing volume. Print qualities as measured by ink density and ink gloss were strongly dependent on pigment particle size and packing volume. Inks used in the printers influenced printing qualities. This is confirmed by recent results [13,27].

Calendering improved the smoothness of the surfaces for all formulations. Ink gloss and ink density consequently increased [29]. However, it is believed that the low

solids content of the coatings prevents the smooth application of the coating due to base sheet roughening by the absorption of coating water. Research is therefore needed to determine ways to control the penetration of the coating water into the base sheet. Base sheet sizing, coating solids, the application and formulation of a base coating, and coating rheology should be considered for topics of future research.

From the results of these experiments, it is evident that the blended coatings of fumed metallic oxide and conventional pigments had comparable optical properties and printing qualities to the coatings of fumed metallic oxides alone.

References

1. Mills, Ross N., "Inkjet printing – Past, Present and Future", *IS&T NIP10*, pp 410 – 413 (1994).

2. Kulmala, A., Paulapuro, H. and Oittinen, P., "Paper requirements for electrophotographic printing," *Proceedings of the IS&T's 10th International Congress on Advances in Non-Impact Printing Technologies*, Springfield VA, 1994, pp. 466-470.

3. Casey, P. James, "Pigment Coating", *Pulp and Paper*, Chapter 22, Wiley, Inc., New York, NY, 1980, p.2181.

4. Bristow, J.A., *Advanced Printing Science & Technology*, 20: 193(1990).

5. *Measurement and Control of the Optical Properties of Paper*, Second edition, Technidyne Corporation, p.7.5-7.6, 1996.

6. Aksoy, Burak, Joyce, Margaret K. and Fleming, Paul D., "Comparative Study of Brightness/Whiteness Using Various Analytical Methods on Coated Papers Containing Colorants", *Proceedings of the TAPPI Spring Technical Conference & Trade Fair*, Chicago, May 2003.

7. Burak Aksoy, Paul D. Fleming and Margaret K. Joyce, "New Measures Of Whiteness That Correlate With Perceived Color Appearance", in Review for *Applied Optics*.

8. Burak Aksoy, Paul D. Fleming and Margaret K. Joyce, "Whiteness Evaluations On Tinted And FWA Added Papers", in Review for *Applied Optics*.

9. Rolf Griesser, "Whiteness not Brightness: A new way of measuring and controlling production of paper", *Appita J.*, v. 46, no. 6, Nov. 1993, 439-445.

10. Rolf Griesser, "CIE Whiteness and Tint: Possible Improvements" *Appita Journal*, v. 49, no. 2, 105-112., (March 1996).

11. TAPPI Standard, T480 m51.

12. D. W. Donigan., J. N. Ishley, K. J. Wise, "Coating Pore Structure and Offset Printing Gloss", *TAPPI Journal*, 80, 5, 163 (1997).

13. Renmei Xu, Paul D. Fleming III and Alexandra Pekarovicova, "The Effect of Ink Jet Papers Roughness on Print Gloss and Ink Film Thickness" *Proceedings of the IS&T NIP20: International Conference on Digital Printing Technologies*, Salt Lake City, 2004.

14. Kubelka, P. and Munk, P., "Ein beitrag zur optik der farbanstrich", *Z. Tech Phys.* 12:593-601, 1931.

15. TAPPI Standard, T1214 sp98.

16. Mourad, S., Emmel, P., Simon, K., and Hersch, R. D., "Extending Kubelka-Munk's theory with Lateral Light Scattering", *IS&T NIP 17*: pp469-473 2001.

17. Lee, Hyunkook, "The influence of fumed metallic oxides on coating structure and their relationships to print quality", Western Michigan University, MS thesis 1998.

18. Lee, Hyunkook, Joyce, Margaret K. Fleming, Paul D. and, Cameron, John, "Production of a Single Coated Glossy Inkjet Paper Using Conventional Coating and Calendering Methods", *Proceedings of the TAPPI Coating Conference*, May 2002 and TAPPI J. in press..

19. Ramakrishnan, Raja, "Coating and Basesheet Influences on the Development of Gloss for Ink Jet Papers Containing Fumed Metallic Oxides." Western Michigan University, MS thesis, 1999.

20. Cawthorne, E. James, "Use of a Chemically-Modified Clay as a replacement for Silica in Matte Coated Ink Jet Papers." Western Michigan University, MS thesis, 1999.

21. Cawthorne, James E., Joyce, Margaret and Fleming, Paul D., "Use of A Chemically Modified Clay as A Replacement for Silica in Matte Coated Ink Jet Papers", *J. Coat. Tech,* 75, No. 937, pp 75-81, Feb. 2003.

22. Fetso, M. Jacqueline and Zettlemoyer, C. Albert., "Factors Affecting Printing Gloss and Uniformity", TAPPI Journal, August 1962, p.667-681.

23. TAPPI procedure T 452 om-92.

24. Fleming, Paul D., Cawthorne, James E., Mehta, Falguni, Halwawala, Saurabh, and Joyce, Margaret K., "Interpretation of Dot Area and Dot Shape based on Image Analysis", *IS&T NIP18* pp 474-477 2002, and *JIST* Sept.-Oct. 2003.

25. Chinmayanandam, T. K., Phys. Rev. 13:96 (1919).
26. Frimova, A., "Particle Size Analysis of Commercial Printing Inks and Their Press Stability and Printability", MS Thesis, Western Michigan University, April 2003.

27. Veronika Chovancova, Paul Howell, Paul D. Fleming III and Adam Rasmusson, "Printability of Different Epson Ink Jet Ink Sets", *Proceedings of the IS&T NIP20: International Conference on Digital Printing Technologies*, Salt Lake City, 2004.

28. Frimova, Andrea, Pekarovicova, Alexandra, Fleming, Paul D., "Particle Size of Printing Inks; Stability, Colorimetry and Printability", In Preparation.

29. Hyun-Kook Lee, Margaret K. Joyce, Paul D. Fleming, and James E. Cawthorne, "Influence Of Silica and Alumina Oxide On Coating Structure and Print Quality Of Ink Jet Papers", *TAPPI Journal*, in press.

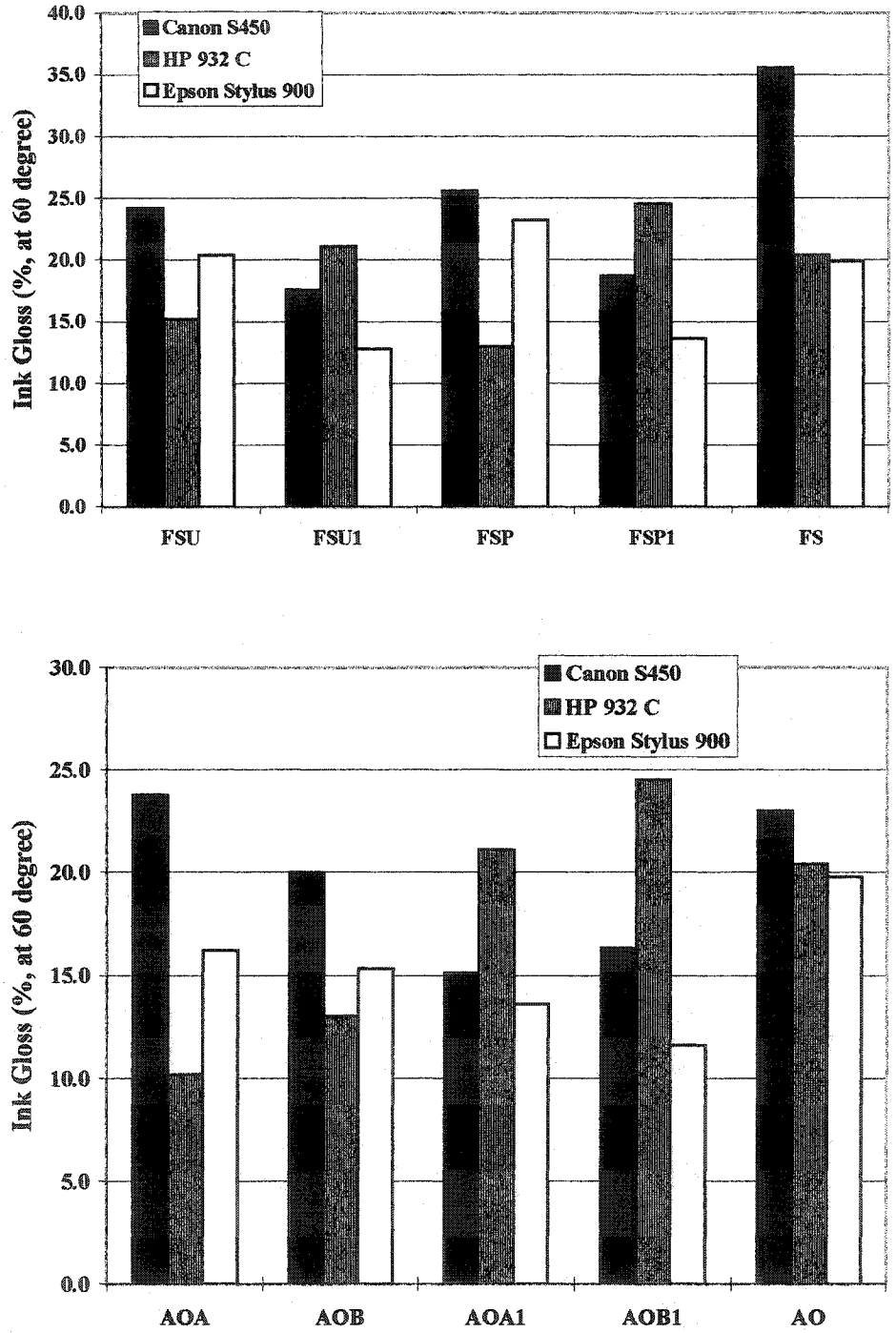

Figure 82. Ink gloss comparison of each coating formulations (Coat wt.: 12 g/m^2, Color: black).

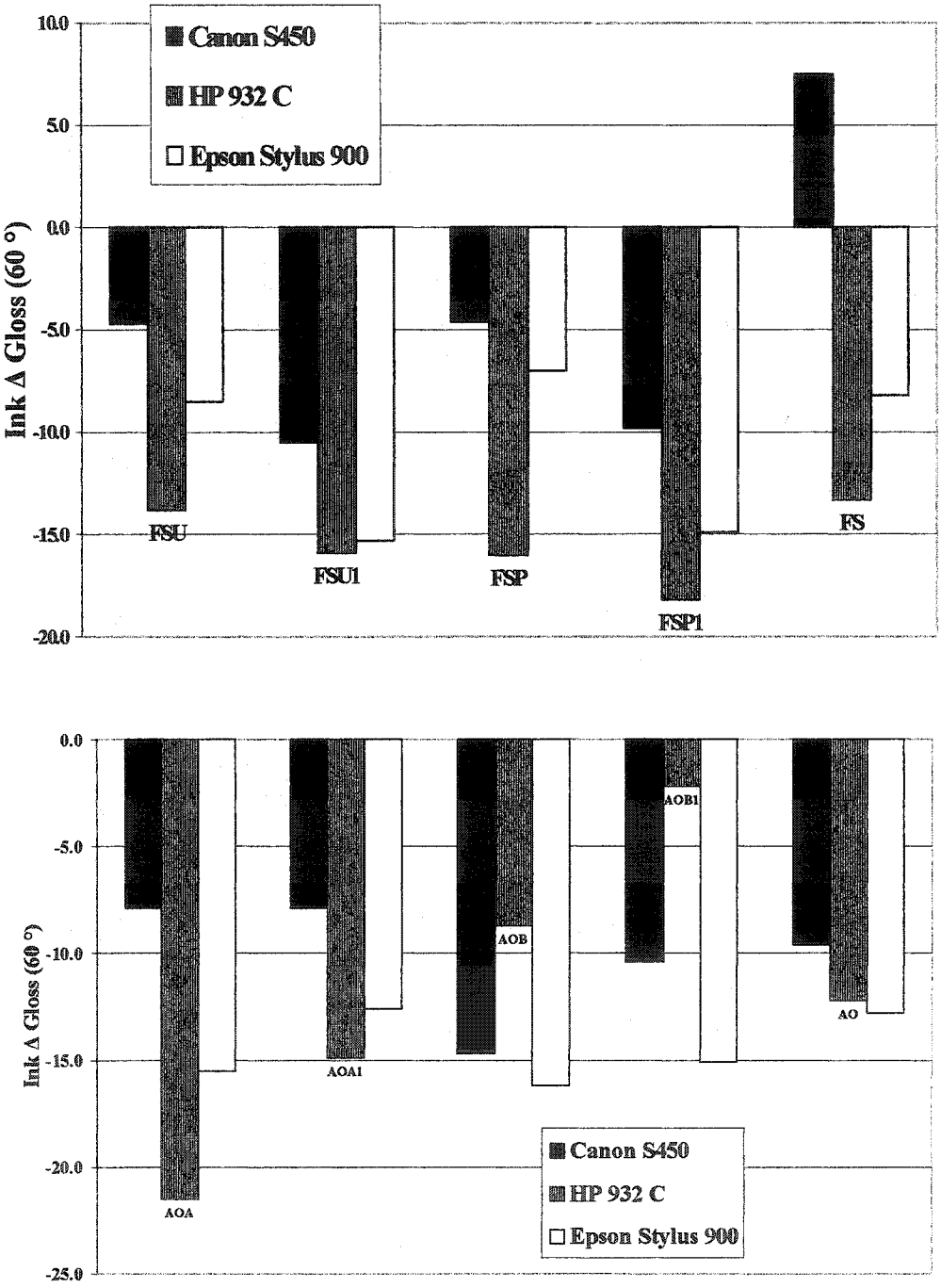

Figure 83. Ink Δ gloss for different coating formulations
(Coat wt.: 12 g/m2, Color: Black)

Appendix A

Standard deviation of optical and physical properties on calendering samples

Sample A

Coat Weight (g/m^2)	Brightness	Gloss	Smoothness	Porosity
6	0.16	1.21	1.02	0.72
8	0.26	1.12	1.11	1.03
10	0.08	1.21	1.13	0.83
12	0.13	1.03	1.07	0.98

Sample A-1

Coat Weight (g/m^2)	Brightness	Gloss	Smoothness	Porosity
6	0.40	0.15	0.05	0.89
8	0.99	0.07	0.03	0.54
10	1.14	0.08	1.03	0.86
12	0.97	0.08	0.07	0.94

Sample B

Coat Weight (g/m^2)	Brightness	Gloss	Smoothness	Porosity
6	0.10	0.67	0.09	0.77
8	0.09	0.78	0.82	0.56
10	0.13	0.74	0.87	0.76
12	0.08	0.78	0.92	0.67

Sample B-1

Coat Weight (g/m^2)	Brightness	Gloss	Smoothness	Porosity
6	0.33	0.06	0.03	0.24
8	1.29	0.14	0.01	0.86
10	0.77	0.09	0.02	0.74
12	1.91	0.12	0.01	1.04

Sample C

Coat Weight (g/m^2)	Brightness	Gloss	Smoothness	Porosity
6	0.06	0.78	0.23	0.12
8	0.15	0.83	0.23	0.16
10	0.13	0.78	0.27	0.16
12	0.12	0.87	0.12	0.08

Sample C-1

Coat Weight (g/m^2)	Brightness	Gloss	Smoothness	Porosity
6	1.43	0.24	0.09	0.61
8	0.31	0.17	0.07	0.84
10	0.15	0.85	0.13	0.21
12	0.33	0.87	0.02	0.1.96

Sample D

Coat Weight (g/m^2)	Brightness	Gloss	Smoothness	Porosity
6	0.15	1.12	0.24	0.87
8	0.10	1.11	0.38	1.12
10	0.08	1.10	0.78	1.34
12	0.07	1.15	0.78	1.07

Sample D-1

Coat Weight (g/m^2)	Brightness	Gloss	Smoothness	Porosity
6	0.17	0.14	0.04	3.20
8	0.18	0.08	0.05	5.00
10	0.45	0.16	0.05	3.20
12	0.67	0.11	0.05	2.00

Sample E

Coat Weight (g/m^2)	Brightness	Gloss	Smoothness	Porosity
6	0.11	0.89	1.25	0.97
8	0.08	1.09	0.89	1.23
10	0.11	0.98	0.79	1.29
12	0.10	1.08	1.02	0.93

Sample F

Coat Weight (g/m^2)	Brightness	Gloss	Smoothness	Porosity
6	0.12	1.09	1.21	1.07
8	0.25	1.12	0.93	0.98
10	0.07	1.09	1.19	0.89
12	0.13	1.18	1.23	0.97

Appendix B

SEM (scanning electron microscope) pictures of coated papers

(3000X magnification)

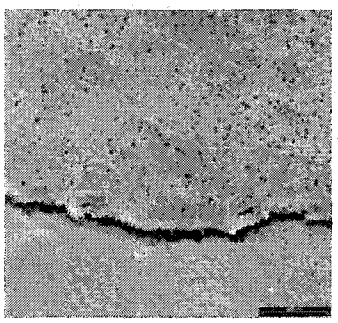

Sample E (100% FS)

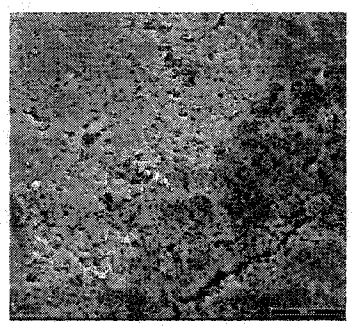

Sample A
(70% FS:30% UFGCC)

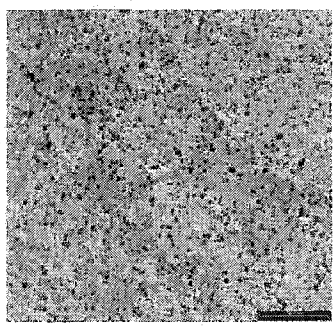

Sample A-1
(50% FS: 50% UFGCC)

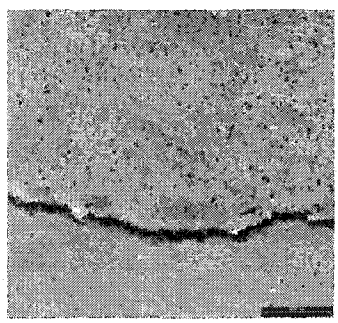

Sample E (100% FS)

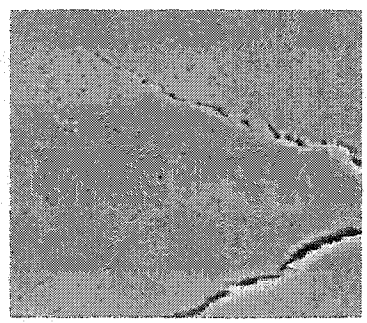

Sample B
(70% FS:30% PCC)

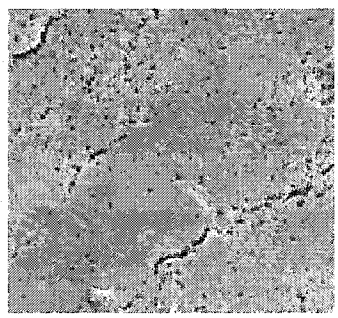

Sample B-1
(50% FS: 50% PCC)